INFORMATION TO USERS

This manuscript has been reproduced from the microfilm master. UMI films the text directly from the original or copy submitted. Thus, some thesis and dissertation copies are in typewriter face, while others may be from any type of computer printer.

The quality of this reproduction is dependent upon the quality of the copy submitted. Broken or indistinct print, colored or poor quality illustrations and photographs, print bleedthrough, substandard margins, and improper alignment can adversely affect reproduction.

In the unlikely event that the author did not send UMI a complete manuscript and there are missing pages, these will be noted. Also, if unauthorized copyright material had to be removed, a note will indicate the deletion.

Oversize materials (e.g., maps, drawings, charts) are reproduced by sectioning the original, beginning at the upper left-hand corner and continuing from left to right in equal sections with small overlaps.

Photographs included in the original manuscript have been reproduced xerographically in this copy. Higher quality 6" x 9" black and white photographic prints are available for any photographs or illustrations appearing in this copy for an additional charge. Contact UMI directly to order.

Bell & Howell Information and Learning
300 North Zeeb Road, Ann Arbor, MI 48106-1346 USA
800-521-0600

Characterization of *FIG2* in *Saccharomyces cerevisiae*

by

Chong Jue

A dissertation submitted to the Graduate Faculty in Biochemistry in partial fulfillment of the requirements for the degree of Doctor of Philosophy, The City University of New York.

2001

UMI Number: 9997099

Bell & Howell Information and Learning Company
300 North Zeeb Road
P.O. Box 1346
Ann Arbor, MI 48106-1346

This manuscript has been read and accepted for the Graduate Faculty in Biochemistry in satisfaction of the dissertation requirement for the degree of Doctor of Philosophy.

10/13/00
Date

Chair of Examining Committee

January 19, 2001
Date

Executive Officer

Supervisory Committee

The City University of New York

Abstract

Characterization of *FIG2* in *Saccharomyces cerevisiae*

by

Chong Jue

Adviser: Professor Peter Lipke

The complete genome sequence of the yeast *Saccharomyces cerevisiae* has been available since 1996. One of the most immediate, albeit difficult, consequences of this is the ability to investigate the functions of genes that have not been previously characterized.

One such previously uncharacterized open reading frame, *YCR089W/FIG2*, has some of the structural characteristics of a cell wall mannoprotein. Construction of a fusion protein consisting of this open reading frame and jellyfish green-fluorescence-protein indicated localization to the cell wall.

Mutant strains were constructed in which this gene was either deleted or overexpressed. These strains were then characterized in terms of cell wall structure and function. *FIG2* was found to be constitutively expressed in both **a** and α haploid mating-type cells.

With respect to the structure of the cell wall, it was found that loss of *FIG2* resulted in aberrant cell morphology in cells of either mating type grown to stationary phase. When cells of either mating type were induced with the appropriate mating pheromone from the opposite type, *FIG2* expression was increased. This induction of *FIG2* expression was greater in α cells than in **a** cells.

With respect to functionality, the sexual agglutinability of *fig2Δ* α mating-type cells was significantly higher than the corresponding wild type strain. Conversely, the overexpression of *FIG2* in α cells resulted in decreased agglutinability. However, when *FIG2* was either deleted or overexpressed in **a** cells, no changes in agglutinability were observed. The time course of the pheromone induction of **a** cells was not altered by deletion of *FIG2*.

The molecular basis of the inhibition of α cell agglutination by *FIG2* was partially characterized. Increasing the gene dosage of *FIG2* did not affect the level of transcription of α-agglutinin. It was therefore hypothesized that the decrease in agglutinability of α cells overexpressing *FIG2* could be the result of specific binding of Fig2p to α-agglutinin. Experiments measuring the binding of soluble, labeled α-agglutinin to whole α cells, both wild type and *FIG2* delete, did not indicate any specific binding.

Acknowledgements

For my mother and my father.

Table of contents

List of Tables

List of Figures

Introduction

The Biology of Reproduction

Reproduction is one of the most important biological processes that define life. Higher eukaryotes generally reproduce sexually, whereas the lower eukaryotes and prokaryotes may commonly reproduce either sexually or asexually. In asexual reproduction, the only genetic variability that an offspring will inherit is through spontaneous mutation, which will produce genetic variability at a far lower rate than the process of recombination, found in sexual reproduction. This increase in genetic variability, made possible by the process of meiosis, is perhaps the most important benefit of sexual reproduction. Genetic variability within a species allows a higher survival rate when the species is faced with environmental changes (Ram et al 1998b). Higher rates of genetic variability coupled with dramatic changes within environments drives the process of speciation. New species are able to exploit new niches in the biosphere. Different species do not compete for resources directly because of their occupation of unique niches. This has led to a geometrical expansion of forms in order to fill all possible niches in the biosphere.

Saccharomyces cerevisiae reproduces either asexually via mitotic division or sexually via conjugation. When conditions allow the possibility of mating, haploid cells will preferentially reproduce sexually despite the fact that these conditions also allow them to reproduce asexually. In complete medium, a pure culture of wild type haploid cells of a specific mating type (**a** or α) is capable of switching a portion of their population to the opposite mating type which generates a culture of two opposite mating types (Haber 1992; Klar et al 1979). When two opposite mating type haploid cells come into direct contact, the two cells fuse to form a diploid zygote, the process of which is known as mating. On solid media, when two opposite mating type haploid cells are in proximity, but not in contact with each other, they will undergo cellular morphogenesis in an attempt to reach out to each other so that they can conjugate, despite the fact that these cells are non-motile (Palkova et al 1997). This mating morphogenic event requires a major remodeling of the cell wall. In the process of fusion, the choreography must be orchestrated precisely to further remodel the cell wall while avoiding cell lysis. It is highly likely that multiple factors are involved.

In this dissertation, an attempt was made to further the understanding of the role of cell wall components in the regulation of mating. Vast amounts of research have been done on either cell walls or mating alone. Yet, the functions of essential proteins in the cell wall that are specific for mating remain largely elusive. In this introduction, I wish to review the basic and some of the latest work on both cell wall and mating related events.

Overview of the General Architecture of the Cell Walls

The cell wall comprises about 26-32% of the dry weight of *S. cerevisiae* (Nguyen et al 1998). The major components of the yeast cell wall are glycoproteins (30%) and glucan (70%) (Nguyen et al 1998). Minor components include chitin and lipids (Ballou 1982; Fleet 1985; Orlean 1997). The generally accepted model of the cell wall is that it is composed of three layers (Linnemans et al 1977; McMurrough & Rose 1967; Zlotnik et al 1984). The outermost layer is comprised of mannoproteins. These outer mannoproteins are covalently attached to the second layer, which is essentially a complex of glucan interspersed with a small amount of chitin (Zlotnik et al 1984). The inner layer is the periplasmic space, outside of the plasma membrane, where various

enzymes and mannoproteins reside (Linnemans et al 1977; Marsh & Rose 1997; McMurrough & Rose 1967).

The Cell Wall Structure Observed in Electron Microscopy

As observed in electron micrographs, the entire wall is about 150-200 nM in thickness (Gruler 1981; McMurrough & Rose 1967). The outer layer is seen as a dark band. When appropriate fixing and staining techniques are used, the outer layer can be seen as a fuzzy band, which is thought to represent bundles of mannoproteins projecting into the medium (Kappeli et al 1984; Tokunaga et al 1990). The electron-dense outer layer disappears when the walls are incubated with protease (van der Vaart et al 1995; Zlotnik et al 1984), implying that the outer layer is made of protein. The middle layer is often seen as an electron-transparent band, which, as mentioned, is widely believed to be glucan (van der Vaart et al 1995). The inner layer (periplasmic space) of the cell wall, located between the plasma membrane and the glucan layer, is often difficult to detect by electron by microscopy, and its existence is not universally acknowledged. However, the cytoplasm does not appear to be in direct contact with the glucan layer. The separation between these two layers is estimated to be about 20 nm (van der Vaart et al

1995) and freeze fracture electron microscopy has revealed some small vesicles on the outer surface of the cell membrane (Barug & de Groot 1983). In addition, there is some biochemical evidence for the existence of an inner cell wall layer (See The Inner Layer of Cell Walls, Below).

Although the evidence for the existence of an inner layer or periplasmic space is not overwhelmingly strong in *S. cerevisiae* or *C. albicans*, such is not the case for *C. neoformans*. In the latter, immunogold electron microscopy localized most mannoproteins to a region between the cytoplasm and the glucan layer (Vartivarian et al 1989).

The Outer Layer of Cell Walls

The glycoproteins of the outer layer consist of *N*-linked and *O*-linked mannoproteins. The *N*-linked glycoproteins are decorated extensively by relatively long mannose polysaccharides (Ballou 1982; Herscovics & Orlean 1993). These mannose chains may have as many as 200 mannose units. These polysaccharide chains have a main backbone of mannose joined through α, 1-6 linkages. Branching off the main mannosyl backbones are short chains of mannose units linked together

through α1-2, or α 1-3 linkages. The reducing end of the backbone is attached to an asparagine residue of the protein (Herscovics & Orlean 1993).

The second type of glycoprotein is the *O*-linked mannoprotein. In these glycoproteins, the mannose chains are short, usually 2- 5 units per chain, and linked together in α1-2 and α1-3 configurations (Mormeneo et al 1989; Zueco et al 1986). These mannose chains are linked to the proteins at serine or threonine residues. The entire complex of mannose chains and proteins are traditionally called mannan, or mannoproteins.

The majority of the mannoproteins, about 84%, of the outer layer are called GPI-CWP (Caro et al 1997; Hamada et al 1998a). The last 12-15 residues of the *C*-terminal ends of these proteins are hydrophobic (Hamada et al 1998b). When these proteins are synthesized in the endoplasmic reticulum, the hydrophobic residues are cleaved at glycine or asparigine residues and a glycosyl phosphatidylinositol (GPI) is attached to the *C*-terminus of the proteins (Udenfriend & Kodukula 1995). The proteins are then secreted to the plasma membrane, where part of the GPI structure is cleaved and the proteins are transferred to a

β1-6 glucan chain (Jiang et al 1996; Lu et al 1995). These glucosylated proteins are then eventually transferred to the main β1-3 glucan chain in the cell wall. The linkage of GPI-CWPs is therefore CWP-GPI-β1-6-glucan-β1-3glucan, which is sometimes extended with chitin (Smits et al 1999). GPI-CWPs are consequently sensitive to β1-6 glucanase.

Another class of wall mannoproteins (16%) on the outer cell wall layer is termed Pir2-CWP (Proteins with Internal Repeats- Cell Wall Proteins). Pir2-CWP is alkali sensitive and β1-6 glucanase insensitive, and Pir2-CWPs do not have a GPI anchor (Kapteyn et al 1999; Mormeneo et al 1994). The proportion of GPI-CWPs and Pir2-CWPs varies depending on the relative activities of their genes (see below, The Dynamic of Cell Walls).

Some mannoproteins on the outermost surface are cross-linked, through sulfydryl linkages, to other mannoproteins in the outer layer. An example of such a mannoprotein is Aga2p, which can be released into the media by treatment with reducing agents (Cappellaro et al 1994; Orlean et al 1986). In the Yellow Y strains,Ywp1 protein is extractable by β-mercaptoethanol, indicating Ywp1 is linked to the cell wall via

disufide linkages (Ramon et al 1999). When cells are treated with hot citrate or hot SDS, some mannoproteins are released into the medium (Mrsa et al 1999; Pastor et al 1982). It is not clear exactly where these latter mannoproteins are located. It is possible that these represent non-covalently attached proteins from all three layers of the cell wall (Valentin et al 1984).

The Middle Layer of Cell Walls

The middle layer of the wall is primarily composed of β1-3 glucan (van der Vaart et al 1995). The β1-3 glucan is branched through β1-6 linkages to other β1-3 glucan chains. These β-glucan main chains are typically about 1500 residues long (Manners et al 1973a). Some shorter β1-6 glucan chains (about 5%), with an average of 140 residues, are branched with β1-3 glucan, through has β1-3 linkages (Manners et al 1973b). These glucan polymers are further strengthened by different degrees of cross-linking to chitin (β1-4 poly-*N*-acetylglucosamine), rendering them differentially soluble in acid or alkali (Hartland et al 1994; Kollar et al 1995). In addition to chitin reinforcement, these glucans are intertwined into triplexes, providing further rigidity to the

cell wall (Duffus et al 1982). Glucan is thought to be the primary component that gives the cell walls its shape and strength.

The Inner Layer of Cell Walls

The inner layer of the cell wall is also known as the periplasmic space. The best-characterized proteins residing in this space are acid phosphatase and invertase (Harsay & Bretscher 1995; Linnemans et al 1977). Recently, Moukadiri et al. have shown that Icw1p (Inner Cell Wall protein) is localized to the inner cell wall (Moukadiri et al 1997). The Serine and Threonine content of Icw1p is over 40%, and it has a putative GPI attachment signal. Disruption of *ICW1* resulted in an increased sensitivity to Zymolyase, suggesting a structural role for Icw1p.

The Genomic Organization of Cell Wall Proteins in *S. cerevisiae*

Saccharomyces cerevisiae has a small genome (13.5 Mb), a large number of chromosomes (16), and few introns (Olson 1991). As a prelude to the determination of the entire genome, the third chromosome, being the smallest, was chosen for sequencing by a collaboration of the European Community's Biotechnology Action

Programme (Oliver et al 1992). Eventually, through an international collaboration of efforts, the sequence of the entire genome was determined (Goffeau et al 1996).

In the genome of *S. cerevisiae*, there are a total of 6218 opening reading frames that potentially code for proteins. Caro et al. made an attempt to identify *in silicio* cell wall proteins (Caro et al 1997). Approximately 10% of the genome, 686 potential proteins, have an *N*-terminal sequence that signals entry into the secretory pathway. Of this group of secretory proteins, 58 have been found to contain a potential glycosyl-phosphatidylinositol (GPI)-attachment signal. These proteins with potential GPI attachment may be directed to plasma membrane or cell wall, depending on the GPI signal. The presence of dibasic amino acids at the *N*-terminal ends of the GPI-cleavage sites are characteristic of plasma membrane proteins. The absence of such dibasic amino acids is indicative of cell wall proteins. Of the 58 proteins with signal sequences, 20 appear to be plasma membrane type, the remaining 38 being presumptive cell wall type. Of the 38 cell wall proteins, the 13 genes that have been described are *SAG1, AGA1, CWP1, CWP2, TIP1, TIR1/SRP1, TIR2, FLO1, FLO5, FLO11, SED1, FIG2* and *YLR392w-a.*

These confirmed cell wall genes contain the aforementioned secretion signal in addition to the wall anchorage signal; they all contain serine and threonine rich regions, which indicates probable glycosylation by mannose side chains.

Potential cell wall proteins, both studied and unstudied, are also classified into families based on sequence homology. The Tir family consists of *TIR1*, *TIR2*, *TIR3*, *TIR4*, *TIR5*, *TIR6*, *TIP1*, *CWP1*, and *CWP2*. In addition, there are the Sed1 family and the Yel040 family. Additional families are defined on the basis of functionality. The Flo family consists of genes involved in flocculation and includes *FLO1*, *FLO5*, *FLO9*, and *FLO11*. There is also a family of agglutination-related cell wall genes, comprised of *SAG1* and *AGA1*. Those cell wall genes which have either been described or studied, or belong to a homologous or functional family account for 21 of the 38 potential cell wall genes. The remaining 17 are, as yet, largely uncharacterized.

Although Caro et al. (1997) established a general groundwork for analysis of cell wall components, their work was far from complete (Caro et al 1997). These authors only described GPI-anchored wall

proteins; and the algorithm that they used to predict the presence of a signal peptide, was only about 75-80% accurate. It is now known that anchorage to the cell wall is not limited to a GPI mechanism. Non-GPI anchored cell wall proteins constitute up to 16% of the cell wall. In a β1-6 glucan deficiency strain, over 80% of the cell wall proteins are such non-GPI cell wall proteins (Kapteyn et al 1999). In addition, a few genes listed as unknown in the paper are now known to be cell wall proteins, for example, *DAN1, UTR2, CRH1*, and *PRY3*. Other recently identified wall proteins, such as *PIR1, PIR3, CIS3, FIG1, FIG3* and *FIG4*, were not mentioned (Erdman et al 1998; Mrsa et al 1997). In addition, the assumption of these authors that the presence of two basic amino acids at the GPI cleavage site is an indication of a membrane-bound, as opposed to a cell wall-bound protein has since been shown to be unreliable. For example, Gap1p and Yap3p were originally predicted to be membrane bound by this criterion, but eventually proven to be cell wall bound (De Sampaio et al 1999).

Since the original estimate of 38 cell wall genes was based on what is now known to be an undependable predictor, it may safely assumed that the total number of cell wall genes is probably greater than 38. Clearly,

this indicates a continuing need to further evaluate the yeast genome for presumptive cell wall genes via increasingly comprehensive methods.

One of the obvious ways to study these wall proteins is to perform gene disruptions on their open reading frames. So far, through worldwide efforts, about a third of the genome has been disrupted (Winzeler et al 1999). Disruption of a single cell wall gene only sometimes results in a measurable phenotype. Often, several genes must be disrupted for any effects to be seen. One paper reported that as many as four genes needed to be disrupted before any noticeable changes occurred (Mrsa & Tanner 1999). Unfortunately, in such multiple disruptants, multiple phenotypes appear simultaneously. Such cells often exhibit slow growth rates, hypersensitivity to Calcoflour White and Congo Red, as well as mating defects. This makes it difficult to assign any one gene to a specific function. Cappellaro et al. have reported that 3 out of 4 bona fide cell wall genes disrupted showed no detectable cell wall phenotypes (Cappellaro et al 1998). In another case, of 6 genes singlely disrupted, no phenotype was found in respect to gowth, mating or sporulation (Lafuente & Gancedo 1999).

The Unexpected Complexity of the Cell Wall

In addition to its more obvious functions, the cell wall also serves as a repository for certain enzymes. Glycolytic enzymes, such as enolase, 3-phosphoglyceraldehyde dehydrogenase, and triophosphate isomerase, have been isolated from the walls of *C. albicans* (Angiolella et al 1996; Eroles et al 1997; Kanbe et al 1996; Sentandreu et al 1995) and from *S. cerevisiae* (Cappellaro et al 1998; Edwards et al 1999). Although some of these authors, such as Cappellaro at al., believe these enzymes to be contaminants, the purification procedures used were specifically designed to isolate cell wall only. These authors also appear to be unaware that glycolytic enzymes, enolase and others, have also been isolated from cell walls of streptococci (Pancholi & Fischetti 1992; Pancholi & Fischetti 1998), and *C. albicans* (Angiolella et al 1996; Eroles et al 1997; Kanbe et al 1996; Sentandreu et al 1995). It can therefore be argued that the finding of glycolytic enzymes in the cell wall fraction is not artifactual. Possibly, all of the enzymes necessary for the generation of ATP through glycolysis exist in the cell wall. This may provide ATP to fuel biochemical reactions at the cell surface. Since the genes for these glycolytic enzymes do not contain signal sequences,

the mechanism by which they may be transported to the cell surface remains a mystery.

The Dynamic of the Cell Wall

Yeast cells are capable of altering the chemical compositions of their cell walls in response to environmental changes or mutations. As will be described (see results), the sensitivity of cells to Zymolyase, a complex of cell wall digesting enzymes, varies depending upon growth temperature, nutrients or growth phase. The loss of a cell wall gene often leads to a change in the composition of the cell wall designed to compensate for the loss of that particular gene product. For example, deletion of the *GAS1* gene results in the release of β1-3 glucan into the medium (Ram et al 1998a). Examination of the cell wall reveals a coincident increase of chitin and mannan contents, an enhanced expression of the *CWP1* gene, and an increase in β1-3 glucan synthase activity.

The majority of mannoproteins connect to β1-3 glucan through β1-6 glucan, while a small portion (16%) of the mannoprotein is connected via an alkali-sensitive linkage, the precise structure of which is unknown

(Kapteyn et al 1999). In β1-6 glucan deficient mutants, the alkali-sensitive wall proteins are increased from 16% to 80%. The incorporation of Pir2p/Hsp150p is also increased.

The characteristics of a- and α- haploids and a/α diploids

In nature, *S. cerevisiae* can exist in either haploid or diploid forms. Haploids are one of two mating types, either **a** cells or α- cells. Diploids do not mate and are the product of the mating of **a**- and α-cells. The ellipsoid diploid cells are generally larger (5 X 6 μm) and more elongated than spheroid haploid cells (4 μm) (Sherman 1998). In addition, diploids can undergo sporulation and remain in a dormant state when nutrients are in poor supply. Aside from being to able to survive better under harsh conditions, heterozygous diploids, but not homozygous diploids, also enjoy an ability to resist ionizing radiation better than haploids (Friis & Roman 1968; Heude & Fabre 1993). The sizes and compositions of haploids and diploids are listed in Table 8 (Sherman 1998).

a and α cells are different genetically only at the *MAT* locus (Dranginis 1986; Sherman 1998). The *MATα* locus encodes two proteins, Matα1p

and Matα2p. Matα1p, working together with Mcm1p, activates a set of α-specific genes (Hagen et al 1993). Matα2p, working together with Mcm1p, Tup1p, and Ssn6p, specifically represses **a**-specific genes (Patterton & Simpson 1994). When both *MATα1* and *MATα2* are deleted, cells behave like **a** cells. This is because **a**-specific genes are constitutively expressed. Therefore, in the absence of expression of α genes and in the absence of repression of **a** genes, cells act like **a** cells (Strathern et al 1981).

In **a** cells, *MAT**a**1* and *MAT**a**2* are two open reading frames corresponding to the two frames of the *MAT*α locus. A function for Mat**a**2p has not yet been published, although some preliminary results have been obtained in which a phenotype has been observed in *mat**a**2* mutants (A. Dranginis, personal communication). Mat**a**1p has no known role in haploid cells. In diploids, Mat**a**1p combines with MATα2p to work as a repressor for MATα1p. Consequently in diploids, α-specific genes are turned off. In addition, the Mat**a**1p-Matα2p complex also represses haploid-specific genes (Dranginis 1990). Therefore **a**-specific genes are also turned off.

Mating-type Switching

Under stringent conditions (i.e. nutrient depletion), diploid cells will undergo meiosis to produce 4 haploid spores (2 spores of mating-type **a**, and 2 of α mating type.). These spores are contained in a protective shell (ascus), which allows them to survive until conditions improve, at which time the haploid spores will be released from the ascus and divide by mitosis (budding) (Sherman 1998).

When the spores are released from an ascospore, each will undergo an initial mitotic division to produce a first generation bud of like mating type. Thus, each of the two **a**-spores will bud to produce an **a**-mating-type daughter cell, and each of the two α-spores will bud to produce an α mating-type daughter cell. In the subsequent division, while each of the maternal cells again bud to produce a cell of like mating-type, the daughter cell from the first division will switch mating-type upon division, and produce a daughter cell of switched mating type. That is, each daughter **a** cell from the first division will bud to produce an α cell daughter, while itself becoming an α cell. The α daughter cells from the first division will undergo a similar transformation to **a**-mating-type while producing **a**-mating-type daughters. In the divisions that follow,

this pattern will be maintained. Maternal cells will continue to breed true for mating type, while daughter cells switch. Thus, in wild type strains, any haploid culture will be of mixed mating type, even if started from a single spore (Haber 1998).

MAT Switching, the Cassette Model

Mating type control is regulated by the *MAT* locus. If the *MAT* locus contains a Y_α sequence, the cells are α mating type. On the other hand, if the *MAT* locus contains a Y_a sequence, the cells are **a**-mating type (Oshima & Takano 1971). Every haploid cell contains one copy each of unexpressed Y_α and Y_a, at the *HML* and *HMR* loci, respectively. When conditions are appropriate, an endonuclease, HO, excises a donor copy of either Y_α or Y_a and transposes it into the *MAT* locus (Nasmyth 1983). The selection of the donor is a specific event, known as donor preference. The cell lineage and selection of a donor are meticulously orchestrated at the molecular level (Klar et al 1982; Weiler & Broach 1992). This mechanism drives the phenomenon of mating type switching and enables haploid cells to form diploid zygotes at high frequency.

Overview of Signal Transduction

Haploid yeasts undergoing vegetative growth devote their metabolic energy toward growth and mitotic division. When 2 haploid cells of opposite mating type interact as a prelude to mating, they transcribe a new set of mating genes that are normally shut-off during vegetative growth (Udden & Finkelstein 1978; Wilkinson & Pringle 1974). Mating interactions are initiated by intercellular signaling of each mating type via external stimulation by the appropriate pheromone from the opposite mating type. The binding of these secreted peptide pheromones on cell surface receptors results in intracellular signal transduction, which initiates a series of effects including G1 arrest and cell-cycle synchronization, increased agglutination, increased transcription of mating-specific genes and selective inactivation of other genes (Betz & Duntze 1979; Kurjan & Lipke 1986; Moore 1983). Chronic exposure to pheromone results in a dramatic cellular morohogenesis to a form known as a shmoo (Moore 1983).

Signal transduction initiated as a prelude to mating is not the only phenomenon capable of radically altering the morphological state of yeast cells. Under conditions of nitrogen starvation, yeasts are

stimulated to form pseudohyphae, which allows these non-motile cells to reach out for essential nutrients (Gimeno et al 1992). The formation of these structures represents a radical departure from normal cell morphology, and is undoubtedly mediated through quantitative and/or qualitative changes in the composition of the cell wall. The relationship between this effect and the equally profound cell wall changes (shmoo formation) seen in response to stimulation by mating pheromone remain unclear.

α-Pheromone

α-Pheromone is secreted by α cells into the extracellular medium. α-Pheromone is a tridecapeptide, the sequence of which is Trp-His-Trp-Leu-Gln-Leu-Lys-Pro-Gly-Gln-Pro-Met-Tyr (Stotzler & Duntze 1976). *MFα1* and *MFα2* are two unlinked loci that code for α-pheromone (Kurjan 1992; Singh et al 1983). *MFα1* encodes for 4 copies of α-pheromone and *MFα2* for two. Five copies of the α-pheromone gene are identical. The remaining copy contains two conservative changes (Asn-4, Arg-7). The biological activities of both of the peptides are similar (Kurjan & Lipke 1986).

The primary translation products encoded by *MFα1* and *MFα2* are called prepro-α-pheromone. Successive processing by membrane-bound proteases generates the mature pheromone. The *KEX2* gene product cleaves the peptide at a Lys-Arg linkage, turning the prepro-α-pheromone into pro-α-pheromone (Fuller et al 1986; Julius et al 1984).

All pro-α-pheromone has two or three X-Ala dipeptides at the amino terminus, while four of the copies also have Lys-Arg dipeptides at the carboxyl terminus. The *STE13* gene product removes the *N*-terminal dipeptides (Julius et al 1983), while the carboxyl terminus is further processed by the *KEX1* gene product (Dmochowska et al 1987). *Kex2* and *ste13* mutants are sterile. The *kex1* mutant is not sterile because one of the five copies of pro-α-pheromone does not need processing at the carboxyl end.

a-Pheromone

a cells secrete two slightly different **a**-factors, the sequences of which are Tyr-Lle-Lle-Lys-Gly-(Val/Leu)-Phe-Trp-Asp-Pro-Ala-Cys (Betz et al 1987). Two unlinked genes, *MFa1* and *MFa2* encode these dodecapeptides; each gene encodes a single polymorphic gene product

(Brake et al 1985). Like α-factor, the primary translational products of **a**-factor require processing to generate mature molecules. An Asp-Asn dipeptide is removed from the *N* terminus and three amino acids are processed from the carboxy terminal end. In addition, the terminal Cys is farnesylated. **a**-factor is farneslyated by the *RAM* gene product, making **a**-factor hydrophobic (Powers et al 1986). Mutation in the *RAM* gene results in sterility (Wilson & Herskowitz 1987). **a**-factor is transported to the cell surface by the *STE6* gene product. Mutations in *STE6* also cause sterility (Wilson & Herskowitz 1984).

Receptors

a and α cells have cell surface receptors that recognize the appropriate pheromone and generate intracellular signals. Once pheromone is bound to the appropriate receptor, the signals are transmitted via a cascade of intracellular proteins. This results in the start of transcription of a number of mating-specific genes.

a-Factor and α-Factor Receptors

The *STE3* and *STE2* genes encode **a**-factor receptor and α-factor receptor respectively (Burkholder & Hartwell 1985; Sprague et al

1983b). The sequences of *STE2* and *STE3* are structurally similar to other receptors in that they contain seven transmembrane domains. Rhodopsin, the β-adrenergic receptor, and the muscarinic acetylcholine receptor are several examples of this class of protein (Burkholder & Hartwell 1985; Hagen et al 1986; Marsh & Herskowitz 1988). In the plasma membrane, the seven hydrophobic domains are clustered together to form a channel-like structure. The stimulating ligand is thought to bind to one or more of the hydrophobic segments (Strader et al 1987). It is likely that **a**-factor and α-factor bind to hydrophobic segments of the appropriate receptors since α-factor is inserted into lipid vesicles and **a**-factor is farneslyated (Betz et al 1987; Wakamatsu et al 1987; Wakamatsu et al 1986).

Mutations in *STE2* and *STE3* genes result in cell-type specific sterility. Expression of normally pheromone-inducible genes is absent in these mutants. However, constitutive production of pheromones in these mutants is normal. Furthermore, *ste2* mutants have been shown to exhibit weaker binding to **a**-factor. This demonstrates that the *STE2* gene product is indeed the **a**-factor receptor (Konopka & Jenness 1991).

Polarized Growth, Budding versus Mating Projection

When **a** cells are placed in a spatial gradient of α-pheromone, the Ste2p have been shown to localize to the tip of the tip of mating projection (Jackson et al 1991). The deletion of the carboxy-terminal cytoplasmic tail of Ste2p results in defects in the mating projection (Konopka et al 1988). Because of this, it has been hypothesized that Ste2p interacts with other proteins required for the establishment of polarized growth.

Polarized growth occurs in both budding and mating projection formation. Budding follows a set pattern. Haploids bud axially (buds form next to old bud scar), whereas diploids bud bipolarly (buds form at the distal end for the daughter cells and at the proximal end for the mother cells) (Chant & Pringle 1991; Sheu et al 1998). The mating projections of haploids in mating mixtures or pheromone gradients, on the other hand, can protrude anywhere relative to the old bud scar (Madden & Snyder 1992; Segall 1993). To achieve this, genes governing the axial mechanism for budding must be turned off. Indeed, Axl2p and Bud4p axial-specific proteins are depleted when the cells are treated with pheromone (Roemer et al 1996; Sanders & Herskowitz 1996).

G-proteins

The binding of pheromone to its appropriate receptor triggers a signal that propagates through a series of proteins and eventually alters gene expression. The most widely studied of these signal transduction proteins are the G-proteins. G-proteins are heterotrimeric and are composed of an α, β and gamma subunits (Kurjan 1992). When pheromone binds to its receptor, the α-subunit dissociates from the β/gamma subunit, allowing the latter subunit to interact with down-stream components in the signal transduction cascade (Kurjan 1992).

The α-subunit is a GTP-binding protein and is homologous to its mammalian counterpart. The α subunit gene in yeast (*SCG1/GPA1*) was first isolated by Dietzel & Kurjan and Miyajima et al. (Dietzel & Kurjan 1987; Miyajima et al 1987). Mutations in *scg1* can be partially restored by complementing the defect with rat G_α protein (Dietzel & Kurjan 1987). When *SCG1* is overexpressed, the cells become less sensitive to stimulation by ligand. This implies that *SCG1* is a negative regulator in the signal transduction cascade (Dietzel & Kurjan 1987). When *SCG1* is

deleted, the cells become enlarged and are unable to mate (Miyajima et al 1987).

The MAP Kinase Pathway Leads to the Activation of *STE12*

The $G_{\beta\gamma}$ (the β subunit and the γ subunit of G-protein) has been shown to interact with Ste20p and Ste5p (Akada et al 1996; Hasson et al 1994; Leberer et al 1992). The Ste5p acts as a scaffold protein holding different members of the MAP kinase cascade together (Choi et al 1994). In the MAP kinase pathway, the function of Ste20p is to activate Ste11p, Ste7p, and eventually Fus3p/Kss1p (Lee & Elion 1999; Zhou et al 1993). The two known substrates for Fus3p/Kss1p phosphorylation are Ste12p and Far1p. Ste12p, a transcription activator, activates a number of genes that are involved in mating functions (e.g. agglutination, projection formation, cell fusion) (Dolan et al 1989; Fields & Herskowitz 1987).

The MAP Kinase Pathway Activates Mating Projection Formation

More interestingly, aside from activating the MAP kinase cascade as above, Ste20p also interacts with Cdc42p (Simon et al 1995; Zhao et al 1995). Cdc42p interacts with Cdc24p to transport Ste20p to the shmoo

tip. Other proteins that are localized to the shmoo tip are actin, Bem1p, Bni1p, Bud6p, Pea2p, Spa2p, and Rom2p (Amberg et al 1997; Evangelista et al 1997; Manning et al 1997; Sheu et al 1998; Valtz & Herskowitz 1996). These proteins are also localized to areas of polarized growth in budding. Mutations in any of these proteins will give rise to defects in mating projection formation (Chenevert et al 1992; Gehrung & Snyder 1990; Manning et al 1997; Read et al 1992). Thus, shmooing and budding share a number of the same components. Major differences between shmooing and budding are site selection, axial budding for haploids, and projection toward to the pheromone gradient in shmooing.

α-Agglutinin

α-Agglutinin is one of the most studied cell wall genes. α-Agglutinin interacts with **a**-agglutinin to facilitate mating, especially in liquid medium (Hauser & Tanner 1989; Lipke & Kurjan 1992). α-Agglutinin is coded by *SAG1/AGα1*. Sag1p is 650 amino acid residues long. Like a typical GPI-CWP, it has an *N*-terminal secretion signal, a *C*-terminal GPI cell wall anchorage signal, and high serine and threonine content (Lipke et al 1989). As determined by deletion analysis, the *C*-terminal

end, from 326 to 650 is not required for binding activity (Wojciechowicz & Lipke 1989). α-Agglutinin has been proposed to belong to the immunoglobulin superfamily. The secondary structure is known to be largely β-sheet, a structure that is consistent with the Ig super-family (Lipke et al 1995).

a-**Agglutinin**

a-agglutinin consists of two subunits encoded by the *AGA1* and *AGA2* genes. *AGA1* has been isolated by screening **a**-specific agglutination defective mutants (Roy et al 1991). These *aga1* mutants mated efficiently on solid media, but not in liquid media. As in the case of α-agglutinin, **a**-agglutinin is not an absolute requirement for mating, but does facilitate mating, especially in liquid media (Roy et al 1991). The *AGA1* gene codes for a protein of 725 amino acids with a rich serine and threonine content. A hydrophobic signal for secretion was found at the *N*-terminus. At the *C*-terminus, another hydrophobic signal is thought to initiate attachment to a glycosyl phosphatidylinositol anchor. The fact that *aga1* mutants secrete active **a**-agglutinins supports the idea that the *AGA1* gene product is responsible for the attachment of the binding subunit of **a**-agglutinin to the cell wall (Roy et al 1991). Interestingly,

AGA1 transcripts were detected in both **a** and α cells when induced by appropriate pheromones.

AGA2 codes for the binding subunit of the **a**-agglutinin (Cappellaro et al 1991). However, the Aga2p secreted into the medium from the *aga1* mutant had low specific activity and proved difficult to purify (M. Shen, personnal commuication). When *AGA1* lacking GPI anchor was co-expressed with *AGA2*, the specific activity of Aga2p increased by fifty fold, possibly by stablizing the proper tertiary structure for binding to α-agglutinin (L. Wang, personnal communication).

Fusion

An overview of fusion can be described as follows. Haploid cells of opposite mating come together in close proximity. The cells signal each other and prepare for mating. Mating projections form in the direction where the mating partner is located (Jackson et al 1991). The walls of the mating cells come into contact (Shimoda & Yanagishima 1975). The walls are degraded while maintaining osmotic stability (Philips & Herskowitz 1997). Membranes are fused (Osumi et al 1974). Cytoplasms are mixed (Osumi et al 1974). The nuclei are brought

together and finally fused (Osumi et al 1974). Diploidy is established and budding gives rise to diploid progeny.

In the senario described above, nuclear fusion is the event that is best understood, whereas cell fusion or the cytoplasmic mixing event, plasmogamy, is much less well studied (Marsh & Rose 1997). Many mating mutants are defective in nuclear fusion or in the machinery that brings the nuclei together. Most of these mutants have defects in their cytoskeletons, which are complex organelles. In addition, mutations in proteins that are responsible for the establishment of polarity are often isolated as mating mutants. Once again, it would appear that the mechanisms of budding and mating projection formation share many of the same components. Virtually, all mutations in mating projections result in defects in mating.

The Mating-Related Cell Membrane Proteins

The integral proteins in the cell membrane that are responsible for plasma membrane fusion remain largely elusive (Marsh & Rose 1997). As of yet, no mating defective mutant has been isolated with a defective gene for a membrane protein. It is possible that these proteins are

redundant and overlapping in function, which would make their identification difficult.

The Mating-Related Cell Wall Proteins

Clearly, changes in cell wall structure must play a significant role in the mating process. Yet, as L. Marsh and M. Rose have noted, "It is perphaps surprising that no cell wall synthesis enzymes have been directly implicated in the cell wall remodeling steps of cell fusion" (Marsh & Rose 1997). Nonetheless, recent research has begun to shed some light on the roles of the cell wall in mating.

There is little doubt that the process of cell wall fusion, during which cell walls must open and reseal, must be carefully choreographed so that the cells maintain osmotic stability (Philips & Herskowitz 1997). It follows that there must be a number of cell wall proteins, which have essential mating-specific functions. However, in the many experiments in which sterile mutants have been examined, few have been identified as cell wall-related. Most sterile mutants discovered to date have been related to signal transduction, establishment of polarized growth, or nuclear fusion.

The Pheromone Responsive Cell Wall Proteins

Induction of haploid cells by pheromone results in a number of cell wall changes. Lipke et al. and Crandall et al. have shown that pheromone-induced cells are more sensitive to Zymolyase lysis (Crandall et al 1977; Lipke et al 1976). The shmoo tips of induced cells appear to be fuzzier and there is a reduction of mannosylation of mannan. Chitin is reported to deposit on the necks of shmoos (Chuang & Schekman 1996). In addition, induced cells were more sensitive to glucanases, indicating cell wall changes. In the more than twenty years since these studies were originally published, further progress in the understanding of mating-related cell wall proteins has been slow.

Some of the best-studied mating related genes of the cell wall are the agglutinins. It is known that opposite mating-type cells adhere to each other during mating because of the agglutinins. However, the role of the agglutinins is essential for mating only in liquid media. On solid media, mating can occur without agglutinins, albeit at lower frequency (Lipke & Kurjan 1992).

CHS1 and *CHS3*, the chitin biosynthesis genes, are up-regulated by pheromones (Shaw et al 1991). *GFA1/GCN1*, which is required for the synthesis of hexosamine precursors of chitin, is also inducible by pheromones (Watzele & Tanner 1989). This is consistent with the observation that chitin is deposited on the shmoo neck during mating. However, *chs3* disruptants mate normally (Shaw et al 1991). *FKS2*, a homolog of the putative glucan synthase *FKS1*, is inducible by pheromone treatment (Mazur et al 1995). Therefore, the *FKS2* gene may be involved in cell wall remodeling during mating. Interestingly, Fks2p requires Ca^{++} influx and calcineurin to synthesize glucan. In addition, *FKS2* is also under the control of protein kinase C. The observation that *fks1 fks2* double mutants are nonviable and *fks1* deletion is viable shows that the *FKS2* gene compensates for the loss of *FKS1*. It further indicates that Fks2p is involved in important cellular processes outside of mating.

The Recent Progress in Mating Related Cell Wall Proteins

Additional progress has been made in understanding cell wall genes related to fusion. Cappellaro et al. have isolated seven cell wall proteins and characterized three (Cappellaro et al 1998). All three proteins are

potential glucanases. Again, single disruption of any of the three genes individually showed no apparent phenotype. In either mating type, the double knockout of *SCW4* and the homologous gene *SCW10* results in slower growth, increased release of proteins from intact cells by DTT, and sharply decreased mating efficiency. It has been suggested that these genes may be endoglucanases or transglucosidases. The authors, however, failed in an attempt to demonstrate glucanase activity *in-vitro*, making it more likely that these genes are transglucosidases. Double knockout mutants were shown to have a decrease in the amount of laminarinase-extractable proteins. In addition, an increased amount of protein is found in the supernatants of the growth culture. These observations suggest these two proteins may have a role in the anchoring of proteins to β1-6 glucan. Such anchoring would, at some point, require transglucosidase activity. The disruption of *BGL2*, an endoglucanase, in the *scw4 scw10* double mutants led to the restoration of the wild type phenotype. The authors postulated that the *BGL2* gene product degrades the glucan polymers, leading to an unstable cell wall. A stable cell wall is a prerequisite for mating. The Scw4p and Scw10p are the first cell wall specific proteins shown to be involved in mating.

The Post-Genomic Approach

Now that the entire genome of *S. cerevisiae* has been sequenced, systematic disruption of cell wall genes, in singles or in multiples, can be done easily and rapidly. As previously mentioned, a number of reports have shown that many cell wall single gene disruptions show no specific phenotype. One interpretation of these results is that many cell wall genes are redundant. This would explain the absence of cell wall specific genes in sterile mutant hunts, as described earlier. Although multiple gene disruptions have been used in recent experiments, this approach has its limitations. The work done by Mrsa and Tanner is a good example (Mrsa & Tanner 1999). The *CCW5, CCW6, CCW7*, and *CCW8* genes were studied in this paper. Single disruption showed no apparent phenotype. When all four genes were disrupted, nonspecific phenotypes, such as slow growth, aberrant morphology, sensitivity to wall binding chemical dyes (Calcoflour White or Congo Red), and mating defects were observed (Mrsa & Tanner 1999). These multiple phenotypes associated with multiple disruptions allow, at best, a vague understanding of the functions of these gene products. Random disruptions of putative cell-wall genes have proven to be a relatively inefficient method for discovering those cell wall proteins involved in

mating. However, the availability of the entire yeast genome makes it possible to screen selectively for genes that have sequences indicating that they are regulated by pheromones. Since pheromones induce mating- related functions, such genes are more likely to reveal mating related phenotypes, even in single-disruption experiments. This was the approach used in the experiments that follow.

The *FIG2* Gene

FIG2/YCR089W, a putative pheromone-regulated gene, was chosen as the subject of this dissertation research. When experiments began (1993), there were no published reports of studies on this gene, other than as an unknown open reading frame in chromosome III. Whether or not other laboratories might be carrying out coincident studies was unknown until 1998, when a paper was published describing the partial characterization of *FIG2* (Erdman et al 1998).

In regard to *FIG2*, Erdman et al. examined potential mating functions almost exclusively. This dissertation, on the other hand, investigates a number of different potential cell wall related functions for *FIG2*, of which, mating is only one. As a consequence of this, although a few of

the findings of Erdman et al. either overlap or augment those found in this dissertation, the two studies are quite distinct.

Erdman et al. carried-out a large-scale transposon tagging screen to identify pheromone regulated genes. Of the 189 genes identified in the screen, a total of 20 were either novel genes, or not yet identified as pheromone regulated. Four of these genes, *FIG1*, *FIG2*, *KAR5/FIG3* and *FIG4* were chosen for partial characterization. The results obtained for *FIG2* are described below.

Erdman et al. constructed *fig2::lacZ* mutants in which they observed no differences in viability, cell cycle arrest, adaptation, or pheromone production. They reported that, in the presence of isotropic α-factor, *fig2Δ* **a** cells exhibited no change in the morphology of mating projections as compared to wild type **a** cells. Interestingly though, they describe "hyperpolarization" in some cells in mating cultures. This hyperpolarization is represented by a rather subjective observation of more distinct projection formation in some cells. Further, these cells represent a very selected sample of only a few cells from a large field of

non-distinctive cells. In addition, the mating type of these few hyperpolarized cells cannot be determined.

Erdman et al. conducted a number of experiments to determine possible mating phenotypes for *fig2* mutants. It was determined the mating efficiency of mutant cells could be either better or worse than wild type, depending upon type of medium and temperature. In liquid medium at 30^0C, the mating efficiency of *fig2Δ* **a** cells was 3 fold higher than wild type in unilateral (*fig2Δ* **a** cell x wild type α cell) matings. In bilateral (*fig2Δ* X *fig2Δ*) matings, the efficiency was 7 fold higher. Interestingly, when mating was carried out on filters, as opposed to in liquid, bilateral mating efficiency was about 7 fold lower than wild type. When mating in liquid medium took place at 16^0C, unilateral mating occurred at a rate 5 fold less than wild type, and bilateral mating 18 fold less than wild type. The mating efficiency of mating in bilateral wild type crosses, unilateral *fig2Δ* **a** cell crosses with wild type α and in bilateral *fig2Δ* mutant crosses was significantly reduced when mating occurred in the presence of Polymixin B, EGTA, or α factor. In each of these crosses, the presence of PEG led to significant increases in mating efficiency.

These results are neither unexpected nor profound. It is well known that PEG is a potent enhancer of mating efficiency (Sipiczki & Ferenczy 1977). PEG also mediates a potent enhancement of the transformation of yeast or *E. coli* by plasmids (Bruschi et al 1987) (Brzobohaty & Kovac 1986) (Klebe et al 1983). The addition of exogenous α-factor has already been described as reducing mating efficiency, presumably by destroying the pheromone gradient in the mating mixture (Udden & Finkelstein 1978). EDTA is known to bind to Ca^{++} ions, which, in turn, are known to be important to many intercellular interactions (Prasad & Rosoff 1992) (Ohsumi & Anraku 1985). Polymyxin B, of course, is well known as a membrane-disrupting agent (Boguslawski 1986). Not surprisingly, except for PEG, Erdman et al. found that all of these chemicals reduced mating.

When these agents were present in various mutant mating mixtures (i.e. *fig1*, *fig2*, *fig3*, and *fig4* of Erdman et al.), an enhancement of the effect of each was observed. That is, PEG was more potent in its stimulation of mating, and the other reagents were more potent mating inhibitors. This was true for both unilateral and bilateral mutant mating mixtures. Erdman et al. attempted to correlate potential functions for these mutants

with the results of the chemical inhibitions/enhancement of mating. However, they report the results from only one unilateral mixture (*fig2Δ* **a** cells x wt α cells).

By means of a qualitative agglutination assay, the details of which were not reported, these authors observed increased agglutination in a single tube experiment involving a bilateral agglutination of *fig2* mutant cells. They also mention increased agglutination in a unilateral experiment for which the results are not shown, and the mutant mating type is not specified. The authors then propose that the increased mating efficiencies seen in liquid medium might be due to increased agglutination.

Erdman et al conducted a few experiments in order to determine the possible structural role, and subcellular localization of Fig2p. By microscopic examination of mating pairs and zygote formation, they suggested that *fig2Δ* mutants form abnormally narrow conjugation bridges during mating. They imply that this indicates that *FIG2* may function in the development and maintenance of a normal conjugation

bridge. They also constructed a *FIG2* β-gal fusion protein. This construct localized to the cell periphery via indirect fluorescence.

Materials and Methods

Strains and Plasmids

Yeast strains are listed in Table 1. *Escherichia coli* strains used in this study are listed in Table 2. All yeast and E. coli strains were stored respectively in YEPD and LB media containing 15% glycerol at -70^0C. Yeast and *E. coli* cells were streaked out on to agar plates containing appropriate nutrients every three months. Plasmids used and constructed are listed in Table 3.

Culture Conditions and Media

All *E. coli* with plasmids containing Amp^R markers were maintained in petri dishes containing LB with Ampicillin (100 μg/ml) medium in 2% agar. LB consisted of 1% Bacto tryptone, 1% NaCl, and 0.5% Bacto yeast extracts. When needed, colonies were inoculated in LB or LB-Amp and were grown at 37^0C for 18 hours unless time is otherwise specified. Yeast were maintained in petri dishes containing YEPD (yeast extract, peptone, dextrose) or YNB (yeast nitrogen base)- supplemented with appropriate amino acids in 2% agar at 4^0C. YEPD medium consists of 0.5 % yeast

extract, 1% Bacto peptone, and 2% glucose. Colonies were inoculated into YEPD or YNB supplemented with appropriate amino acids at 30^0C for 18 hours as stock culture. The stock cultures were diluted into fresh media and grown to the appropriate O.D. for the particular experiment. With induction experiments, the haploid cells were grown to mid-log phase in which cells were at 0.3 OD or less. **a** cells were induced with α factor at 40 ng/ml for agglutination assays, and at 400 ng per ml for other inductions. α-cells were induced with **a**-factor at 400 ng/ml in all experiments. The standard time for induction of **a** cells was 30 mins, and for α-cells was1 hour, all at 30^0C with shaking.

Chemicals

All chemicals were reagent grade, from Sigma-Aldrich Chemical Company. Molecular biology reagents for restriction analysis, ligation, and DNA modification were purchased from either Life Technologies or New England Biolab. DNA labeling utilized a Random Priming Kit purchased from Amersham. Total RNA isolation reagent, Trisolve, was purchased from Tropix. The poly-A RNA isolation kit was purchased from Pharmacia. DNA fragment purification was done with Gene Clean from Bio101.

Total DNA Isolation from yeast

The DNA templates for PCR reactions were isolated as follows: 5 ml of *W303-1A* was grown to saturation in YEPD. Cells were centrifuged at 5,000 RPM for 5 minutes in an SS34 rotor and resuspended in 1 ml of water. Cells were transferred to a 1.5 ml microfuge tube and spun for 5 seconds in a Fisher Scientific microcentrifuge. The pellet was resuspended in 1 ml of Sorbitol solution (1 M Sorbitol, 50 mM Tris pH7.5, 10 mM DTT, 0.2 mg/ml Zymolyase 100T), and incubated at 30°C for 60 minutes with gentle rocking. The suspension was then spun for 10 sec. in a microcentrifuge. Cells were resuspended gently in 0.25 ml 50 mM EDTA. An additional 0.25 ml 50 mM EDTA, 0.6% SDS was added and mixed well. The suspension was then heated at 65°C for 15 min after which 0.1 ml 5M KOAc was added. Cells were then spun in the microfuge for 5 min after which 0.5 ml of the supernatant was transferred to a new tube. 0.35 ml of isopropanol was then added and incubated for 5 minutes at room temperature. Tubes were then spun for 2 minutes and the pellets were decanted and drained for 5 minutes. The resulting DNA pellet was dissolved in 0.5 ml of 10 mM Tris (pH8), 1 mM EDTA. The DNA was extracted once with an equal volume of phenol. 0.3 ml of 5 M NH_4 acetate was added and the DNA was precipitated by the addition of 0.5 ml isopropanol. The DNA was pelleted by spinning for 2

minutes in the microcentrifuge, rinsed with 70% ethanol and dried in a vacuum for 10 minutes. The DNA was then redissolved in 50 µl 0.2X TE for 3 hours at room temperature. This resultant DNA was stored at 4^0C indefinitely.

Oligonucleotide Sequences and Syntheses

Oligonucleotides OCJ931 (5' ATG AAC TCA TTT GCG TCA TTA GGT) and OCJ932 (5' TAT TGA GTT TGA AGT CAA AAC ATC) were synthesized by the Hunter College RCMI (Research Center for Minority Institutes) DNA Synthesis and Sequencing Laboratory. OCJ931 is derived from the first 18 nucleotides at the *N* terminus of the *FIG2* gene. OCJ932 complements the non-mRNA strand at position 931 to 954 of *FIG2*. Lyophilized oligonucleotide powders were deprotected by adding an equal volume of concentrated ammonium hydroxide and incubation at 55^0C for 18 hours. PCR primers were purified via NEN NENSORB (New England Nuclear) column using procedures recommended by the manufacturer. Briefly, the column was washed with 10 ml of methanol and further washed with 5 ml of 0.1 M TEAA (Triethylamine acetate), pH 7.0. The column was loaded with oligos in NH_4OH, and washed with 2 ml of 2 % NH_4OH. The column was then washed with 10 ml of acetonitrile/0.1 M TEAA, pH 7.0,

(1:9) to remove failure sequences. The trityl group was then cleaved with 25 ml of 0.5% TFA and the column was neutralized with 10 ml 0.1 M TEAA, pH 7.0. The oligos were eluted with 5 ml of 35% methanol in 5 X 1 ml fractions. The oligos were evaporated in a Speed Vac 18 hours with the heat on.

PCR Procedures: PCRs were performed on a thermocycler manufactured by Coy Instruments. Melting temperatures were calculated using Microsoft's Excel program on a Macintosh computer, model 180, according to the following formula (Sambrook S et al 1989).

DNA/DNA: $T_m = 16.6 * \log (Na^+) + 0.41 * \%GC + 81.5 - 0.62 * \%F - 500/\#BP$

The Tm for OCJ931 is 50 ^{0}C and the Tm for OCJ932 is 41 ^{0}C. The thermocycler was programmed to cycle at 94^{0}C for 30 seconds, 42^{0}C for 30 seconds and 72^{0}C for 1 minute, and the number of cycles was 30. The PCR mix contained 1 μg of yeast total DNA, 0.5 μg each of OCJ931 and OCJ932, 1X buffer that was supplied by Cetus, and 2 units of Taq DNA polymerase.

Screening of *FIG2* from a Yeast Library

A yeast genomic library (2J351) was obtained from Dr. Jean Hirsch of Mount Sinai Medial School. The genomic library was contained in the vector YEp351, which contained the *LEU* marker. The library represents 3.8 X genomes and contains 85% inserts with an average size of 6-8 Kb. It was constructed by cloning a *Sau3A* partial digestion of total yeast genomic DNA into the *BamHI* site in the multiple cloning site of the vector. The library is in strain MC 1061, which is not α-complementing for *lacZ*. The library was titrated and plated to 2000 cells per LB plate supplemented with 100 μg /ml Amphicillin. Colonies were grown to pin point size on the plate. Cells were replica plated on Nylon membranes (Nytran circles) by the following method. Nytran circles were laid on each of the plates. Orientation markers were marked on the filter and on the plate with a needle and India ink. After 30 seconds, the filters were peeled off the plate. Filters were sequentially transferred, colony side up, to paper towels saturated with 0.5 M NaOH, 1 M Tris pH 7.5-8.0, 1 M Tris/1.5 M NaCl pH7.5. Lysis took place in 5 minutes on each bed of filters. The filters were soaked briefly in 2X SSPE (sodium sulfate phosphate EDTA) and baked at 80^0C for 30 minutes in a vacuum oven. Duplicate filters were prepared from all plates to be screened.

Labeling PCR Product with [^{32}P]-dCTP

A Random Priming kit from Boehringer Mannheim was used according to the manufacturer's instructions.

5 µl of DNA (25 ng) was added to 5 µl of water and boiled for 2 minutes. The denatured DNA was placed on ice for 5 minutes. To the DNA, 3 µl of dNTP, 2 µl of Reaction mix, and 5 µl of [^{32}P]-dCTP were added and incubated for 30 minutes. The labeled probes were added without purification.

Prehybridization Conditions

60 ml of the prehybridization solution was prepared by mixing 15 ml of 5X SSPE, 6 ml of 50X Denhardt's solution, 0.6 ml of 100 µg/ml denatured Salmon sperm DNA, and 38 ml of water. 20 (set A) filters were placed in one bag and sealed while the duplicate 20 (set B) filters were in another bag. The nylon filters were hybridized at 42^{0}C for 18 hours.

Hybridization Conditions

Prehybridization solutions were removed from the plastic bags and replaced by hybridization solution of the following composition: 20 ml of 50 % Formamide, 10 ml of 5X SSPE, 0.8 ml of 50X Denhardt's solution, 0.4 ml of 100 μg/ml Salmon Sperm DNA, 1.6 ml of 10% SDS, 10^6 CPM probe and 7.2 ml of water. The probes were hybridized at 42^0C for 18 hours. After removal of filters from the bags, the filters were washed twice with 2X SSPE, 0.1% SDS for 15 minutes at room temperature. The filters were further washed with 0.2 X SSPE, 0.1 % SDS at 42^0C for 1 hour. After blotting dry and wrapping in Saran Wrap, the filters were then put into cassettes with X ray film and an intensifying screen and exposed for 18 hours. Films were then matched to the master plate to identify the *E. coli* colonies.

Small *E. coli* Plasmid Preparation

E. coli cells were grown overnight to saturation in 1 ml of LB broth with 100 μg /ml of Amphicillin. Cells were spun 3 minutes in an Eppendorf centrifuge. Cells were resuspended in 100 μL of 50 mM glucose, 25 mM Tris pH 8.0, 10 mM EDTA. 200 μl of 0.1% SDS, 0.2 N NaOH was added for 5 minutes to lyse the cells. 150 μl of KOAc pH 4.8 was added to

neutralize the lysis solutions. Precipitates were removed by spinning in a microcentrifuge for 5 minutes. 400 µl of this DNA solution was added to a new tube containing 280 µl of isopropanol. After 5 minutes incubation at room temperature, the tubes were spun for 5 minutes in a microcentrifuge. The DNA pellets were washed with 1 ml of 70% ethanol and dried under vacuum. The plasmids were redissolved in 50 µl of TE. 1 µl of plasmid DNA was used for PCR as described above to positively identify the clones.

Large Scale Plasmid Preparation

Single colonies of cells were grown to saturation in 500 ml of LB with Ampicillin (100 µg /ml). Cells were spun at 5000 RPM for 5 minutes in a GSA rotor. Cells were resuspended in 18 ml 50 mM glucose, 25 mM Tris pH 8.0, 10 mM EDTA. 40 ml of 0.1% SDS, 0.2 N NaOH was added for 5 minutes to lyse the cells. 20 ml of 5 M KOAc pH 4.8 was added to neutralize the lysis solutions. Precipitates were removed by spinning in a centrifuge for 15 minutes. The solution was filtered into a new bottle, 50 ml of cold isopropanol was added, and the solution then placed on ice for 10 minutes. DNA was pelleted at 8000 RPM for 15 min. The supernatant was discarded and the pellet was dried under vacuum. DNA was resuspended in 11 ml of TE and transferred to a 15 ml tube. 12 g of CsCl and 1 ml of

ethithium bromide (10mg/ml) were added. Debris was removed by spinning in a tabletop centrifuge for 2 minutes. The supernatant was transferred to a quick seal centrifuge tube and the plasmid was banded by ultracentrifugation at 65,000 RPM for 18 hours. The bottom plasmid band was extracted with a 3 ml syringe and 18g needle. Ethidium bromide was removed by extraction with equal volumes of isopropanol five times. DNA was precipitated by two volumes of water, and 6 volumes of ethanol. After 10 minutes incubation on ice, this DNA was pelleted at 7000 RPM for 10 minutes. The pellet was washed with 70 % ethanol, dried in a vacuum, and resuspended in 0.5 ml of TE. The concentration of DNA was measured by UV absorbance at 260 nM. It was assumed that 1 absorbance unit represented 50 μg per ml.

DNA Sequencing

The 5' end and the 3' end of the inserts of positive library clones were determined by DNA sequencing. Primers were purchased from Keystone DNA Synthesis laboratory. The primer used to determine the 5' end was Universal primer that was supplied with the DNA sequencing kit and the primer used to determine the 3 ' end was OCJ934 (5' ACACTTTATGCTTCCGGC3'). A Sequenase Kit was purchased from United States Biochemical. Protocols for DNA sequencing were those

recommended by the manufacturer. 4 μg of DNA was denatured in 0.02 M NaOH at 37^{0}C for 30 minutes. DNA was precipitated by 0.4 volumes of 5M ammonium acetate pH 7.5 and 4 volumes of ethanol on ice for 10 minutes. The pellet was spun for 5 minutes, washed with 70% ethanol, dried under vacuum, and redissolved in 7 μl of water. Annealing of template to the primers was done by mixing 1 μl of primer (0.03 OD/ml), 2 μl Sequenase Buffer, DNA 1.5 μg and 7 μl of water. Tubes were incubated at 65^{0}C for 2 minutes and cooled to room temperature over 30 minutes. The labeling mix (dGTP) was diluted 10 fold with distilled water. Sequenase was diluted 1: 8 with cold TE. To 10 μl template-primer were added the following: 1 μl of DTT (0.1M), 2 μl of Diluted Labeling Mix, 0.5 μl of ^{35}S ATP, and 2 μl of diluted Sequenase. 2.5 μl of ddNTP Termination mix was placed into 4 separate tubes, ddA, ddC, ddG, and ddT respectively. 3.5 μl of template-primer mix were added to each termination mix and incubated at 37^{0}C for 10 minutes. 4 μl of dye was added to stop the reactions.

DNA Sequence Analysis by Computer

DNA sequences were determined via GCG program on a minivax or SGI computer through the computer network at Hunter College.

Construction of p102

In order to maximize the unique restriction sites in the *FIG2* open reading frame of p101, the yeast DNA from p101 was subcloned into a pUC18 vector which is smaller than the YEp351 vector. p101 was digested with *SmaI* and *SphI* as recommended by the manufacturer. pUC18 was also digested with *SmaI* and *SphI*. The digested material was loaded on 0.7% agarose in 1X TAE buffer. The 5 Kb fragment containing the yeast insert from p101 and 2.8 Kb pUC18 were excised from the agarose. The bands were purified by GeneClean (purchased from Bio101). Briefly, NaI solution (3 volumes) was added to each gel slice. The band was incubated at 45^0C for 5 minutes to melt the gel. 5 µl of glass milk was added to the DNA and incubated at 40C for 30 minutes. The glass milk was spun and washed three times with WASH solution. The glass milk was resuspended in 50 µl of water and eluted at 45^0C for 10 minutes. DNA concentration was determined by loading 3 µl of elutate on a 0.1% agarose gel containing ethidium bromide (1 µg /ml).

The two fragments were ligated in the following mix: 100 ng of vector DNA, 100 ng of insert DNA, 2 µl of 10X ligation buffer, 2 Weiss Units of ligase and sufficient water to make a final volume of 20 µl. The ligation mix

was incubated at 16^{0}C for 18 hours. The ligation mix was then transformed into E. coli JM109 competent cells as follows. 200 µl of competent cells were thawed on ice for 10 minutes. 5 µl of ligation mix was added to the cells, and incubation continued on ice for 3 minutes. Cells were heat-shocked at 42^{0}C for 2 minutes and returned to ice for 2 minutes. 500 µl of LB was added and the cells were incubated at 37^{0}C for 1 hour to recover and to initiate of growth. 200 µl of cells were plated on LB plates containing 100 µg per ml Ampicillin. Plates were incubated at 37^{0}C for 18 hours until colonies appeared. Individual colonies were grown in 2 ml of LB broth with Ampicillin. Mini plasmid preparation was done as described above. Positive clones were identified by *SmaI*, *SphI* restriction analysis.

Construction of p103

p102 was digested with *XcmI* and *Eco47III* to delete 35 base pairs within the open reading frame of *FIG2* in p102. YEp24 was digested with *HindIII* to isolate the 1.1 Kb *URA3* fragment. Both the digested p102 and *URA3* were blunted by PCR reaction as follows. 1 µg of DNA was added to 5 µl of 10X PCR buffer (supplied by the manufacturer), 5 µl of 2 mM dATP, dCTP, dTTP and dGTP and 1 µl (1 unit) of Taq polymerase. The mix was incubated at 55^{0}C for 10 minutes. The fragments were purified by 0.7%

agarose gel to remove all the unreacted nucleotides. Ligation of the two fragments and transformation were done as described above. Positive clones were identified by restriction analysis by cutting with *EcoRI* restriction enzyme.

Disruption of *FIG2* in Yeast

30 µg of the disruption plasmid p103 was digested with *SalI* to release yeast DNA from the vector. Yeast strains *W303-1A*, *W303-1B*, and *W303-A/B* were made competent as follows. 1 drop of saturated starter culture was inoculated into 100 ml YEPD. Cells were grown 12 – 15 hours at 30^0C to mid-log phase ($0.2x10^7$ to $5x10^7$ cells/ml, measured by A_{610}). Cells were spun at 4000 RPM (SS34) for 5 minutes. Cells were washed in 0.2 volume of TE/LiAc. Cells were resuspended cells in 0.2 volume of TE/LiAc and incubated at 30^0C for 60 minutes. Cells were resuspended at 0.02 volumes of TE/LiAc. To 50 µl cells, 10 µg DNA was added and incubation continued at room temperature for 60 minutes. 0.5 ml 40% PEG was added, followed immediately by gentle vortexing. Cells were further incubated 60 minutes at room temperature. Heat shock was done at 42^0C for 5 minutes. Cells were spun at 2000 RPM for 3 minutes and resuspended in 0.2 ml TE. Synthetic, complete plates without uracil were used for selection.

Analysis of Yeast *fig2Δ* Disruptants

Yeast colonies were grown in 5 ml of YNB without uracil for 24 hours to saturation. Total yeast genomic DNA was isolated as described above. 20 µl of DNA was digested with HindIII and RNase and run on a 1% agarose gel in 1X TAE. DNA was transferred onto 2 pieces of Hybond N nylon papers (Amersham) as follows. The DNA in the gel was denatured in 5 volumes of 0.5 N NaOH. The gel was transferred to 5 volumes of 10 SSPE to neutralize the alkali. Two pieces of HyBond N nylon paper were cut to the size of the gel and soaked in 10X SSPE solution. The papers were placed above and below the gel. A one-inch thickness of 3 MM papers was soaked in 10X SSPE and placed on either side of the nylon paper. Two inches of dry paper towel were added to the top of 3 MM filter papers. DNA was allowed to transfer for 4 hours. The nylons were rinsed in 1X SSPE and dried in a vacuum oven at 80^0C for 30 minutes. The 960 bp PCR product from *FIG2* gene and 1.1 Kb *URA3* DNA was labeled with ^{32}P by random priming as described above. The nylons were then prehybridididized and hybridized as described above. The nylons were put into a cassette and exposed to X-ray film overnight.

Isolation of *FIG2* C-terminal DNA Fragment

FIG2 was amplified by PCR reaction using a *S. cerevisiae* genomic template. Due to the large size of the PCR product, two amplifications were attempted. The first attempted product contained the entire *FIG2* coding sequence and the entire upstream sequence. This amplification failed. The second amplification yielded a PCR product that contained the entire *FIG2* coding sequence and 200 bp of the upstream sequence. This amplified product was inserted into pPCRII (purchased from Invitrogen) at the AT cloning site and renamed pP2. Sequence analysis showed the *AgeI* and *NotI* sites were unique and would excise a fragment containing two thirds of the coding sequence in addition to a few hundred base pairs 3' after the translation stop codon. p102 was isolated from the library as previously described. This plasmid contained the entire upstream sequence in addition to 1 kb of the *FIG2* coding sequence. *SalI* and *AgeI* were unique restriction sites that would excise the entire upstream sequence and the 5' end of the ORF of *FIG2*. The yeast shuttle plasmids pRS313 (containing *HIS3* and *CEN*) and pRS423 (containing *HIS3* and 2u) were used for single and multicopy expression respectively. The expression plasmids were cut with *SalI* and *NotI*. The *SalI*, *AgeI* restricted N terminal fragment and the *AgeI*,

NotI C-terminal fragment were three-way ligated into the expressions plasmids.

Construction of Green Fluorescence Protein Tagged *FIG2*

The pEGFP-C1 plasmid was purchased from Clontech. The fluorescence of the pEGFP-C1 protein was 35 times stronger than the wild type green fluorescence protein (GFP). The polycloning sites were inserted between the last amino acid residue and the stop codon. Two oligonucleotides, FEGFP and BEGFP, were synthesized to perform PCR using pEGFP-C1 as template. The sequence of FEGFP was 5' GCGCC**GCAATG**TTCC ATG GTG AGC AAG GGC GAG, where the underlined was the beginning of GFP coding sequence. A *BsrD1* site (in bold) was engineering at the 5' end of the oligo to be fused into the *BsgI* site of the *FIG2* coding sequence. The spacing between the ATG start codon and the engineered site was designed so that the fusion protein would be in frame. The sequence of *BEGFP* was 5' GCGC**GACGTC**TT AGC TTG AGC TCG AGA TCT GAG, where the underlined sequence was the coding sequence of the 3' end of *EGFP*. An *AatII* site (in bold) was engineered between the coding sequence and the GC clamp which simply allowed greater cutting efficiency. The 3' end of *EGFP* was fused to the *AatII* site of *FIG2* in frame. PCR was performed using a

PCR kit purchased from Boehringer Mannheim and was carried out according to the manufacturer's instructions. The cycling conditions were 94^0C for 20 seconds, 49^0C for 30 seconds, and 68^0C for 2 mins. 25 cycles were performed. The PCR product was digested with *BsrD1* and *AatII* and purified with gene clean to remove the trimmed ends. YCp*FIG2* and YEp*FIG2* were digested with *BsgI* and *AatII* to remove part of the internal coding sequence and ligated with PCR products. The resulting plasmids were transformed into wild type *W303* haploids and diploids. The transformation procedure was described previously (Ito et al 1983). pRS313, the parent plasmid without insert, was also transformed as control.

Northern Analysis

Total RNA was isolated by Trisolve Reagent. 5 ml of cells were grown to log phase. Cells were centrifuged in a clinical centrifuge for 5 minutes at 5000 rpm. The volume of the cell pellet was estimated visually, and an equal volume of Trisolve reagent was added. An equal amount of acid-washed glass beads (425-625 micron) was added to the suspension. The mixture was vortexed 6 times at 30 seconds intervals. A needle was used to puncture a hole at the bottom of the tube, and the liquid contents drained into a larger tube. The liquid was spun at 5,000 RPM for 5 minutes. The upper

phase was aspirated and mixed with an equal volume of isopropanol to precipitate RNA. The RNA was then dried lightly under vacuum, and dissolved in 100 µl of TE. The RNA was stored at -70^0 C. Formaldehyde gels were prepared as in Sambrook et al. (Sambrook et al 1989). 20 µg of RNA was loaded for routine analysis. 100 µg of RNA was loaded for analysis of low-level constitutive expression of *FIG2*. The gel was washed and transferred to Hybond N nylon paper according to the manufacturer's instructions. The RNA was crossed linked to the Nylon by a UV Cross Linker (Stratagene) in automatic mode. The nylon paper was prehybridized and hybridized as previously described. ^{32}P labeled probes were made using an Amersham Mega Prime kit available commercially (Amersham). Normally, 10^6 cpm per ml was used for hybridization, which was carried out overnight. For low expression, 10^8 cpm per ml was used instead. The blots were washed with 0.2X SSC, 1% SDS. Films were exposed between 20 minutes and10 days based on Geiger counter readings.

Agglutination Assay

Agglutination between haploid a and α cells was measured as previously described (Terrance & Lipke 1981). Briefly, a and α cells were grown separately in YNB at 30^{0}C to an optical density between 0.1 and 0.2 (A660).

Cells were washed and resuspended in fresh medium. Cells to be induced were then incubated at 30^0C with pheromone from the opposite mating type (40ng/ml) for up to one hour. Cells were then harvested by centrifugation, washed twice with distilled water, and adjusted to 0.3 (A660) in 0.1 M NaAc pH5.0 containing 10 μg /ml cyclohexamide. Aliquots of cells (1.5 ml) of each mating type were mixed in 13 X 100 test tubes. Control tubes contained 3 ml of either **a** cells or α cells alone. Cells were spun in a table top centrifuge at 900 rpm to lightly compact the cells. Cells were then resuspended in a controlled fashion, using a homemade cell resuspender consisting of a paddle spinning at 1000 rpm.via a constant speed device. Each tube was resuspended for 10 sec, and then allowed to settle for 20 min at room temperature. Cell density in each tube was then read by light scattering at 660 nM. Agglutinated cells settle to the bottom and form suspended aggregates that scatter light less than unagglutinated cells. The agglutination index was calculated according to the following formula:

$$A.I. = 1-((2 \text{ X } OD_{(a+\alpha)})/(OD_a + OD_\alpha))$$

Liquid Mating Assay

Tester mating strains were N435-1A (*MAT**a** his7 lys7(ts) met6 arg1 gal4 MAL2 SUC*) and N435-2A (*MATα his7 lys7(ts) met6 arg1 gal4 MAL2 SUC*). **a** and α cells were grown in YEPD at 30^0C to 0.3 O.D. 1.0 ml of cell suspension of each mating type was placed in a 50 ml sterile Corning tube. Cells were shaken at 300 RPM at 30^0C for 4 hours unless otherwise specified. Cells were then collected and washed with 1 ml of water to remove growth media. Cells were diluted to 10^5, 10^4, 10^3 cells per ml. 100 µl of cells at 10^5 and 10^4 cells per ml. were plated on minimal plates in triplicate in order to select diploid cells. 100 µl of cells at 10^4 and 10^3 cells per ml were plated on YNB supplemented with adenine, leucine, uracil, tryptophan and hisitine to select for both the diploids and *W303*. Plates were grown for 3 days before scoring. Mating Efficiency was calculated as follows:

M.E.= number of diploid / (number of diploid + *W303* haploids)

Solid Phase Mating Assay

Strains used in solid mating experiments were identical to those used in the liquid experiments. Cells of opposite mating type were grown in appropriate

media to between 0.1 to 0.3 O.D. A ratio of 1.5 to 1 of tester strains to *W303* with different *FIG2* gene dosages were mixed and vacuum filtered onto nitrocellulose paper. Total cells per filter were always maintained at 10^7 cells/filter to allow close contact. The filters were placed on a YEPD plate at 30^0C for 2 or 4 hours. The cells on the filters were resuspended in 10 ml of sterile water and diluted to 1 X 10^3 and 1 X 10^4 cells per ml. 100 µl each of the dilution was plated in triplicate on YNB minimal plates to detect diploids and on YNB supplemented with with adenine, leucine, tryptophan and hisitine for diploids and *W303* haploids. Mating efficiency was calculated as above.

Spheroplast Formation Assay

A single colony of cells was inoculated into YEPD or YNB with appropriate amino acids overnight at 30^0C. Aliquots of 100 µl (for YNB) or 30 µL (for YEPD) of cells were inoculated into 100 ml of fresh YNB or YEPD media respectively. Cells were grown at 30^0C unless otherwise specified for 18 hours to reach 0.3 OD at 660 nM. Cells were collected by centrifugation at 4000 RPM for 5 minutes, and washed with 25 ml of water. Approximately 40 ml of lysis buffer (100 mM Citrate pH5.0, 10 mM EDTA) was added to the cells. The final OD of the cells was adjusted with buffer to

0.6. Cell suspensions, 3 ml each, in triplicate, were placed in 100 X 13 mm test tubes. Fresh Zymolyase was prepared at 10 mg/ml. 30 μL was added to each cell suspension. Tubes were read at 660nm at three or five minute intervals.

RNA Protection Assay (RPA)

RPA is a radio-labeled method used to detect the presence of RNA. RPA's differ from Northern blots in that they offer greater sensitivity in detecting mRNA. From previous experiments, it was known that the constitutive transcription of *FIG2* is low. Therefore, I employed RPA to detect the transcription levels of *FIG2* under conditions in which cells were uninduced and induced by pheromone. One of the findings in this study is that agglutination decreased in α-cells in which *FIG2* was overexpressed. Likewise, α-cells containing a defective copy of *FIG2* hyperagglutinate. One of the possible mechanisms that can explain the inverse relationship of agglutination in α-cells and *FIG2* expression is that the transcription of α-agglutinin is repressed by the *FIG2* gene products. Three probes, Act1, Sag1 and Fig2 were prepared to quantitate the transcription levels of actin, α-agglutinin, and *FIG2* respectively. Actin is considered to be a household gene, and its transcription should not be altered by pheromone treatment.

Therefore, the level of actin transcripts can be considered as control for the amount of mRNA isolated. The *FIG2* probe should allow detection of *FIG2* transcripts under induced and uninduced conditions. The transcription level of α-agglutinin would be determined in the presence of normal expression of *FIG2* versus high expression of *FIG2*.

Probe Design: The sequence of T3 promotor is ATT AAC CCT CAC TAA AGG GAC. In the presence of ATP, CTP, GTP and radiolabeled UTP, proper templates with a T3 promotor sequence, and T3 RNA polymerase, a radiolabeled RNA can be transcribed.

A pair of primers was selected by computer using *FIG2* as template. The sequence of *FIG2-1* is CTC ATT TGC GTC ATT AGG TCT G, and the Tm of this oligonucleotide is 51.7^{0}C. The sequence of *T3FIG2-2* is ATT AAC CCT CAC TAA AGG GAC TCT TTG GAG ATG TTG AAC CTG (T3 promotor sequence underlined) and the Tm is 50.6. The primers were synthesized by GibcoBRL Company.

Besides the *FIG2* probe, Agα1 and actin probes were prepared in a similar manner. The primer employed for Agα1 was SAG-1 with sequence of CGC CTC GCT TAA TAT AGT CAG CAC. The sequence of the T3SAG-2 was

ATT AAC CCT CAC TAA AGA GAC CCA ATC CGC TAA GGA AAT AGT AGC TG (T3 promotor sequence underlined). The T_m of T3SAG-1 is 56.4 and T_m of T3SAG-2 is 56.7. The *SAG1* PCR product was 362 base pairs. The primers used to generate actin PCR products were Act-1 with sequence of CCT CGT GCT GTC TTC CCA TCT ATC and Act-2 with sequence of ATT AAC CCT CAC TAA AGA GAC TGG AGC TTC AGT CAA AAG AAC AGG. The Tm's of Act-1 and Act-2 are 1 57.9^{0}C and 56.6^{0}C respectively. The length of the ACT1 PCR product was 245 base pairs. The PCR reagent kit was purchased from Boehringer Mannheim. It was used according to the manufacturer's instructions.

The PCR reaction was performed in a Perkin Elmer Model 9600 machine. Mix A and Mix B were mixed immediately prior to the start to obtain the best results. Each cycle was at 94^{0}C 20 seconds, 5^{0}C for 30 seconds and 68^{0}C for 2 minutes. Routinely, reactions continued for 25 cycles. The PCR products were purified on Agarose gels to remove primers, nucleotides, and buffer. The full-length transcripts generated by T3 DNA polymerase are limited to less than 400 base pairs.

Radiolabeled RNA probe: In-vitro transcription was performed using the Ambion Maxiscript kit. The manufacturer's procedure was followed without modification.

Each reaction was composed of 7 μl Distilled water, 1 μl DNA template (1 μg / μl) from the PCR, 2 μl 10 X buffer, 1 μl 10 mM ATP, 1 μl 10 mM GTP, 1 μl 10 mM CTP, 5 μl ^{32}P UTP, and 2 μl T3 DNA polymerase (1U/μl).

The reactions were incubated at room temperature for 2 hours. 1 μl of RNase-free DNase was added to the solution and incubated continued at 37^{0}C for 5 minutes to digest the DNA templates. 5 μl was loaded onto a 5% acrylamide gel for PAGE analysis. The gel was made as follows: 7.2 g Urea, 3 ml 5X TBE, 1.9 ml 40% acryamide (19:1 acryamide:bis), ~10 ml distilled water to make 15 ml, 10 μl 10% APS, and 16 μl TEMED.

PAGE was run at 100 volts for 30 minutes. The gel was exposed to X-ray film for 1 minute. The mobility of band on the developed autoradiographs was measured against an RNA standard. This was an important control, because brand-new Eppendorf tubes will occasionally contain measurable RNase. Once the radiolabeled RNA was proved to be correctly synthesized,

the probes were purified via acryamide gel. Briefly, the entire 90 µl of reaction mix was loaded onto prepratory gels of composition identical to those described above. The desired band was localized by autoradiography, and excised from gel. The excised band was minced to generate a greater surface area. This mince was then eluted with TE.

Poly-A RNA isolation. An RNA isolation kit, Poly (A)PURE, was purchased from Ambion Inc. The manufacturer's procedure was followed, with some modifications. 10 ml cultures of *W303-1A*, *W303-1A*(*YEPFIG2*), *W303-1B* and *W303-1B*(*YEpFIG2*) were grown to 0.3 O.D. Half of each culture was induced with the appropriate pheromone at a concentration of 400 ng/ml for 1 hour. The cells were washed twice with water. 1 ml of lysis solution and 2 ml. of dilution solution were added to each cell suspension. Sufficient glass beads were then added until the meniscus was covered. The cells were vortexed 10 x 1 minute, with 1 minute cooling periods (on ice) between vortexings. The content from one vial of oligo-dT was added to the lysate. The lysate was incubated with oligo dT at room temperature for 1 hour. Lysate was removed by centrifugation in the microcentrifuge. 10 ml of binding buffer was added, and the supernatant was aspirated off after an additional centrifugation. Beads were washed twice with binding buffer and

three times with wash buffer. 200 µl of pre-warmed elution buffer was added to the beads to elute mRNA. The eluate containing the polyA RNA was stored at -70^{0}C. The concentration of RNA was determined by A_{260}. 1 O.D. was equivalent to 40 µg /ml. RNA.

The RPA exhibits extreme sensitivity in the detection of specific mRNA molecules. Briefly, radiolabeled specific mRNA probe was hybridized to total cellular mRNA. The mixture was digested with RNase to remove non-hybridized single stranded RNA. The labeled RNA:RNA* duplex is analyzed by PAGE and detected by autoradiography (ARG).
In a microtube, 10^4 CPM of probe (*FIG2*, *SAG1*, or *ACT1*) was mixed with 0.6 µg of poly (A^+) RNA. In addition to experimental tubes containing labeled probe + yeast RNA, two control tubes were prepared. One of these contained only labeled Fig2 probe. This tube remained undigested and was analyzed via ARG to determine the total probe radiation per lane. The other control contained labeled Fig2 probe and total mouse RNA. This latter control was digested and analyzed via ARG to determine the blank binding value, since any binding of yeast probe to mouse RNA is non-specific. Each mixture was adjusted to 0.5 M with NH_4OAc and 2 volumes of ethanol were added. Tubes were placed on ice for 20 minutes and spun for 10 minutes.

Supernatant was removed and the pellet was air-dried. The pellet was suspended in 20 µl of hybridization buffer supplied by the manufacturer. The samples were heated to 90^0C for 3 minutes and hybridized for 18 hours at 42^0C. Stock RNaseA/RNaseT1 mixture was diluted with RNase digestion buffer in a ratio of 1:100. GlycoBlue, a glycogen carrier, was added to the diluted RNase at a ratio of 1:100. To the all the tubes except for the one control tube, 200 µl of diluted RNase was added. The samples were incubated at 37^0C for 30 minutes. After digestion, 300 µl of inactivation/precipitation solution was added to each of the tubes. Samples were precipitated at -20^0C for 20 minutes and pelleted by centrifugation. The samples were dried and suspended in 20 µl of loading buffer. The samples were loaded onto a urea PAGE gel. The gel was run at 100 volts for 2 hours. The gel was wrapped in plastic sheets and exposed overnight to a Kodak XAR5 film, which was subsequently developed.

Agar Diffusion Assay

W303-1A and *W303-1Afig2Δ* were grown to 1.0 X 10^6 cells per ml in YNB with complete amino acids and YNB without uracil respectively. Identical aliquots of media (90 ml each) containing 2% agar were melted by microwave and cooled to 45^0C in a water bath. 10 ml of the appropriate cell

culture was diluted into each 90 ml of cooled agar. Each of the cooled agars was poured into petri dishes (20 ml. per dish) and set aside until solidified. Drugs samples were dissolved in either water or DMSO at 1 to 10 mg per ml. Duplicate aliquots (20 µl) of each drug were absorbed onto 10 mm Whatman paper circles. The paper circles were then placed on *W303-1A* and *W303-1Afig2Δ* seeded agar plates and incubated at 30^0C overnight. The cells on the seeded agar could be seen as a lawn of confluent cells in the background. Drugs that inhibited growth caused a region of reduced cell density around the paper circles. This zone of clearance was measured (mm.), and recorded as "size of clearance" or "kill zone".

Results

General characterization of *FIG2*

When *Saccharomyces cerevisiae* undergoes mating, haploid cells of opposite mating type, a and α, fuse to form a diploid zygote. In this process, haploid cells make and maintain contact with cells of the opposite mating type through the process of sexual agglutination. The molecule on α cells that is responsible for agglutination is a single polypeptide called α-agglutinin. *Agα1/SAG1*, the gene that encodes for α-agglutinin, was first independently isolated by two different laboratories (Hauser & Tanner 1989; Lipke et al 1989). The corresponding molecule on **a** cells, **a**-agglutinin is composed of two subunits- the binding subunit and the core subunit, which are encoded by the *AGA2* and *AGA1* genes respectively (Cappellaro et al 1994; de Nobel et al 1995; Roy et al 1991). The *AGA2* gene product has been isolated and characterized (Cappellaro et al 1994) (de Nobel et al 1995). Aga2p is a single peptide that is composed of 87 amino acids. The binding of Aga2p to α-agglutinin occurs at the *C*-terminal half. *AGA1* is the core subunit that connects Aga2p to the cell wall.

AGA1 has also been isolated and characterized (Roy et al 1991). Aga1p is a single polypeptide of 725 residues with 2 clusters of 5 cysteine residues that are responsible for binding to Aga2p. In order to find proteins that have high homology to *AGA1*, the program in the Stanford University Saccharomyces Genome Database was used to search for similar sequences (http://genome-www.stanford.edu/saccharomyces/). It was found that *FIG2* has homology to *AGA1* (YNR044) protein, as shown in Table 4. The alignment of *AGA1* and *FIG2/YCR089W* is shown in Fig 1. In the alignment, the beginning of *AGA1* coincides with the middle portion of *FIG2*. The similarity is largely due to the high serine and threonine content. Otherwise, the few short exact matches of *AGA1* and *FIG2* are YTTWCP and TEVCSH motifs, the importance of which is unknown. However, it is notable that the YTTWCP sequence is also found in other cell wall genes (Staab & Sundstrom 1998).

FIG2/YCR089W is an open reading frame located in chromosome III and is 1610 amino acid residues long (Oliver et al 1992). The first 23 amino acids are hydrophobic, which is a signal for secretion into the endoplasmic reticulum. This should result in processing and ultimately, transportation to either the plasma membrane or to the outside of the cells (Erdman et al

1998). The *C*-terminal end of *FIG2* is also hydrophobic, which is likely a signal for the protein to be anchored to the cell wall (Benghezal et al 1995; De Sampaio et al 1999; Hamada et al 1998b). Similar to many other cell wall proteins, *FIG2* has a high serine and threonine content, 26.1% and 18.0% respectively, as shown in Table 5. As shown in Figure 2, there are 17 *N*-glycosylation sites, concentrated mostly around the *N*-terminal half. In addition, there is an identical internal repeat positioned at residues 396 to 472 and 505 to 581. Although it is common for some cell wall proteins to have internal repeats, the significance of these repeat sequences is not known. To make sure that these internal repeats are not a sequencing error made by the genome database, each was partially sequenced to be certain that they are authentic (Data not shown).

Isolation of *FIG2* from Genomic DNA

The DNA probe was prepared by PCR using primers as described in the Materials and Methods section. The DNA probe was labeled with ^{32}P and used to screen 20,000 *E. coli* colonies as described in Materials and Methods. Three positive colonies were identified, one of which (designated p101a) was partially sequenced to identify the cloned sequence (Figure 3). The sequence inserted into p101 was found to contain 4998 base pairs of

yeast DNA. At the 5' end, the cloned sequence contained the *YCR086W* open reading frame, the *YCR087W* open reading frame, *YCR088C* (Actin binding protein), and part of *FIG2*. The promotor of *FIG2* was present, however, only 960 bp of the *FIG2* structural gene was isolated. Although only a portion of the coding sequence was isolated, this was sufficient to create a disruption construct.

Construction of p102a

The backbone of the p101a plasmid contained a yeast *LEU* gene, which might complicate the disruption process by directing a homologous recombination into the *LEU* locus instead of the *FIG2* locus. Therefore, the insert of the library plasmid was transferred to the pUC18 plasmid via the *Sma*I and *SphI* sites. The newly constructed plasmid was designated p102a (Figure 4). The yeast DNA in this plasmid was exclusively the DNA of interest. Further, p102a was smaller than p101a, due to the smaller backbone of the parent plasmid. Therefore, p102a contained more unique restriction sites for cloning.

Construction of p103a

The *URA3* DNA to be inserted in *FIG2* was isolated as a 1.1 kb fragment from *YEp24* by *HindIII* digestion. p102a was digested with *XcmI* and *Eco47III*, deleting 35 base pairs from *FIG2*. The ends of both fragments were filled in by PCR reaction. After ligation and transformation, the proper clone was verified by restriction analysis. The resulting disruption plasmid was called p103a, and is illustrated in Fig 5. After the construct was made and verified by restriction digest, the plasmid was digested with *SalI* to release the integrative fragment. The plasmid was then transformed into *W303-1A*, *W303-1B*, and *W303-A/B*. Individual transformants were isolated and stored at -70^0C.

Southern Analysis of Disruptants

Individual yeast colonies were grown in 5 ml YNB without uracil to saturation. The genomic DNA was purified as described in Materials and Methods. The DNA was further digested with *Hind III* and run on a 0.7% agarose gel to separate the fragments. The DNA was transferred onto nitrocellulose paper. Duplicate gels and transfers were prepared. The nitrocellulose paper was prehybridized and hybridized as described in Materials and Methods. One blot was hybridized to the *FIG2* probe, while the other was to be hybridized to the *URA3* probe. It was expected that the

FIG2 band would be larger (4.3 Kb) in the disrupted haploids than in the wild type haploids (3.2 Kb) due to the presence of the *URA3* disruption construct in the former. For the *URA3* probe, the wild type is expected to show one band (1.1 Kb), and disruptants expected to show two bands- one for the original, genomic *URA3* gene (1.1 Kb), the other, corresponding to the *URA3* located in the disrupted *FIG2* locus (4.3 Kb).

The results of the Southern blots are shown in Figure 6 and Figure 7. In Figure 6, the Southern Blot was probed by the *FIG2* 960 bp fragment. Lanes 13, 14, and 15 contained wild type DNA isolated from a, α, and a/α cells respectively. The band obtained was the expected 3.2 Kb. Lanes 1 to 4 were individual isolates from **a** cells that were disrupted at the *FIG2* locus. Lane 5-8 were individual isolates from α-cells disrupted at the *FIG2* locus. These haploids all show a single band at the expected 4.3Kb. Lanes 9-12 represent the DNA isolated from diploids. One wild type band and one disrupted band were observed and were to be expected since double integration would be a very low probability event. The diploid represented by lane 11 was an exception. In this particular clone, only the 3.2 Kb fragment is seen. This is unlikely to represent a reversion to wild type *URA3*, since the mutation in the genomic 1.1 Kb *URA3* involves a deletion. This

may indicate that, in this case, *URA3* integrated into the genome at a location other than at the *FIG2* locus. It is possible that, in this clone, *URA3* integrated into a very large *HindIII* fragment. Such large fragments do not transfer onto nitrocellulose, and are thus not observed.

Figure 7 represents an experiment identical to that shown in Figure 6, except that the DNA was hybridized with the *URA3* probe. In this blot, the genomic *URA3* was seen as a 1.1 kb fragment, as expected from restriction digests by *HindIII*. In the mutant haploids, an additional band of 4.4 kb was observed. The 4.4 kb band, of course, was the same as the 4.4 kb band detected by the *FIG2* probe. This 4.4 kb band contains a *URA3* fragment flanked by two *FIG2* fragments, one 5 and the other 3' of the *URA3* gene. In the mutant heterozygous diploids, the same pattern was observed as in the haploids. Diploids contain two copies of genomic *URA3*, as well as the *URA3* within the disrupted *fig2* gene. The fact that lane 11 once again exhibits only a single band at 1.1 Kb is further confirmation that the disruption construct did not integrate into Fig 2 in this particular case.

FIG2 is a Non-essential Gene

One possible outcome of disrupting a gene is that disrupted cells might no longer viable if the gene happens to be essential. Typically, one would disrupt a certain gene in diploids so that only one copy of the gene is disrupted while the homologous copy remained as wild type. The diploids are then sporulated, and the spores, being haploids, are tested for viability. In the case of disrupting *FIG2*, both haploids and diploids were used. Viable transformants from the haploids indicated *FIG2* is not essential. As shown in Figure 8, wild type a, α and a/α diploid cells, as well as the corresponding mutants all showed typical, almost identical growth curves. In Figure 9, the log of the cell density was plotted over time during mid log phase. The essentially identical slopes indicate that both mutants and wild type strains grow at the same rate.

FIG2 Disruptants Exhibited Abnormal Morphology in Stationary Phase

Wild type cells and *fig2* disruptants were examined by microscopy to see if mutants have abnormal morphology. If *FIG2* is a cell wall gene of significant structural importance, the disruptants (mutants) may exhibit aberrant morphology. As shown in Figure 10, the morphologies of wild type and mutant **a** cells were similar in both size and shape when the cells were

harvested from mid-log growth. There seemed to be a slight enlargement of the mutant cells as compared to the wild type, but visual examination is often subjective. Similar results were observed for α-cells and heterozygous diploids (data not shown). Interestingly, when *fig2* mutants, either **a** or α-cells, were in stationary phase, the cells appeared to be aberrant, larger in size as a whole and larger in the size of the vacuole. As shown in Figure 11a and Figure 11b, the morphological difference between wild type and mutant **a** cells was quite pronounced. Similar observations could be made about α-cells (Figure 12a and Figure 12 b). The differences between the heterozygous diploid mutants and wild type were more subtle. There was possibly as much similarity as difference in these cells (Figure13).

A spheroplast Formation Assay Showed Cell Wall Integrity

One of the possible biological functions of *FIG2* is that its gene product plays a role in supporting the rigidity of the wall. Although the strength of cell wall is largely provided by β1-3 glucan, some mannoproteins may further support cell wall rigidity and shape. A cell wall integrity assay was developed based on the rate of cell wall lysis in the presence of zymolyase, which is mixture of β1,3glucanase and protease (Zlotnik et al 1984). In this assay, cells are suspended in a hypotonic solution and the density of cell

suspension is measured by spectrophotometric absorbance at 660 nM. The optical density of a cell suspension is directly dependent on the light scattering caused by intact cells. As Zymolyase digests cell walls, cells expand by osmosis and lyse. Therefore, the decrease in optical density is proportional to the degree of cell lysis, which, in turn, is a function of cell wall strength. As shown in Figure 14, cells grown in different media and at different phases of the growth curve showed differences in the strength of their cell walls. The walls of cells that were in log phase were weaker than their stationary phase counterparts. These results were expected. Cells in log phase are actively growing and dividing. Consequently, their cell walls are in a constant state of flux. As the cells expand, the cells carefully orchestrate glucan synthesis and glucan degradation, which allows addition to the glucan chain. To accomplish the task of cell division, such cells keep their cell walls relatively thin, as compared to cells in stationary phase. When cells enter stationary phase, they are no longer dividing. Their walls become thicker to afford extra protection.

Also, as shown in Figure 14, media play a role in the strength of cell walls. The walls of cells that were grown rich medium, YEPD, were weaker than the walls of cells grown in defined medium, YNB. There is no obvious

explanation for this. One can speculate that a faster growth rate (in rich media) may result in weaker cell walls. Alternatively, cells grown in the presence of proteins and peptides (in rich media) might loosen up the "pores" in their cell walls in order to allow high molecular weight nutrients to enter the cell. The opening of such pores may result in a weaker cell wall. Nevertheless, the spheroplast lysis assay is a valid measurement of cell wall strength.

As shown in Fig 15, the integrity of cell walls from wild type cells was measured against the *FIG2* deletion mutants. The bottom four curves were cells that were grown to log phase in two different media. In the case of YEPD grown cells, the wild type and mutants curves were virtually superimposed on each other, indicating no difference in lysis rate. Therefore, the strength of the walls generated from wild type and the mutants were no different. When the cells were grown in YNB, the curves appeared to be slightly different. The wild type cell appeared to be stronger than mutants. However, statistics with 95% confidence level (Student's T-test) showed that these two curves are not different.

The upper four curves in Figure 15 showed the rate of lysis of cells that were grown to stationary phase. The general observation was that the walls from

these conditions were stronger than the cell walls in log phase. Whether the cells were grown in YNB or YEPD, there was little difference in the strength of walls between the wild type and the mutants.

It was possible that *FIG2* only expressed itself in cells grown at lower temperatures, but not 28^0C. Therefore, cells grown at different temperatures were tested for cell wall strength. As shown in Figure 16, the spheroplast lysis assay showed there was no difference between the wild type and the mutants in respect to cell wall integrity whether the cells were grown at 10^0C or 28^0C. Interestingly, the walls of cells that were grown at the lower temperature appeared to be stronger than the walls from cells grown at higher temperature. One may speculate that cells grown at higher temperature, having a faster growth rate, might exhibit weaker cell walls. This would be consistent with results seen in cells grown in rich medium vs. minimal medium.

The Agar Diffusion Assay Showed that Disruptants Were Weakly Resistant to Econazole

Agar Diffusion assays are commonly employed to test for antimicrobial activity in clinical settings, and in the pharmaceutical industry (Franzin et al

2000; Soni et al 1999). This technique was therefore used to examine both wild type and *fig2* mutant cells, since disruption of a putative cell wall gene might be expected to alter the sensitivities of cells to antibiotics.

The modes of action of many antifungal agents are understood in some detail. Because of this, when a mutation in a gene exhibits altered sensitivity to a drug with a known molecular target, specific roles for the product of that gene can immediately be suggested. For example, disruption of *FKS1* (the putative glucan synthase-1) produces cells dependent solely on *FSK2* (glucan synthase-2). Consequently, such mutants have a greatly reduced overall level of glucan synthase activity. Predictably, these mutants exhibit super sensitivity to FK506, a drug that is known to inhibit glucan synthase (Douglas et al 1994; Foor et al 1992). If an unknown mutant shows a specific sensitivity to FK506, it is likely that the mutation is either in *FKS1*, *FSK2*, or in some other gene in the pathways leading to, or regulating, glucan synthase activities.

A limited set of antifungal drugs, with known targets, was tested versus *fig2*-disrupted strains and wild type strains (Table 6). The modes of action of these compounds are described briefly below. Cycloheximide is known to interfere with eukaryotic ribosomal protein synthesis (Diment & Blinova

1976). Echinocandin B inhibits glucan synthase (Debono & Gordee 1994; Debono et al 1995; Lee et al 1990). Aculeacin A is another β1-3 glucan synthase inhibitor, which, along with Echinocandin B, is localized to the plasma membrane (Bozzola et al 1984; Mizoguchi et al 1977; Mizuno et al 1977; Yamaguchi et al 1985). Tunicamycin has been reported to be a mannoprotein glycosylation inhibitor (Dean 1995; Lagunas et al 1986). Cerulenin is a potent, noncompetitive inhibitor of fatty acid synthase (Inokoshi et al 1994; Mago & Khuller 1989; Watkins et al 1998). In fact, this latter compound has been used to screen for genes that are related to fatty acid synthesis (Oskouian & Saba 1999). Econazole is an azole derivative that inhibits ergosterol synthesis (Vanden Bossche et al 1990).

As shown in Table 6, *fig2Δ* haploids, of both mating types, are slightly less sensitive to econazole. The zones of clearance for the disruptants are about 2 mm smaller than for the wild types.

Pheromone Response Elements (PRE) were Located Upstream of *FIG2*.

In the effort to understand the biological functions of *FIG2*, no evidence was found that *FIG2* was responsible for cell wall integrity. I therefore examined the possibility of a function for this gene in mating. Genes that

are involved in mating are commonly known to have specific regulatory elements in the upstream sequence (Trueheart et al 1987). In response to the stimulation of haploids by pheromone, Ste12p binds to the upstream of many mating genes to activate transcription. The consensus sequence for the Ste12p binding sequence is TGAAACA (PRE sequence) (Trueheart et al 1987) (Sengupta & Cochran 1990). A number of pheromone-regulated genes, such as *STE2*, *STE3*, *FUS1*, and *SAG1*, are known to have a PRE sequence upstream of the gene (Lipke et al 1989).

There are four PRE sequences found upstream of *FIG2*. Two of the four sequences were an exact match, while the other two have 6 of 7 matching bases. The most obvious implication of these PRE sequences is that *FIG2* may somehow play a role in mating.

The Mating Projection (Shmoo) Produced by *FIG2* Disruptants Appeared to Be Normal

FIG2 was a cell wall gene candidate, and it was thought to be pheromone regulated. Perhaps *FIG2* plays a role in shmoo formation. When haploid cells are chronically induced by pheromone (high concentrations for 4 hours), the cells undergo a morphological change. The cells become larger, and the shape of the cells changes from round or oval to pear-like or peanut-

like (shmoos). Many important proteins for mating are directed to the surface of the shmoo tip. I compared the morphology of pheromone-induced *FIG2* disruptants relative to the wild type. As shown in Figure 17, a standard yeast strain, *2180-1A*, was induced by α-factor at 400 ng/ml for 4 hours. When examined under the microscope in 40X, the change in morphology was obvious. The wild type uninduced *X-2180* was observed to be round or oval in shape, while the induced *X2180-1A* was observed to have shmooed. Interestingly, the *2180-1A* strain was capable of forming only "uni-pod" shmoos, while the *W303-1A* strain could form more than one projection. In Figure 18, *W303-1A* and its isogenic *FIG2* disruptant were compared. Wild type *W303-1A* was capable of forming mono-polar and bi-polar projections when induced by α-factor. The corresponding disruptants showed a similar morphology.

The Constitutive Expression of *FIG2* was Approximately 3600 Fold Lower than that of Actin Expression

Although *FIG2* exists in the genome as an open reading frame, it is still possible that *FIG2* is a pseudo-gene which is not naturally expressed. Numerous attempts were made by Northern analysis to detect *FIG2* transcripts, but none were detected by normal procedures. Consequently, an

unusually hot ^{32}P probe, 10^8 CPM per ml, was employed. After exposure for 10 days, *FIG2* transcripts were finally detected in non-induced cells (Figure 19). For control, an equivalent probe specific for actin transcripts was made. The actin blot required only 40 minutes to detect actin transcripts. Constitutive *FIG2* expression was calculated to be 3600 fold weaker than actin expression, according to the following formula:

((10 days X 24 Hr/day X 60 Min/Hr) / 40 Min) = 360 fold more exposure time.

The intensity of the actin bands was estimated to be at least 10 fold greater than the *FIG2* bands. Therefore, the difference in expression is at least 360 X 10 = 3600 fold. Thus, the constitutive expression of *FIG2* can be estimated to be at least 3600 lower than actin.

In the uninduced state, the level of transcription from **a**, α, or **a**/α cells appeared to be equivalent. In addition to the band representing *FIG2*, two extra bands appear on the gels labeled with the super-hot probe for long periods. These bands are the same size as rRNA, which has no homology to

FIG2. Probably, these represent non-specific binding brought on by the extreme labeling conditions.

***FIG2* Expression was Inducible by Pheromones**. The RNase protection assay (RPA) is a much more sensitive technique than Northern blots to detect rare transcripts (Crotchfelt et al 1998; Samani et al 1987; Woodcock et al 1996). In this assay, purified Poly-A mRNA is hybridized to ^{32}P labeled probe in solution directly. No transfer from gel to nylon membrane is required. The directly hybridized mRNA/probe (RNA/RNA) complex is subjected to single-strand-specific RNase digestion to remove the remaining unhybridized probe. The hybridized complexes are then subjected to acrylamide gel electrophoresis and exposed to X-ray film. In Figure 20a, the levels of actin expression in a or α cells were unaltered by induction with the appropriate pheromone at 400 ng/ml. However, as shown in Figure 20b, *FIG2* transcripts were increased in induced **a** or α cells as compared to non-induced cells. Therefore, the RPA data is consistent with the discovery of PRE sequences upstream of *FIG2*.

***FIG2* is a Cell Wall Gene**

As mentioned in the general characterization section of "Results", *FIG2* is a strong candidate as a cell wall gene based on the existence of i) high homology to *AGA1*, which is a cell wall gene, ii) high serine/threonine content, iii) internal repeats, iv) an extracellular signal sequence, and v) a cell wall anchorage signal. In an attempt to further confirm this experimentally, I constructed a fusion protein in which the jellyfish green-fluorescence-protein (*GFP*) (Ram et al 1998b) was inserted, in frame, in the middle of *FIG2* (see Fig 5A). The construct was made and transformed into *W303-1A* and *W303-1B* haploid cells. Mid log cells were then induced by their appropriate pheromones at 400 ng/ml. The cells were then suspended in 10 mM Tris pH 8.0, 1 mM EDTA at 4^0C for 18 hours to allow the GFP fusion protein to fold properly. These cell suspensions were then observed for fluorescence. As shown in Figure 21a, induced *W303-1A* cells appeared somewhat larger than normal under bright field microscopy.

When the cells were examined under the excitation of UV light, fluorescence was exhibited in two distinct patterns (Figures 21 & 22). Most cells showed a speckled pattern of light fluorescence, which was distributed relatively evenly across the periphery of the cell. A smaller, but significant number of cells exhibited an uneven distribution, which appeared as a

crescent of fluorescence along one side of the cell. Interestingly, for each pattern, the fluorescence in a few cells was much brighter than in the majority of cells.

Clearly, in at least some cells (2 out of 66 in Fig 22), the fusion protein appears to be unevenly distributed. This might be internal fluorescence due to entrapment of the protein within some intracellular organelle such as endoplasmic reticulum, caused perhaps by improper folding. It is also possible that the distribution of this protein in the cell wall is polarized to a limited section of cell wall. If that portion of the cell surface that contains fusion protein faces the camera directly, fluorescence will appear to be evenly distributed. If it happens to be tangential to the line of sight, the observed crescent pattern will result. The different intensities seen may also be a reflection of how the localized fluorescent patch is oriented. If it is located on the on the upper surface of the cell, the unobstructed view should result in a bright observed fluorescence, whereas fluorescence on the lower surface would be obscured by the overlying non-fluorescent cytoplasm and cell wall.

Even though a precise interpretation of the observed pattern of fluorescence labeling is problematic, these experiments show some peripheral staining. Since peripheral staining would be expected for a cell wall protein, these results serve to support the idea of a role for *FIG2* in mating, since uninduced cells of either mating type do not exhibit fluorescence.

Deletion of *FIG2* in α-cells Led to Hyperagglutination

In mating, opposite mating-type cells must first come into contact with each other. The cells then adhere to each other to allow fusion of cell walls, cell membranes, and nuclei to form diploids. This cell-cell adhesion process is known as sexual agglutination. Sexual agglutination is all but essential for mating in liquid media, since, under these conditions, the mating efficiency of α-agglutinin deleted strains is 10^{-7} that of wild type (Lipke et al 1989). On solid media, sexual agglutination is not an absolute requirement for mating. However, on solid media, the mating efficiency of α-agglutinin deleted strains was 2-4 fold less than the isogenic wild type (Lipke et al 1989).

Both the α-agglutinin and **a**-agglutinin are regulated by pheromone induction. There is a distinct possibility that *FIG2* plays a role in

agglutination since it has been shown to be a cell wall gene with little role in maintaining cell wall structure, but inducible by pheromones.

Our laboratory has established a quantitative agglutination assay (Terrance & Lipke 1981). Utilizing this assay, *FIG2* deletion strains were agglutinated with wild type strains in various combinations. As shown in Figure 23, the four agglutination pairs were wild type a versus wild type α, *FIG2* deleted **a** cell versus wild type α, wild type **a** cells versus *FIG2* deleted α-cells, and *FIG2* deleted **a** cells versus *FIG2* deleted α-cells. When *FIG2* is deleted in α-cells, the agglutination index increased by about 35%. A similar increase was seen when *FIG2* was deleted from both **a** and α-cells. When the same deletion was performed on the **a** cells alone, the increase in agglutination index was only about 8%. Therefore, it appears that agglutination may be up-regulated by deleting *FIG2* in α-cells.

The Overexpression of *FIG2* Led to Repression of Agglutination

The absence of *FIG2* expression in α cells led to hyper-agglutination. Thus, overexpression might lead to hypo-agglutination. This idea was put to the test. The *FIG2* gene was constructed with its natural promotor in the multicopy plasmid pRS423. Transformation by this plasmid should raise the

gene dosage by about 10 fold over the wild type. The overexpression plasmid was transformed into *W303-1A* and *W303-1B*. The transformants were then agglutinated with the isogenic wild type in various combinations. As shown in Figure 24, the four combinations were wild type **a** cells versus wild type α-cells, overexpressing **a** cells versus wild type α cells, wild type **a** cells versus overexpressing α cells, and overexpressing **a** cells versus overexpression α cells. As expected, the level of agglutination of overexpressing α-cells was repressed relative to wild type, while overexpressing *FIG2* in **a** cells produced little change in agglutination index. These results were consistent with the hyper-agglutination of α-cell null mutants.

The Dose Response of a-factor Induced Hyper-agglutination was Less than 50 ng/ml

When α-cells are induced by a-factor, the transcription of α-agglutinins is increased (Terrance & Lipke 1981). This leads to an increase in agglutination, as measured by the quantitative agglutination assay. At the same time, **a**-factor also induces *FIG2*, which somehow represses

agglutination. Attempts were made to determine the dose of **a**-factor that is required to produce optimal agglutination in the absence of interference by *FIG2*. This experiment was done in the *FIG2* deletion strain. As shown in Figure 25, agglutination clearly increased in cells induced by **a**-factor. Because there were just a few points on these curves, the dose of **a**-factor needed to produce optimal agglutination could only be estimated to be less than 50 ng/ml. The dose that produced half of the maximal response could not be determined. The agglutination of the wild type, once again, was lower than that of the *FIG2* mutant, a result that was consistent with the Figure 23.

Due to its hydrophobic nature, **a**-factor is only reliably soluble in organic solvents, such as DMSO or isopropanol. Once an organic stock solution of **a**-factor is diluted into aqueous media, indeterminant amounts of **a**-factor may precipitate. Therefore, dose-response experiments with **a**-factor, and their interpretation, are somewhat problematic.

Similar experiments were performed on **a** -cells induced by α -factor. As shown in Figure 26, the agglutination index reached 0.7 when α-factor induction was increased from 0 to 20 ng/ml. Addition of more α-factor did

not increase agglutination significantly. Again, there was little difference in the dose response between the wild type and the *FIG2* deletion mutant

It is clear that, at least in α cells, *FIG2* inhibits agglutinability without altering the final levels of transcription of agglutinin (Figs 24 and 28). Precisely why agglutination might need to be down-regulated is not clear, but the evidence presented so far makes a strong case for the existence of such down-regulation. One possible scenario is that *FIG2* expresses itself at the end-stage of agglutination, allowing cells to revert to a normal state should a mating partner not be found.

It has been known for some time that the time required for maximal induction of agglutination is about 80 minutes for **a**-factor and 20 minutes for α-factor (Terrance & Lipke 1981). These experiments, however, were performed in the presence of the normal constitutive expression of *FIG2*. It is possible that modulation of *FIG2* expression would alter this time course.

Shown in Figure 27 is a time course of induction experiment in which various combinations of cells, both wild type and *fig2* mutants, were agglutinated. As expected, the highest levels of agglutination were found in combinations in which the α-cells had *FIG2* deleted. In all cases, the time

required for maximal induction of **a**-cells was about 20 minutes, a result that was in agreement with previous findings (Terrance & Lipke 1981). There was no difference in terms of time to maximal induction between the wild type **a**-cells or the *fig2* mutants. Significantly, all combinations showed a similar decline in agglutinability when incubation with pheromone was continued well beyond the point of maximal induction. The facts that deletion of *FIG2* did not slow this decline, and that the decline began only after 50 to 100 minutes of induction, argue against a role for *FIG2* in causing a more rapid return to constitutive levels of agglutinability.

Overexpression of *FIG2* Did Not Interfere the Transcription of α-agglutinin

So far, the data presented have suggested a role for down-regulation of agglutination in α cells. There are many possible mechanisms through which this might be achieved. The expression of *FIG2* might down-regulate the transcription of α-agglutinin. Alternatively, *FIG2* might interfere with the translation of α-agglutinin, or possibly its post-translational modifications. Other possibilities are that the *FIG2* gene product could specifically bind to α-agglutinin and prevent proper folding of this molecule, or bind to agglutinin near the active site and thereby interfere with the

specific binding of **a**-agglutinin. Since *FIG2* is a relatively large cell wall protein, it may simply interfere with agglutination in a non-specific manner. For example, *FIG2* could act as a "huge umbrella" on the cell surface, shielding α-agglutinin from the extracellular matrix. Finally, the expression of large amounts of *FIG2* may simply create competition with α-agglutinin for space available for secretion or space for anchorage onto the cell wall.

An RNase Protection Assay (RPA) experiment was performed to examine the level of α-agglutinin expression in cells with different doses of *FIG2*. As shown Figure 28, the level of pheromone-induced α-agglutinin transcripts (lane 6) was much greater than that of uninduced transcripts (lane 5). When the cells were transformed to harbor a multicopy plasmid containing *FIG2,* the level of α-agglutinin transcripts was unaltered. The control experiment is shown in the left-hand panel autoradiograph (ARG) in Figure 28. In this experiment, an actin sequence was used as the hybridization probe. The actin gene is not pheromone-inducible. The bands in all the lanes were roughly similar, indicating the amounts of actin mRNA isolated were similar.

Disruption of *FIG2* Did not Show Defects in Mating on Solid Media.

Since sexual agglutination facilitates mating, disruption of agglutination may affect normal mating behavior. The disruption of *FIG2* caused the cells to hyper-agglutinate; such disruptants may show unusual mating behavior. **a** and α tester strains carrying specific nutritional makers were mated with *W303,* which has a different set of axoutropic makers complementing the tester strains. The resulting diploids are able to grow on minimal media which will not support either haploid. A qualitative mating assay was performed on solid agar in an attempt to detect mating defects in *fig2* disruptants. The results are shown in Figure 29. Qualitative observations of the mating patterns of *fig2* α cell disruptants often seemed to indicate hypermating in comparison to wild type. Results, however, were far from consistent. Since mating experiments on solid media provide only qualitative measurements of mating competency, assays performed in liquid media were also carried out. Unfortunately, the results of these experiments were inconsistent, and therefore equivocal.

***FIG2* Did Not Specifically Bind to α-agglutinin Based on ^{125}I-labeled α-agglutinin Binding to Whole Cells**

It has been established that the mechanism of down regulation of α-agglutinin by *FIG2* is not due to down regulation of transcription of α-agglutinin. Therefore, it is possible that *FIG2* specifically binds to α-agglutinin and somehow prevents α-agglutinin from interacting with **a**-agglutinin. To test this idea, purified α-agglutinin was labeled with ^{125}I. The labeled material was allowed to bind induced α cells with *FIG2* deleted, and induced α cells with constitutively expressed *FIG2*. The cells and the labeled material were allowed to bind for one hour at room temperature or one hour at 4^0C. The cells were collected, and washed three times with binding buffer at 4^0C. Radiation in the cell pellets was then measured via gamma radiation counter. Labeled α-agglutinin did not bind measurably to the either α-cells with *fig2* deleted or wild type α-cells (Table 7).

Discussion

Research Goals

The experimental results presented above elucidate biological role(s) of the *FIG2* gene in *S.cerevisiae*, focusing upon potential functions for *FIG2* as either a structural cell wall gene and/or a gene regulating sexual agglutination. In addition, the expression of *FIG2* was determined in haploid vs. diploid, and, in the former, constitutively vs. in response to pheromone stimulation. These choices were governed by the facts that the *FIG2* sequence contains structural features common to cell wall genes, as well as PRE sequences associated with pheromone-inducible genes. Of course, any pheromone-inducible gene is likely to be involved in mating-related functions, and sexual agglutination is one such function that is already known to involve cell wall molecules (e.g. the agglutinins) and may also be mediated by other, as of yet uncharacterized, molecules, such as *FIG2*.

In the discussion that follows, the results obtained in this study are examined and interpreted at length. In those instances in which specific results overlap and/or complement those of Erdman et al (1998), a detailed discussion of, and comparison with the two sets of data are provided.

The Possible Structural Roles of *FIG2*

To characterize *FIG2*, it is helpful to keep in mind the varied roles of the cell wall. One of the most obvious characteristics of the wall is that it provides protection for the cells through its chemical rigidity. β1-3 glucan, β1-6 glucan and chitin form a solid structure that protects the cell from mechanical injury (De Nobel et al 1990; Zlotnik et al 1984). Consequently, any disruption of the biogenesis or assembly of these polysaccharides may result in compromise of the structure of the cell wall.

Any number of factors might affect cell wall integrity. These include growth medium, growth temperature, and growth phase. Indeed, it has been shown that the permeability of cell wall to α-amylase is increased when the cell are grown in rich medium (Rothstein et al 1987) and that such cells are more porous in regards to protein leakage (De Nobel et al 1990). Such changes in the permeability of the cell wall are likely due to differences in the physical structure of cell walls synthesized under different growth conditions.

These results are consistent with the current study. Cells that were grown in YNB were more resistant to Zymolyase than cells that were grown in

YEPD (Figure 15). The increase in sensitivity of YEPD-grown cells to Zymolyase can be explained by a general thinning of cell walls and/or increased access of Zymolase to important structural cell wall molecules. Changes in cell wall porosity in response to growth medium has already been demonstrated to allow increased access by large molecules (De Nobel et al 1990; Rothstein et al 1987). The increased sensitivity to Zymolase seen in this study, therefore, can reasonably be inferred to be due to changes in the porosity of the wall.

The significance of this increased porosity in cells grown in rich medium is unclear. It may be biologically significant if cells grown in rich medium require more porous walls in order to allow the large peptides present in such medium to permeate through the walls and be used as nutrients. Alternately, the increased porosity may simply be incidental, an artifact of differential growth rates. During the exponential phase of growth, the doubling time of haploid strains is approximately 90 minutes in YEPD medium and 140 minutes in YNB at 30^0C (Sherman 1998). The higher growth rate of cells grown in YEPD may simply result in a less tightly-knit cell wall.

The chemical composition of the cell wall is known to be different depending on the growth phase of the cells. In stationary phase, cells are known to be thicker and less porous than in log phase (De Nobel et al 1990; Valentin et al 1987). Shimoi et al have purified a major cell wall mannoprotein, Sed1p, from cells that were grown to stationary phase (Shimoi et al 1998). They have shown that the transcript of *SED1* increases when cells enter the stationary phase. *Sed1Δ* cells grown to stationary phase were shown to be more Zymolyase sensitive when compared to the wild type. However, the *sed1* deleted cells were more resistant to Zymolyase in stationary phase than in log phase, implying that there are other factors in the stationary growing cells that are responsible for the Zymolyase resistance (Shimoi et al 1998). In fact, at least one other protein, *TIP1*, is induced in stationary phase cells (Kondo & Inouye 1991).

Aside from the alteration of the spectrum of cell surface mannoproteins in stationary phase, the glucan on the cell surface is also changed. *FKS1* and *FKS2* are two homologs that synthesize cell wall glucan (Mazur et al 1995). Working under different regulation, *FKS1* is often expressed when *FKS2* is repressed, and vice versa. For example, *FKS1* is expressed in the log phase while *FKS2* is largely repressed. On the other hand, *FKS2* is strongly

expressed in stationary phase while *FKS1* is not expressed. It has been proposed that the glucan synthesized by *FKS2* may be more stable than that derived from *FKS1* (Zhao et al 1998).

As shown in Figure 14, stationary phase cells are more resistant to Zymolyase lysis than log phase cells, regardless of the media in which the cells are grown. This is consistent with the ideas that stationary phase cells may form thicker walls due to slower growth and /or may fortify their cell walls through the differential synthesis of cell wall components.

Yeast cells are also known to express different proteins at different temperatures. For example, *TIP1* and *TIR2*, two cell wall genes of unknown physiological function, are known to be induced when growth temperature is lowered from 30^0C to 10^0C (Kowalski et al 1995). In addition, *FKS2* is thermally induced when cells are shifted from 23^0C to 39^0C (Zhao et al 1998). As shown in Figure 16, cells grown at low temperature are more resistant to lysis. This is consistent with the results obtained from different growth media. In both cases, the more slowly growing cells (defined medium or low temperature) showed greater cell wall integrity. Interestingly, deletion of *FIG2* resulted in no significant difference in the

results obtained by changing growth media, growth phase or growth temperature (Figures15 and 16).

In addition to the Zymolyase resistance assay, it is useful to supplement the results of such assays with data derived from other methods. One such method is simple microscopic examination, since significant alterations in cell wall composition or structure are likely to result in manifest changes in the appearance of cells. As shown in the Figure 10, the shapes and sizes of the wild type and the corresponding *FIG2* deleted exponential **a** cells were not different from each other. However, when the cells were grown to stationary phase, the *FIG2* deleted strains appeared to be significantly larger than the wild type. Interestingly, these results contrast with those obtained from the Zymolyase resistance assay, in which the stationary cells of the wild type and its isogenic *fig2* mutants appeared to be similar.

Based on the results of microscopic examinations, the cell wall structures of the wild type and its *FIG2* deleted strains are different when the cells are grown to stationary phase. As shown in Figure 19 and Figure 20, there was a low level of constitutive expression of *FIG2* in the uninduced state, both in haploid and diploid cells. Perhaps this low-level constitutive expression is

important for maintaining the cell wall in stationary phase (Data not shown). As noted earlier, the expression of wall proteins during stationary phase is different than that of the log phase cells.

As mentioned previously (Introduction), Erdman et al (1998) noted "hyperpolarization" of mating projections in *fig2* mutant haploid cells in unmated mixed cultures - i.e. longer, thinner mating projections. Of potential significance is the fact that this hyperpolarization is not seen in unmixed culture treated with isotropic α factor. However, the interpretation of mating projection formation is, by nature, an intricate endeavour. The strains used, time of incubation, temperature, growth phase, and the composition of the growth medium employed may all affect the results obtained. Even when all of these factors are controlled, results are somewhat variable from experiment to experiment, and highly variable from cell to cell within an experiment. Added to this, is the fact that the visual observations used to "score" morphological changes are necessarily somewhat subjective, as well as only semiquantitative. As a result, comparisons are difficult in the absence of very clear or profound differences.

For these experiments, Erdman et al. employed **a** cell strains derived from s288c with *bar1Δ* engineered. They were able to observed mating projections after only 2 hours of induction with isotropic α-factor (Erdman et al., Fig 3). My experiments were carried out with strains *X2180-1A* and *W303-1A*, both of which have *BAR1* intact. In such cells, the time required to form full mating projections is consistently 3.5 to 4 hours. While *X2180* cells always form a single (unipolar) mating projection (Fig. 17), *W303* cells will sometimes form two, and, occasionally, three mating projections (multipolar projections, Fig. 17). The mating projections formed in *X2180* cells also differ in their shape, tending to be more blunted than the relatively pointed projections formed by *W303* cells (Fig 17). These pointed projections are quite similar in shape to those observed in the *bar1Δ* strains (both WT and *fig2Δ* mutant) utilized by Erdman et al. (Erdman et al., Fig. 3).

It is in the morphologies induced in mating mixtures that Erdman et al. observed a *fig2* mutant phenotype. Firstly, since the cells are mixed, the mating type of each cell observed is uncertain. Therefore, if there are any genuine differences in the morphology of some cells under these conditions, these may simply be representative of α-cells, for which there were no isotropic controls. Secondly, their conclusion is based on a comparison of

selected cells from a field of unmated cells amongst zygotes (Erdman et al., Fig. 6, and Fig. 5, insets). A relatively small field of cells is shown for each condition. However, when these fields are observed in their entirety, a more objective comparison reveals that the morphologies of the few wild type cells and *fig2* mutants actually shown are remarkably similar (Erdman et al., 1998, Fig 5). Experience has shown that, within any given population of induced cells, various forms are often seen. Given the subjective nature of these assays, it can be quite difficult to identify differences between different conditions without a careful comparison between two large populations of cells. Clearly, such a comprehensive analysis was not done by Erdman et al.

Another phenotype observed by Erdman et al. relates to the structure of the zygotes formed by mutant cells. On the basis of electron microscopy, they claim that mutant cells form abnormally-narrow conjugation bridges. Again, this is based on a selected micrograph of a single zygote (Erdman et al., Fig. 8). No indication is given that serial sections were made, to assure that this section represents a full, central section, as opposed to a naturally-narrow, tangential section.

On the basis of these results, Erdman et al. proposed the loss of *FIG2* causes the formation of hyperpolarized mating projections, which eventually result in narrow conjugation bridges. According to them, it is the defect in conjugation bridges that may be responsible for lower mating efficiency.

With the exception of the liquid mating assay results, 7 out of 11 of Erdman et al.'s figures on mating were based on microscopy. Yet, mating is a very dynamic process. Therefore, a mutation might very well somehow directly or indirectly affect the time course of the mating process. Any individual micrograph is merely a snapshot of a single instant in this process, which can only be adequately described by a complete, sequential series of photographs. For example, the increased agglutination of the *fig2Δ* mutant may cause the fusion process to begin earlier, if only because mates are more quickly found. In this case, one might expect that the morphology of mutant zygotes at any given time may differ from the wild type.

Clearly, cell walls protect against mechanical injury. However, yeast cells face many other challenges. Toxins released from other life forms are also a threat to the survival of yeast. Cell walls are the first line of defense against

all challenges from the hostile environment. It has been shown by Yun et al. that strains with deleted *pir1*, *pir2* and *pir3* are more sensitive to tobacco osmotin, an antifungal protein, and that overexpression of any one of the *PIR* gene renders cells resistant to osmostin (Yun et al 1998; Yun et al 1997). These authors postulated that osmotin interacts with specific cell membrane proteins to form pores in the membrane, resulting in leakage of cytoplasm to the extracellular matrix. They proposed that cell wall proteins of the *PIR* gene family act to mask the cell surface receptors that are specific for osmotin.

Other, similar toxin receptors have been extensively studied. For example, killer-toxin K1, a pore-forming protein, is known to bind to β1-6 glucan on the cell surface of yeast (Bussey 1991). KT28, a mannoprotein-binding protein, is another toxin acting via a similar mechanism (Schmitt & Radler 1990). Nisin, a small peptide that is known to be antibacterial, has no effect on wild type *S. cerevisiae*. However, *cwp2* deleted strains showed sensitivity to Nisin (Dielbandhoesing et al 1998). Furthermore, double deletion of *CWP1* (a *CWP2* homolog) and *CWP2* renders the cells hypersensitive to Nisin.

Taken together, the protective properties of the cell walls enhance the survival of yeast. In this study, the sensitivity to known antifungals of *Δfig2 cells* was compared to wild type by means of the agar diffusion assay. Deletion of *FIG2* did not change the sensitivity to a panel of known antifungal drugs, except in the case of econazole (Table 3). For this drug, the kill zone of *FIG2* deleted strain was 4 mm smaller than it was in wild type. By industrial drug testing standards, only a difference of 5 mm or greater is considered to be significant. However, the 5-mm industrial standard is arbitrary. The reasons that *fig2* null mutants are more resistance to econozole were not further investigated. Perhaps the cell wall structure of the *FIG2* deleted strain was altered, thereby limiting the permeability to econozole. Since the enhanced drug resistance of the *FIG2* deleted strain was specific to this drug, it would be interesting to test these strains with other azole or triazole agents.

F*ig2Δ* mutants may help in the discovery of new anti-fungal drugs

The two major classes of compounds that are currently in clinical use for systemic mycoses are Amphotericin B (AmB) and azole drugs. In fact, there are significant problems associated with each of these classes of drug. In the case of AmB, the problem is toxicity. Since the discovery of AmB in 1953,

hundreds of derivatives have been isolated and characterized (Dutcher 1968). Yet, in spite of this, AmB itself is the only one of these compounds ever used clinically. This is because of the high levels of nephropathy and neurotoxicity associated with AmB, which have earned this drug the nickname "Ampho the terrible". Consequently, AmB is generally considered the drug of the last resort. The hundreds of other AmB derivatives are essentially considered unsuitable for clinical use. Forty years of experience with this class of compound has caused the drug industry not to consider or develop any leads based on AmB derivatives. However, this type of compound routinely shows up in screens of new antifungals.

Considerable time must be spent in the isolation and characterization of each of these before it is discovered to be an AmB derivative. This time is invariably wasted, since these compounds have been found to be uniformly toxic. Because of this, it is quite valuable to be able to prevent undesirable classes of compounds from creating what are, in effect, false positives in screening assays. To this end, counter-screens are frequently devised to identify such compounds, thus saving the time needed for isolation/characterization. This procedure is termed "dereplication" in the pharmaceutical industry.

Currently, azoles and triazoles are the drugs of first choice in the fight against deep seeded mycoses. However, these drugs have achieved this status by default to the highly toxic AmB derivatives, since both azoles and triazoles themselves have significant clinical deficiencies. The major limitation of these drugs is that they are only fungistatic (Sohnle et al 1998). There have also been indications that their future effectiveness may be reduced by the recent emergence of resistance (Marichal et al 1999; Rex et al 1995). In addition, the target of azole is the fungal cytochrome P450-dependent lanosterol 14-α-demethylase system (Marichal et al 1999). Since there are 25-30 different P450s in human cells, it is probable that some of these will interact with these drugs. Although the FDA-approved azoles and triazoles are currently considered safe, certain related compounds (i.e. genaconazole, derived from fluconazole and sperconazole, derived from itraconazole) are known to be carcinogenic or tumorogenic , (Anaissie et al 1993)(Heoprich 1995). In this regard, it is worth noting that the information on drug toxicity in the literature may not be complete because there may be a few scientists who are less than enthusiastic about publishing adverse effects of drugs that they hope to eventually develop for use in humans.

Therefore, the seriousness of the toxicity of these drugs may be only partially known.

Because of this, in addition to dereplicating AmB derived compounds, it would be highly valuable to easily identify and thereby eliminate azoles and triazoles from antifungal drug screens. Since econazole is an azole compound, and since *FIG2* mutant cells show a decreased sensitivity to this drug, it is possible to devise an assay to easily and rapidly identify potential azoles. A two-plate diffusion assay, one utilizing *fig2Δ*, and the other utilizing wild type strains could be readily created for this purpose. Identical filter disks saturated with solutions containing potential antifungal compounds placed on each plate would create a zone of clearance proportional to the degree of antifungal activity. An appropriately smaller zone of clearance on the mutant plate, compared to the wild type plate, would be an indication that the antifungal activity is azole-related. Such an assay should be rapid enough to have utility even in the pharmaceutical industry, where screening two thousand natural products in a single week is not uncommon.

FIG2 is Localized to the Cell Wall

As described earlier, the *FIG2* is likely to be a cell wall gene. As mentioned previously (see Introduction) there has been one previous attempt (Erdman et al., personal communication) at localization of *FIG2* to the cell periphery. This was done by means of indirect fluorescence of a *fig2::β-gal* fusion protein. However, this construct did not contain a GPI anchorage signal, the significance of this result is unclear.

In order to properly localize the *FIG2* gene product to the cell wall, a reporter protein was constructed in which green fluorescent protein was placed in the middle of *FIG2*. This technique has been successfully employed by a number of investigators (Lo & Dranginis 1996; Ram et al 1998b). As shown in Figure 21 and Figure 22, induced haploid cells harboring the fusion construct showed fluorescence at the periphery of the cells when the cells were excited by UV light. The fluorescence was only observed when the cells were incubated in TE (10 mM Tris 1 mM EDTA pH8.0) overnight at 4^0C. These observations are consistent with the finding that showed GFP exhibits the brightest fluorescence at pH 8 (Clonetech Inc). The pH of yeast medium, YNB, is about 5.5. If fusion protein is located on the cell wall, the low pH environment may reduce fluorescence. When cells

are incubated at high pH, it may take some time for the protein to fold properly for the exhibition of fluorescence.

The observed fluorescence on the periphery of the cell does not prove that the fusion protein is localized to the cell walls, but it strongly suggests that this is the case. If the fusion protein were localized to the nucleus, one would expect to see a small circle or oval of fluorescence inside the cell. If the fusion protein were localized to the cytoplasm, then the fluorescence would be seen all across the cell, probably with uniform brightness. If, however, the fusion proteins were localized to the cell surface, then fluorescence would be seen as light, uniform fluorescence across the cell, with a bright ring around the cell circumference. Under the microscope, cells are seen in two dimensions. The edge of the cell circumference is a tangential view of cell surface. Therefore, a bright fluorescence ring is expected.

In Figure 21 and Figure 22, the fluorescence pattern of the cells does not appear as a uniform ring. Rather, the fluorescence pattern was irregular, consisting of crescent-shaped areas and spots of fluorescence on the edges of the cells, all interspersed with dark areas of no fluorescence. This pattern

can be interpreted to mean that the distribution of the fusion protein is localized to a relatively small patch on the cell wall. When the proteins are on the side of the cell opposite to the viewer, these cells are observed as having no fluorescence. When most of the fusion proteins are localized to the opposite site of the viewer with a little hanging on the edge, this is seen as a small area of fluorescence on the edge. Finally, when the fusion protein is localized partially front and partially back, the fluorescence appears as a crest.

When induced by pheromone at low concentration (40 ng/ml), haploid cells do not form mating projections (Moore 1983). However, this does not mean cells that these cells do not exhibit any polarization. For example, unconjugated haploid cells have been shown to exhibit asymmetric binding to fluorescent-labeled ConA (Tkacz & MacKay 1979). In fact, many cell wall proteins are polarized after pheromone induction. Proteins that are localized to the shmoo tip are actin, Bem1p, Bni1p, Bud6p, Pea2p, Spa2p, and Rom2p (Amberg et al 1997; Evangelista et al 1997; Manning et al 1997; Sheu et al 1998; Valtz & Herskowitz 1996).

FIG2 is inducible by pheromones

There are four Pheromone Response Elements (PRE's) upstream of *FIG2*. The consensus sequence of a PRE is TGAAACA (Trueheart et al 1987). At –449 and –454 upstream of the AUG codon, there are two such perfect-match PRE's. At –413, a single base mismatch (underlined) PRE, TGAAAAA is found. At –365, is another single base mismatch (underlined) PRE, TAAAACA. These PRE elements are found in front of a number of pheromone inducible genes, such as *FUS1*, *STE2*, *FUS2*, *MFA2*, *STE6*, and *BAR1* (Van Arsdell et al 1987). The PRE's are the binding site of Ste12p, a transcription factor that is pheromone specific. Therefore, the presence of multiple PRE's in *FIG2* strongly implies that the gene is pheromone inducible.

Many fruitless Northern analyses were performed in uninduced haploids in an attempt to detect constitutive expression of *FIG2*. After a number of attempts, it was realized that the probe for this Northern blot had to be unusually hot, and the exposure of the blot to had to be much longer. As shown in Figure 19, the transcripts of constitutively expressed *FIG2* were present at equal levels in a, α, and a/α wild types.

In experiments with *fig2* disruptants, smaller transcripts were observed in the haploids. In the heterozygous disrupted diploid, one normal and a slightly smaller transcript were detected. The slightly smaller *FIG2* transcript is probably fusion *URA3* and *FIG2*. These transcripts existed because the *URA3* was inserted in the *fig2*. In fact, these slightly smaller transcripts in disruptants were more abundant than the full-sized *FIG2* transcripts in the wild type. This could be explained by the fact that the smaller transcripts were driven by the *URA3* promotor, which may be more efficient. In hindsight, the disruption construct would have been better constructed if *URA3* had been inserted in the opposite direction of *FIG2*. Nevertheless, partial expression of normal *FIG2* in disruptants was highly unlikely because *URA3* had its own stop codon and the downstream portion of *FIG2* was out of frame after insertion of *URA3*.

Subsequent to the Northern analysis, an RNA protection assay (RPA) was employed to detect *FIG2* transcripts. As shown in Figure 20, expression of *FIG2* is shown to be induced by pheromone in both a and α haploids. The constitutive expression of *FIG2* in α-cells appears to be higher than that in **a** cells. Furthermore, the induction of *FIG2* transcripts appeared to be higher in α than that in **a** cells. This differential expression may help to explain

increased agglutination in α cells that are *FIG2* deleted (see the discussion of agglutination below).

The cell-type-specific expression of either a or α cells is controlled by transcription activators that specifically bind to the promotor sequence of cell type specific genes. The expression of α specific genes is localized to the PQ box, where transcriptional activators Mcm1p and A1p are known to bind cooperatively. These PQ boxes have been found in the α-agglutinin gene (*AGα1*), **a**-factor receptor gene (*STE3*) and α-pheromone structural genes (*MFα1* and *MFα2*) (Jarvis et al 1988; Kurjan 1985; Kurjan & Herskowitz 1982; Lipke et al 1989). The nearly palindromic sequence of the P box is ACACTAATTAGGAAG (Jarvis et al 1988; Sengupta & Cochran 1990). The consensus sequence of the Q box is CTGTCATTGT (Jarvis et al 1988; Sengupta & Cochran 1990). Significantly, there is an absence of a PQ box upstream of *FIG2*. Consistent with this is that *FIG2* is also inducible in **a** cells. The reasons for greater induction of *FIG2* in α-cells as opposed to **a** cells are not known.

The fact that *FIG2* is sex-pheromone inducible strongly suggests that this gene somehow plays a role in the pheromone signal transduction pathway.

The activation of the pheromone signal transduction pathway in haploid cells results in G1 arrest, increased agglutination, and increased transcription of a number of mating related genes. These functions are important for mating, and, not surprisingly, mutations in many of the genes involved result in sterility. Interesting, deletion of *FIG2* does not result in sterility (Figure 29)(Erdman et al 1998).

Numerous genetic screens have been set up by researchers in the yeast scientific community to search for sterile mutants. In fact, many components in the signal transduction pathway have been found by genetic screens. For example, *STE2*, *STE3*, *STE5*, *STE7*, *STE11*, *STE12* were all found this way (Burkholder & Hartwell 1985; Hagen et al 1986). Presumably, if mutations in *FIG2* caused sterility, it would have been identified in such screens. *FIG2* has a number of sequenced-based homologs that have been studied. The closest homologs of *FIG2* by protein sequence are *FLO11/MUC1*, *FLO1*, *FLO9*, and *AGA1* (*Saccharomyces* genome Database, http://genome-www.stanford.edu/Saccharomyces/). *FLO11* is involved with agar invasion and pseudohyphal growth (Lo & Dranginis 1996; Lo & Dranginis 1998). *FLO1* and *FLO9* are likely

associated with flocculation (Kobayashi et al 1998). *AGA1* plays a role in sexual agglutination. Mutations in these genes do not result in sterility.

There has been a report of a possible role for *FIG2* in mating (Erdman et al, 1998). Mating was found to be more efficient in both bilateral and unilateral (**a** cell mutant x wild type α) mating, but only in liquid medium. Bilateral mating on filters was actually less than in wild type. My results do not concur. As can be seen (Figure 29), both types of unilateral cross resulted in mating that did not appear to differ from wild type controls. This experiment was on solid medium. The results of corresponding experiments in liquid medium were inconsistent and equivocal, and consequently not reported.

The Role of *FIG2* in Agglutination

Another potential phenotype for a mating specific gene is sexual agglutination. Sexual agglutination in yeast has been extensively studied in a number of laboratories throughout the world, including the laboratory in which this study was conducted (Cappellaro et al 1991; Lipke & Kurjan 1992; Yanagishima 1986). In this phenomenon, the pheromone inducible α-agglutinin on α cells binds to the corresponding **a**-agglutinin on **a** cells. The

tightly agglutinated cells then undergo fusion to form diploids. Interestingly, agglutination is not required for cells to mate on solid media, although the efficiency is lowered somewhat. Perhaps, *FIG2* somehow plays a role in glycoprotein mediated agglutination.

As already mentioned (Introduction), hyperagglutination has recently been reported in both uni- and bi-lateral mating mixtures (Erdman et al., 1998). However, these results are difficult to evaluate since there was no description of the growth media used, growth phase of the cells, state of pheromone induction, mutant cell type in the unilateral experiment, or even the mechanics of the agglutination assay itself, which is apparently only semiquantitative.

Clearly, the results of Erdman et al. indicate that *fig2* mutants hyper-mate at 30^0C and hypo-mate and 16^0C. The result shown for bilateral hyperagglutination is also clear, despite the qualitative nature of their assay. As they, themselves, indicate (page 469, second column, line 29),

"... loss of Fig2p reproducibly increases the mating efficiency 3.2-7.2 fold in both unilateral and bilateral matings. Increased mating efficiency through the loss of a gene product in otherwise wild-type cells is a novel phenotype for a gene that functions in mating. The increased mating efficiency for *fig2Δ* strains is likely because of their enhanced agglutination relative to the wild-type cells ..."

Interestingly, Erdman et al. also noted that "Hyperagglutination of *fig2Δ* strains during mating was observed at both 30^{0}C and 16^{0}C, indicating that the cold sensitivity of *fig2Δ* mutant matings is caused by a defect "independent of agglutination". In my view, these statements are contradictory. Although a temperature sensitive mutation would be expected to exhibit a mutant phenotype (in this case, hyperagglutination) at the restrictive temperature (30^{0}C), a normal phenotype would be expected at the permissive temperature (16^{0}C). Yet these investigators observed hyperagglutination at both temperatures. Clearly then, changes in agglutination cannot explain both the hypermating seen at 30^{0}C and the hypomating seen at 16^{0}C. This would indeed require "a defect independent of agglutination", but it is quite difficult to imagine that a random mutation in a single gene product would affect different systems at different temperatures. Understandably, Erdman et al. are at a loss to explain this result.

The agglutination experiments reported here were obtained with a photometric assay that is arguably the most sensitive and quantitative agglutination assay extant (Terrance and Lipke, 1981). In this case, as shown in Figure 23, *fig2* deleted α-cells agglutinated more strongly with

either wild type **a** cells or *fig2Δ* **a** cells than the undeleted wild type. As can be seen, this effect is quite profound. When **a** cells were deleted, these cells agglutinated normally with the wild type α cells. This result too, appears unequivocal. The results therefore clearly demonstrate that increased agglutinability is exhibited only by *fig2* mutant α-cells (Fig 23). If, as has been suggested by Erdman et al. (1998), increased agglutinability is responsible for higher rates of mating in liquid medium, this effect should be specific to mating combinations in which the α-cells are *fig2* mutants. However, these investigators report increased mating efficiency in both bilateral matings and in unilateral matings. The latter matings were between **a** cell mutants and wild type α-cells. Since this latter combination will clearly not result in significantly increased agglutinability, this cannot be the phenomenon underlying increased mating.

Based on the Northern analysis discussed earlier, *FIG2* is expressed in **a** cells, as well as in α-cells. It would seem logical that *FIG2* plays a role in **a** cell agglutination, as it does in α–cell agglutination. Paradoxically, such would appear not to be the case.

To confirm the results of agglutination experiments with *FIG2* deleted strains. A "reverse" experiment was done, in which *FIG2* was overexpressed in each mating type. If the deletion of *FIG2* in α-cells resulted in an increase in agglutination, overexpression would be expected in result in a decrease in agglutination when compared to the wild type. On the other hand, since deletion of *FIG2* in **a** cells showed no obvious effect in respect to agglutination, overexpression of *FIG2* in **a** cells would likely show no effect as well. The results shown in Figure 24 confirm the expectations for both α-cells and **a** cells. Agglutinability in α cells was decreased when *FIG2* was overexpressed. Overexpression in **a** cells produced no change in agglutinability.

Upon exposure to **a**-factor, α-agglutinin transcripts increase 20 fold (Lipke et al 1989). Yet, the corresponding level of surface α-agglutinin is increased by 2-7 fold, and agglutinability is only increased 1.5-2.5 fold (Lipke & Kurjan 1992). Clearly, the increase in transcription of the gene for α-agglutinin is disproportionately greater than the corresponding increases in expressed protein levels or agglutinability. This implies that the regulation of α-agglutinin expression at the cell surface is complex and possibly occurs on many levels. The facts that *FIG2* is inducible by pheromone and appears

to be a down-regulator of agglutinability may, in part, explain the disproportionality seen in those experiments of Lipke et al. (Lipke et al 1989).

As shown in Figure 28, the amount of induced RNA for α-agglutinin remains identical whether or not *FIG2* is overexpressed. This implies that the down regulation of agglutinability by *FIG2* probably does not occur through repression of transcription of the α-agglutinin gene. This suggests that any down regulation is likely to occur posttranscriptionally.

A number of genes that regulate agglutinability have been described (Hartwell 1980; Sprague et al 1983a; Trueheart et al 1987). These mutants have been shown to represent genes for various components of the pheromone response pathway. Not surprisingly, these genes are pleiotropic in their effects. The decreased expression of any number of pheromone-inducible gene products, including the structural genes for the agglutinins, might account for the agglutination defects observed in these mutants. The unaltered expression of **a**-agglutinin (as measured by unaltered agglutinability) as the gene dosage of *FIG2* changes implies that *FIG2* does not affect the gene products in the pheromone response pathway in this cell

type. α-cell agglutinability, on the other hand, is affected by *FIG2*. The lack of apparent pleitropism is evidence that this gene may not play a role in signal transduction, but rather specifically affects α-agglutinin, whether directly or indirectly.

The Mechanisms of Down-Regulation of Agglutination by *FIG2*

The possible mechanisms by which *FIG2* may function in inhibiting α cell agglutination can be narrowed down to the following: i) *Fig2*p reduces translation of α-agglutinin. ii) The *FIG2* gene product binds to α-agglutinin on the cell surface which may result in a) an alteration of the overall structure or stability of α-agglutinin, or; b) specific masking or inactivation of the α-agglutinin active site that binds to **a**-agglutinin iii) *FIG2* alters the post-translational modification of α-agglutinin that is necessary for activity. iv) Fig2p may inhibit cellular components used in, the transport and/or secretion of α-agglutinin, v) *FIG2* may simply compete with α-agglutinin for limited sites on the cell surface. or vi) Being a relatively large molecule, *FIG2* might simply act as a large umbrella, masking the availability of α-agglutinin on the cell surface.

An attempt was made to detect binding of radiolabeled α-agglutinin to whole α-cells with or without the expression of *FIG2*. No binding was found. Using purified *FIG2* protein instead of the whole cells would have been a better experiment. The disadvantage of using whole cells is that the binding sites of cell surface *FIG2* may not be available due to the presence of cell surface α-agglutinin which, being adjacent on the *FIG2*, might have an advantage in binding to Fig2p over the labeled α-agglutinin in solution. Alternately, the Fig2p binding site for α-agglutinin may simply be unavailable to soluble α-agglutinin.

A Human Homolog of *FIG2*

The human *MUC1* gene is at the top of the list in the search for human genes that are homologous to the yeast *FIG2*. The sequence similarity between *MUC1* and *FIG2* is primarily due to their high serine/threonine contents, since they do not share a common motif. Interestingly, in addition to having high serine/threonine contents, both genes code for cell-surface molecules, have internal repeats, and have anti-adhesion properties, as is discussed below.

The Human *MUC1* Gene

The *MUC1* membrane mucin was first identified as the surface molecue resognized by monoclonal anbodies directed towards both normal and cancerous epithelial cells (Taylor-Papadimitriou et al 1999). Mucins exist as both as membrane-bound glycoproteins, and, without their anchorage sequence, as an epithelial secretion. The latter is a major constituent of the mucus that protects and lubricates mammalian epithelia. Mucins are a family of high molecular weight proteins that are heavily *O*-glycosylated through serine and threonine linkages (Rose 1992). These glycoproteins have an extended ectodomain, consisting of 30-90 homologous 20-amino acid repeats that are rich in serine, threonine, and proline (Lagow et al 1999). These repeats are likely to form a polyproline β-helix. The ectodomain of the membrane-bound form can protrude more than 200 nm above the cell surface, whereas most cell surface molecules do not extend beyond 35 nm (Wesseling et al 1996).

The human *MUC1* gene was first isolated and characterized by Lan et al. (Lan et al 1990). Muc-1p is preferentially expressed on the apical surface of most polarized epithelial cells. Its postulated biological functions include physiochemical protection from toxins and mutagens, signal transduction, regulation of cell growth, and adhesion modulation (Winterford et al 1999).

Human Mucin is Implicated in Some Cancers

The expression of *MUC1* has been found to be associated with adenocarcinomas of the breast, pancreas, colon, kidney and ovary (Ho & Kim 1994; Xing et al 1998). In malignant cells, the expression of *MUC1* is up-regulated (Walsh et al 1999). In such cells, *MUC1* is no longer concentrated at the apical surfaces of cells, but rather, is delocalized all around the cell surface (Seregni et al 1997). Additionally, in cancerous cells, Muc-1p has an aberrant glycosylation pattern. This exposes the highly immunogenic internal repeat core peptides (Samuel & Longenecker 1995).

Muc-1p is a Ligand to ICAM-1

MUC1 has been shown to be a ligand for intercellular adhesion molecule 1 (*ICAM-1*) (Kam et al 1998; Regimbald et al 1996). Recombinant Icam-1p readily binds to a murine adenocarinoma cell line transfected with *MUC1* (Kam et al 1998). This binding is inhibited by purified tumor *MUC1*, but not by synthetic *MUC1* peptides of 9 to 24 amino acids. However, a peptide consisting of six tandem repeats of *MUC1* (120 aa's), was as effective an inhibitor as purified *MUC1*.

Muc-1p is a Anti-adhesive Molecule

MUC1 is an anti-adhesive molecule. Wesseling et al. have demonstrated that overexpression of *MUC1* inhibits integrin-mediated cell adhesion to extracellular matrix components (Wesseling et al 1995). *E*-cadherin-mediated cell-cell adhesion is also inhibited by *MUC1*(Wesseling et al 1996). The anticancer drug adriamycin reduces *MUC1* on the cell surface, resulting in increased *E*-cahedrin mediated cell-cell adhesion. In this report, it was proposed that *MUC1* nonspecifically reduced cell-cell and cell-extracellular matrix interactions *in vitro* and *in vivo*, presumably by steric hindrance caused by the extreme length and high density of *MUC1* on the cell surface. Support for this proposal was drawn from the positive correlation between the incremental deletion of the internal repeats of *MUC1* and the progressive diminution of anti-adhesive properties.

All of this raises the possibility of a *MUC1*-based vaccine directed at the deglycosylated proteins of cancerous cells. To investigate this possibility indirectly, researchers in Amsterdam have conducted the following study. They took serum samples from early breast cancer patients who had not yet received treatment, and from non-cancer patient controls, and measured naturally occurring *MUC1* specific antibodies. The progress of the disease

was followed closely. The results showed that the survival of patients is positively correlated with pretreatment serum antibody levels that were equal or higher than the average (von Mensdorff-Pouilly et al 2000).

Biomira Inc. has developed a *MUC1*-based vaccine (THERATOPE) designed to protect against breast cancer. Phase III clinical trials are currently under way (www.biomira.com). Results, so far, are encouraging.

One of the enduring significant problems in cancer therapy is the fact that, in the cancerous state, immune function is repressed (Agrawal et al 1998). Soluble Muc1p has been implicated in this immunosuppression, as it has been shown to inhibit T-cell activation (Agrawal et al 1998; Chan et al 1999). It would be interesting to determine whether or not *FIG2* might also inhibit immune function.

Clearly, *FIG2* and *MUC1* share both structural and functional features. Yet, the definitive biological function(s) of both genes are still uncertain. Might expression of *MUC1* in *S. cerevisiae* affect agglutination? Will adriamycin, which reduces *MUC1* levels in humans, affect *FIG2* expression and agglutination in yeast?

Table 1: Yeast strains used in this study

Strain	Genotype or derivation	Source
W303-1A	*MAT***a** *ade2-1 can1-100 ura3-1 leu2-3, 112 trp1-1 his3-11,15*	R. Rothstein
W303-1B	*MATα ade2-1 can1-100 ura3-1 leu2-3, 112 trp1-1 his3-11,15*	R. Rothstein
W303-A/B	*MAT***a***/ MATα ade2-1/ade2-1 can1-100/can1-100 ura3-1/ ura3-1 leu2-3, 112/ leu2-3, 112 trp1-1/ trp1-1 his3-11,15/ his3-11,15*	R. Rothstein
N435-1A	*MAT***a** *his7 lys7(ts) met6 arg6 gal4 MAL2 SUC*	J. Kurjan
N435-2A	*MATα his7 lys7(ts) met6 arg6 gal4 MAL2 SUC*	J. Kurjan
X2180-1A	*MAT***a** *SUC2 mal mel gal2 CUP1*	Yeast Genetic Stock Center
X2180-1B	*MATα SUC2 mal mel gal2 CUP1*	Yeast Genetic Stock Center

Table 2: *Echerichia coli* strains used in this study.

Strain	Genotype	Source
DH5α	*supE*44 Δ*lac*U169 (ϕ80 *lacZ MAT*ΔM15) *hsdR*17 *recA1 endA1 gyrA*96 *thi*-1 *relA*1	Life Technologies
HB101	*ara*14,*gal*K2,*hsd*S20($r_B^- m_B^+$),*lac*Y1,*leu*B6,*mtl*-1, *pro*A2,*rec*A13,*rps*L20,*sup*E44,9,14,*thi*-1,*xyl*-5, Δ(*mcr*C-*mrr*),F	Clontech

Table 3: Plasmids

Name	Marker	Remarks	Source
2J251	*Amp*^{R}	Yeast library in YEp351	J. Hirsch
pUC18	*Amp*^{R}		Life Technologies
YEp24	*URA3*		Life Technologies
pRS313	*HIS3*		P. Heiter
p101a	*LEU2*	Partial *FIG2* in Yep351	This study
p102a	*Amp*^{R}	Partial *FIG2* in Puc18	This study
p103a	*Amp*^{R}	Partial *FIG2::URA3*	This study
pP2	*Amp*^{R}	Complete Fig2 ORF	This study
YCp *FIG2*	*HIS3*	*FIG2* expression in single copy	This study
YEp *FIG2*	*HIS3*	*FIG2* expression in multicopy	This study
pSM1	*HIS3*	*FIG2::GFP* in single copy	This study
pSM2	*HIS3*	*FIG2::GFP* in multi copy	This study

Table 4: The homolog of *AGA1*. The results of the search for *AGA1* (*YNR044W*) homologs in the Stanford University Saccharomyces Genome Database (SGD) using default parameters. *YCR089W* was the only gene that showed significant homology to *AGA1*. These results are based on the Smith-Waterman algorithm for comparing protein sequences, and were computed using the March 18, 199 version of the SGD database.

Target ORF/Gene Name	Chromosome	P-Value	% Ident	% Align	Gaps
YCR089W	3	6.70e-05	6.8	93.1	3

Table 5: The amino acid and molecular weight analysis of Fig2p.

Calculated Molecular Weight = 166 Kdal
Estimated pI = 4.63

Amino Acid Composition:

Non-polar:		No.	Percent
	Ala	90	5.59
	Val	103	6.40
	Leu	100	6.21
	Ile	80	4.97
	Pro	77	4.78
	Met	14	0.87
	Phe	42	2.61
	Trp	12	0.75
Polar:		No.	Percent
	Gly	47	2.92
	Ser	424	26.34
	Thr	291	18.07
	Cys	26	1.61
	Tyr	40	2.48
	Asn	50	3.11
	Gln	56	3.48
Acidic:		No.	Percent
	Asp	32	1.99
	Glu	57	3.54
Basic:		No.	Percent
	Lys	43	2.67
	Arg	12	0.75
	His	13	0.81

Table 6. Agar Diffusion Assay. The strains used were *W303-1A*, *W303-1B*, *W303-A/B* (a, α, a/α), and the corresponding *ycr089w* deleted strains. Cells were plated on YEPD soft agar at 10^5 cells per ml. The stock concentrations of the drugs were as follows. Econazole=1mg/ml; Tunicamycin=1mg/ml; Cerulenin=0.2 mg/ml; Echinocandin= 1mg/ml; Cyclohexamide=0.5 mg/ml; Aculeain= 1 mg/ml. 10 ul of drug stock solution was spotted on a 10 mm disk and placed on the surface of the agar. Cells were then incubated at 30^0C overnight. The zone of clearance was recorded in mm.

	a	aΔ	α	αΔ	a/α	a/α(Δ)
Econazole	28	24	25	23	26	26
Tunicamycin	14	14	14	13	13	14
Cerulenin	21	20	21	21	21	20
Cyclohexamide	18	18	18	17	19	17
Aculeacin	12	13	13	13	13	13
Echinocandin	18	17	17.5	16	19	19

Table 7: Binding of soluble, labeled α-agglutinin to whole cells. Purified recombinant α-agglutinin was labeled with I^{125} via Boton-Hunter Reagent. *W303-1B* (+) and *W303-1Bfig2Δ*(–) were grown to mid-log phase and induced with a-factor (40 ng/ml). Aliquots representing 10^8 cells of each strain were washed with water and resuspended in 200ul binding buffer (0.1 M NaAc pH5.0, 1 mM PMSF, 10 mg/ml BSA). Labeled agglutinin (10,000 cpm) was added to each cell suspension. One set was incubated at room temperature, and the other at 4^0C. Binding continued for 30 minutes. After binding, cells were washed 3 times with binding buffer at 4^0C. Cell pellets were then collected and counted in a gamma ray counter. (*) indicates pretreatment with un-labled α-agglutinin (100ng/ml, 20^0C, 30 min.)

FIG2 expression	Temperature ^{0}C	CPM	Standard deviation
-	20	485.3	49.6
+	20	561.7	7.6
+*	20	469.0	93.6
-	4	517.7	56.9
+	4	544.3	19.7

Figure 1: The results of alignment of ***YNR044W*** (*AGA1*) vs. ***YCR089W*** as performed by the Stanford University *Saccharomyces* Genome Database (SGC) using default parameters.

```
                20        30        40        50        60        70
YNR044 LLGLTNIALASDPETILVTITKTNDANGVVTTTVSPALVSTSTIVQAGTTTLYTTWCPLT
                                               : : ::  ::|| | :  ::: |||.|| :
YCR089 SNSTETIAVISNIHKTSSNKDYSLTTTQLKTSGMQTLVLSTVTTTVNGAATEYTTWCPAS
              720       730       740       750       760       770

                80        90       100       110              120
YNR044 VSTSSAAEISPSISYATTLSRFSTLTLSTEVCSHEAC-PS--------SSTLPTTTLSVT
                 ::::|:::  ::':|:::||.|||  | :         || :|  :  ' :
YCR089 -----------SIAYTTSIS-YKTLVLTTEVCSHSECTPTVITSVTATSSTIPLLSTSSS
                        780       790       800       810

              130       140       150       160       170       180
YNR044 SKFTSYICPTCHTTAISSL---SEVGTTTVVSSSA--IEPSSASIISPVTSTLSSTTSSN
        : ::| :     ::    | :   ::|::':::::  :   :' :  :  :   '::::::
YCR089 TVLSSTVSEGAKNPAASEVTINTQVSATSEATSTSTQVSATSATATASESSTTSQVSTAS
           820       830       840       850       860       870

               190       200       210       220       230       240
YNR044 PTTTSLSSTSTSPSSTSTSPSSTSTSSSSTSTSSSSTSTSSSSTSTSPSSTSTSSSLTST
        | ::::: : : :::    ::    |    :|:: | :|    |: : :   : : |   : :
YCR089 ETISTLGTQNFTTTGSLLFPA-LSTEMINTTVVSRKTLIISTEVCSHSKCVPTVITEVVT
           880       890       900       910       920       930

               250       260       270       280       290       300
YNR044 SSSSTSTSQSSTSTSSSSTSTSPSSTSTSSSSTSTSPSSKSTSASSTSTSSYSTSTSPSL
        |::: |::::|| : :: :: :: '| :. : '| :   :    : :   '::  ||    .
YCR089 SKGTPSNGHSSQTLQTEAVEVTLSSHQTVTMSTEVCSNSICTPTVITSVQMRSTPF-PYL
           940       950       960       970       980       990

               310          320           330       340       350
YNR044 TSS--SPTLASTSPSSTSISS---TFTDSTSSLG----SSIASSSTSVSLYSPSTPVYSV
        |    | :|| :   '   ·|    ||: ||:||         ':|   : :' :: : ::
YCR089 TSSTSSSSLASTKKSSLEASSEMSTFSVSTQSLPLAFTSSEKRSTTSVSQWSNTVLTNTI
          1000      1010      1020      1030      1040      1050

              360       370       380       390       400       410
YNR044 PSTSSNVATPSMTSSTVETTVSSQSSSEYITKSSISTTIPS-FSMSTYFTTVSGVTTMYT
        .: :' : :    :        : |. '    |   .::  .| :.:|.   : ::|: |:
YCR089 MSSSSNVISTNEKPSS--TTSPYNFSSGY---SLPSSSTPSQYSLSTATTTINGIKTVYT
          1060      1070        1080          1090      1100      1110

              420       430       440       450       460
YNR044 TWCPYSSESETSTLTSMHETVTTDATVCTHESCMPSQTTSLITSSIKMSTKNVATSVS-T
       ||': : :| :::  | : : ::|  | : :     ': :|| :||::: ::::,::'
YCR089 TWCPLAEKSTVAA--SSQSSRSVDRFVSSSK---PS--SSLSQTSIQYTLSTATTTISGL
            1120        1130      1140              1150      1160

          470       480       490       500       510          520
YNR044 STVESSYACSTCAETSHSYSSVQTASSSSVTQQTTSTKSWVS---SMTTSDEDFNKHATG
       :|, :::    |  .|:|  :: | :||::  : |::' :|   |::|| :: :: :
YCR089 KTVYTTW----CPLTSKSTLGATTQTSSTAKVRITSASSATSTSISLSTSTESESSSGYL
           1170          1180      1190      1200      1210      1220
```

```
        530       540       550       560       570       580
YNR044 KYHVTSSGTSTISTSVSEATSTSSIDSESQEQSSHLLSTSVLSSSSLSATLSSDSTILLF
       :  ! | .:|   :   ::::| :|  : |   !:   |:| :!::: .:  |: ::: .:
YCR089 SKGVCS-GTECTQDVPTQSSSPASTLAYSPSVSTS--SSSSFSTTTASTLTSTHTSVPLL
            1230      1240      1250      1260      1270

        590       600       610       620       630       640
YNR044 SSVSSLSVEQSPVTTLQISSTSEILQPTSSTAIATISASTSSLSATSISTPSTSVESTIE
       ! !!: : :!! :.  :!::      !!!:  :: ::':!:: |:':   : :
YCR089 PSSSSISA-SSPSSTSLLSTSLPSPAFTSSTLPTATAVSSSTFIASSLPLSSKS------
     1280      1290      1300      1310      1320      1330

        650       660          670       680          690       700
YNR044 SSSLTPTVSSIFLS---SSSAPSSLQTSVTTTEVSTT--SISIQYQTSSMVTISQYMGSG
       !   :.: !! ::!   ! : . :':: :  :  ! ::!:    :!:: ::
YCR089 SLSLSPVSSSILMSQFSSSSSSSSSLASLPSLSISPTVDTVSVLQPTTSIATLTCTDSQC
            1340      1350      1360      1370      1380      1390

             710       720
YNR044 SQTRLPLGKLVFAIMAVACNVIFS

YCR089 QQEVSTICNGSNCDDVTSTATTPPSTVTDTMTCTGSECQKTTSSSCDGYSCKVSETYKSS
            1400      1410      1420      1430      1440      1450
```

Figure 2: Schematic diagram of the *YCR089W* gene. The hydrophobic sequences of the *N*- and *C*-terminals are shown. The arrows are the potential *N* glycosylation sites. The residues of the internal repeats are shown in the box below.

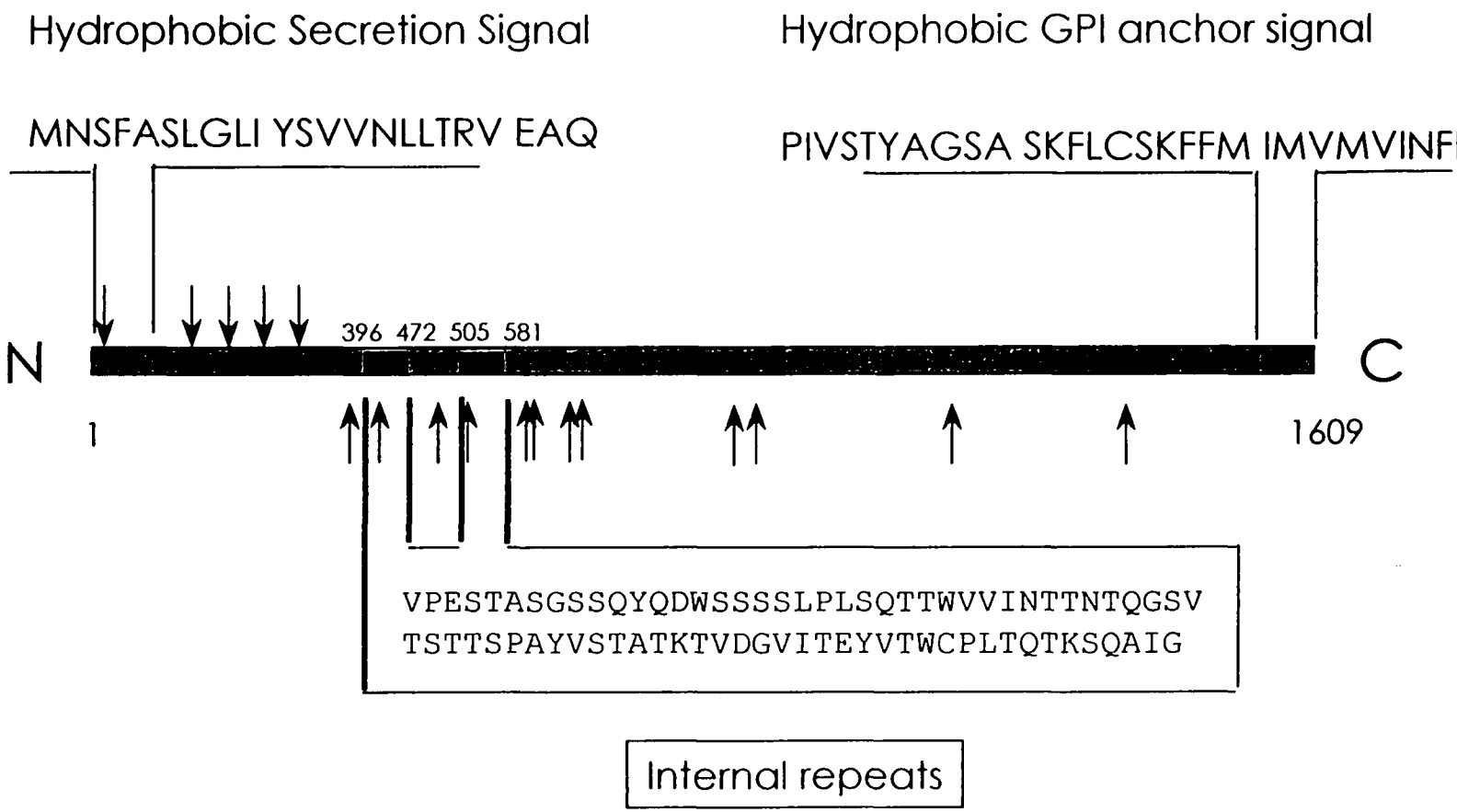

Figure 3: Schematic of the p101a plasmid, which was constructed from YEp351 into which 5 Kb of yeast DNA containing partial sequence of *YCR089W* was inserted between the *SmaI* and *SphI* restriction sites. Hatched sequence indicates yeast DNA. Black heavy lines indicate potential open reading frames.

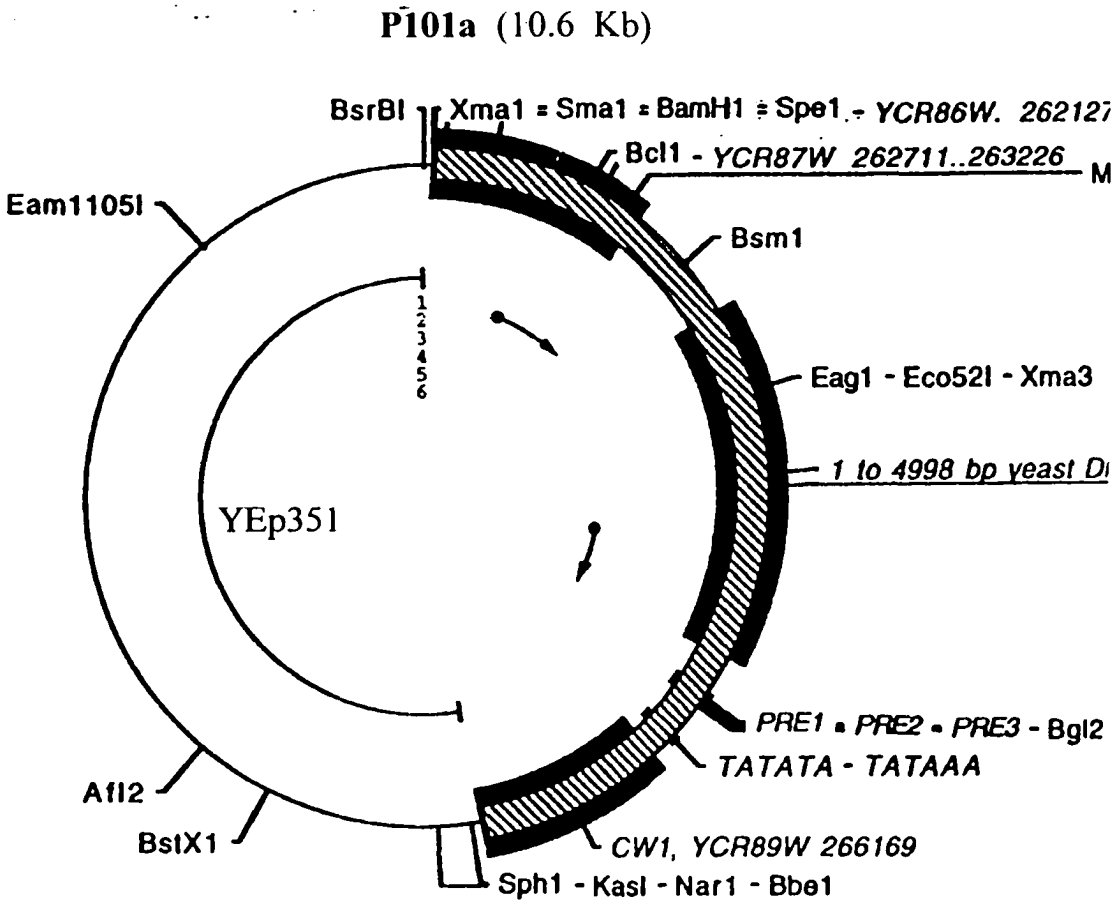

Figure 4: Map of the p102a plasmid, which was constructed by removing the plasmid backbone of p101a by *SmaI* and *SphI* digestion, and replacing by pUC18. Hatched sequence indicates yeast DNA. Black heavy lines indicate potential open reading frames.

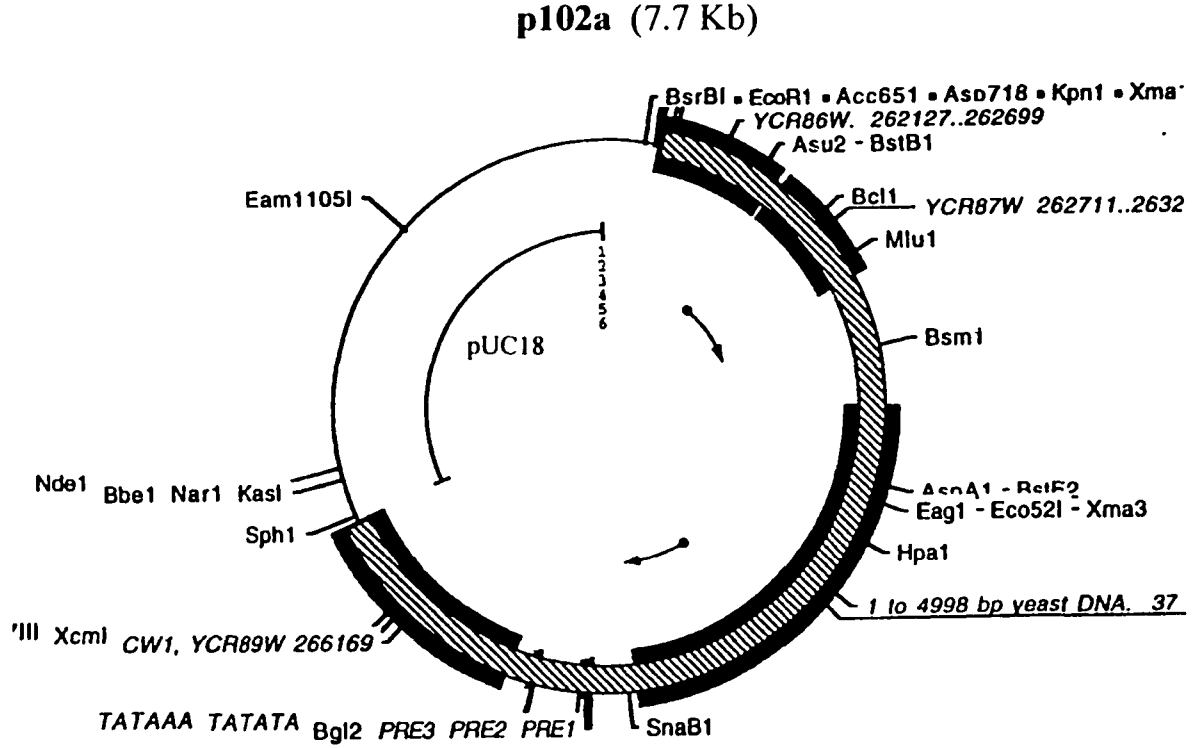

Figure 5: The plasmid map of p103a containing *YCR089W* disrupted by *URA3*.
Hatched sequence indicates yeast DNA. Black heavy lines indicate potential open reading frames.

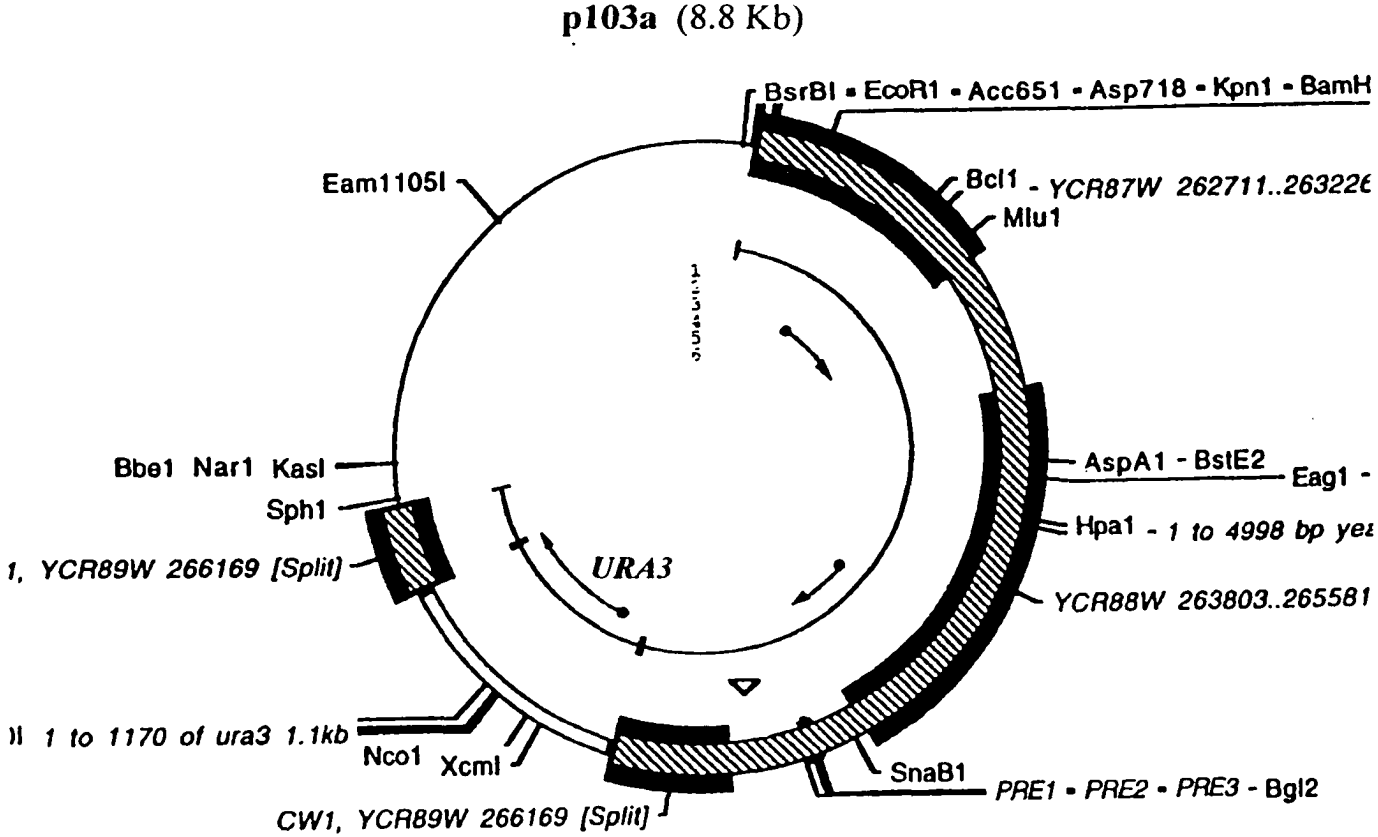

Figure 6: Southern analysis of *YRC089W* disruption by the *URA3* fragment. Genomic DNA was digested with *Hind III*. The blot was probed with a ^{32}P labeled *YCR089W* fragment.
In 6A,, lane 1-4: **a**-cells with *Δycr089;* lane 5-8: α-cells with *Δycr089w;* lane 9-12: **a**/α cells with *Δycr089w/YCR089W*. Lane 13 is wild type **a** cells.Lane 14 is wild type α cells. Lane 15 was wild type **a**/α cells.
In 6B, the position of *URA3* insertion is shown.

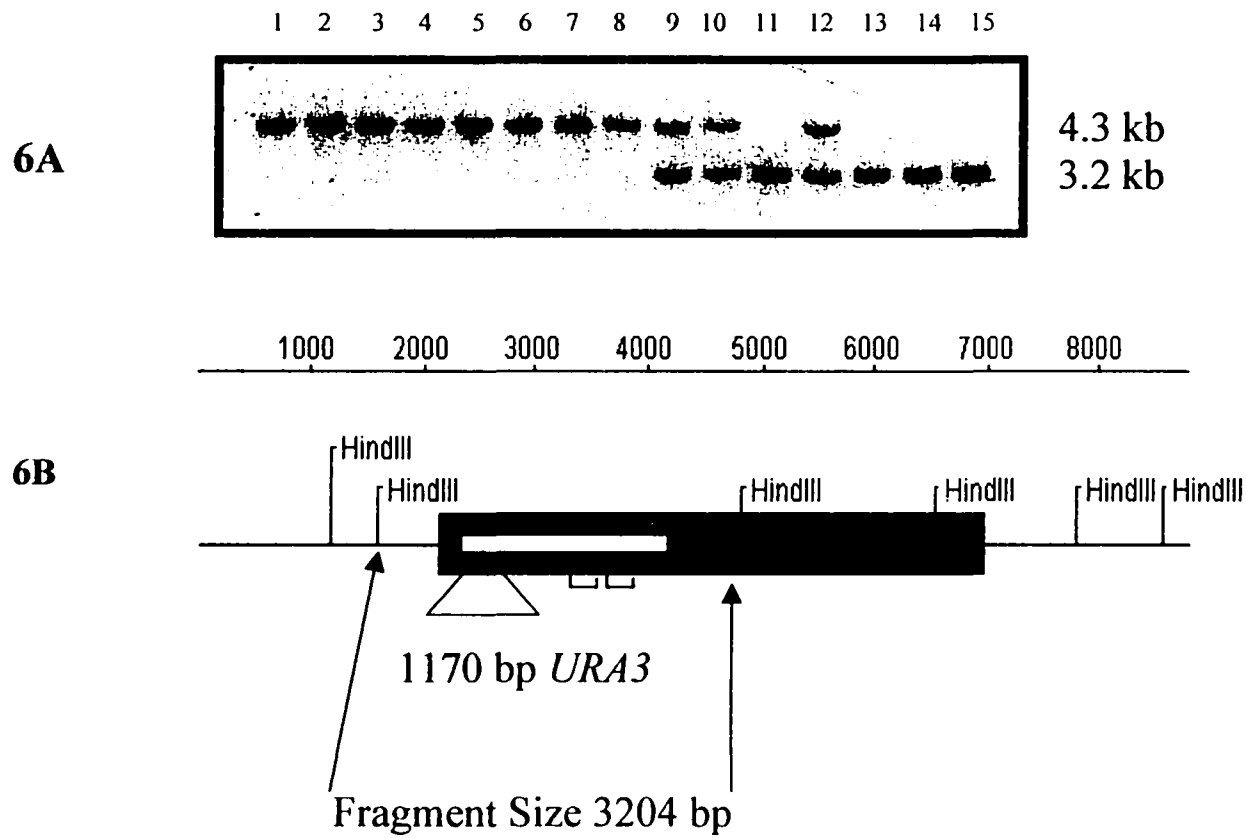

Figure 7: Southern analysis of *YRC089W* disruption by the *URA3* fragment. Genomic DNA was digested with *Hind III*. The blot was probed with a ^{32}P labeled *URA3* fragment.
In 7A,, lane 1-4: **a**-cells with *Δycr089;* lane 5-8: α-cells with *Δycr089w;* lane 9-12: **a**/α cells with *Δycr089w/YCR089W.* Lane 13 is wild type **a** cells.Lane 14 is wild type α cells. Lane 15 was wild type **a**/α cells.
In 7B, the position of *URA3* insertion is shown.

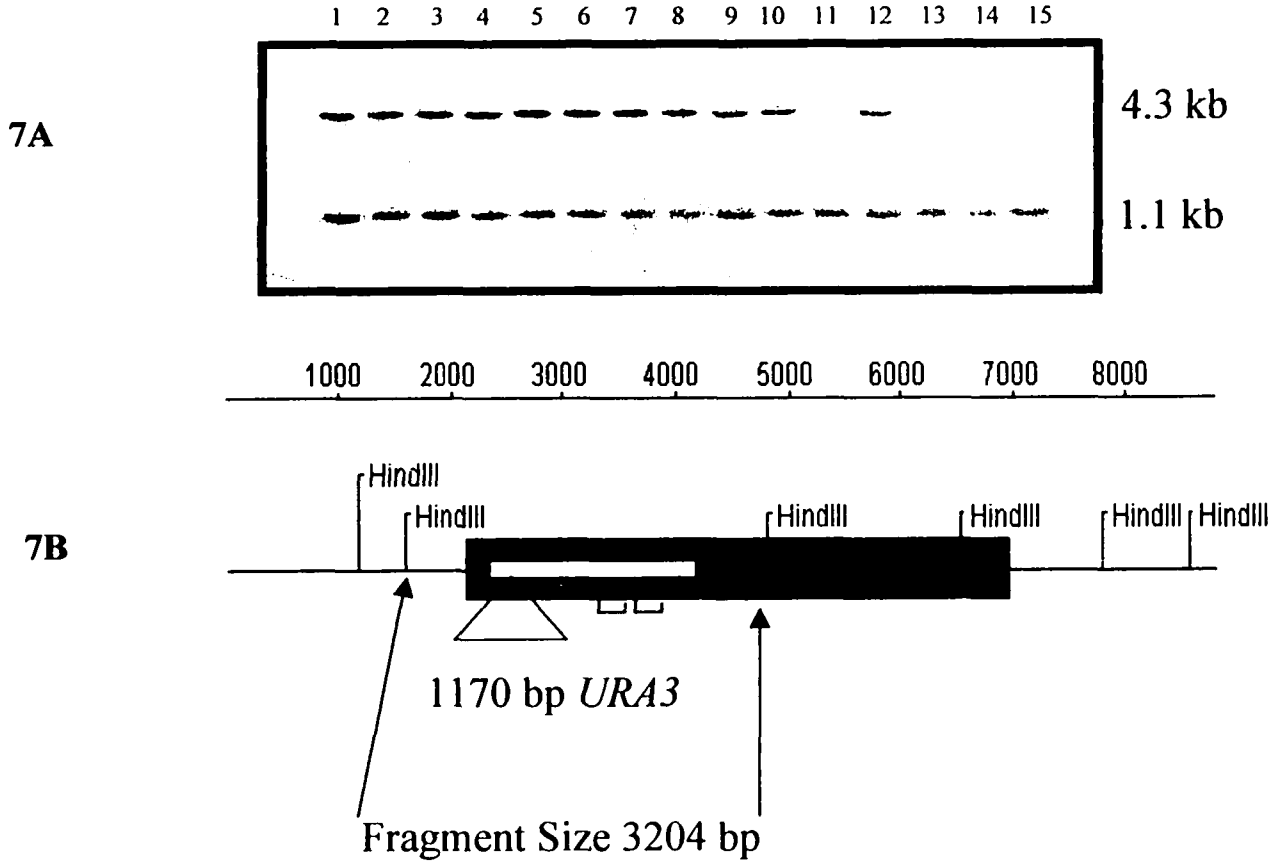

Figure 8: The growth curves of *Δycr089w* and their isogenic wild types. **a**, α, **a**/α cells and their corresponding disruptants in *YCR089W* were grown in YNB supplemented with uracil. Growth was monitored by absorbance at 660nM

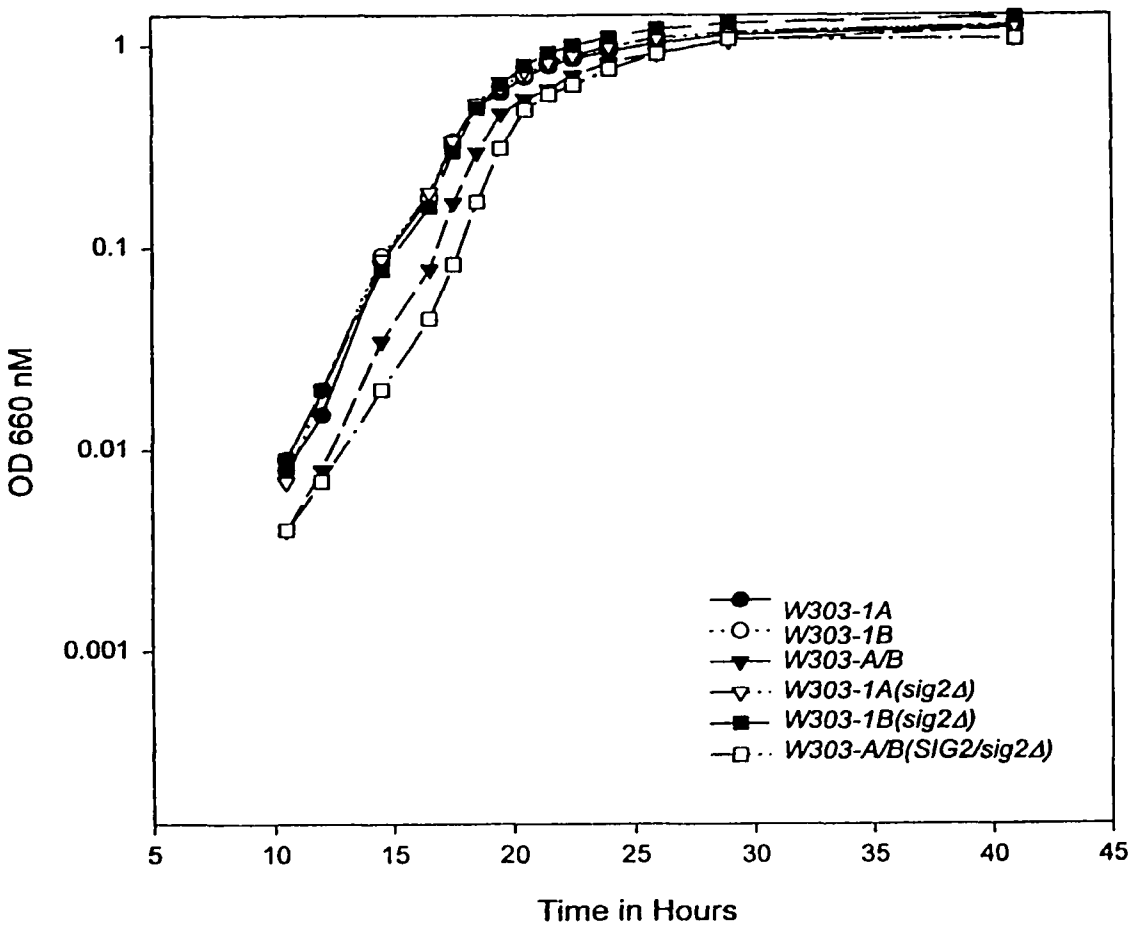

Figure 9: Linear regression analysis of the growth curves of *Δycr089w* and their isogenic wild types. **a**, α, **a**/α cells and their corresponding disruptants in *YCR089W* were grown in YNB supplemented with uracil. Growth was monitored by absorbance at 660nM. Data from the log phase of growth analyzed by Sigma Plot Linear Regression Analysis.

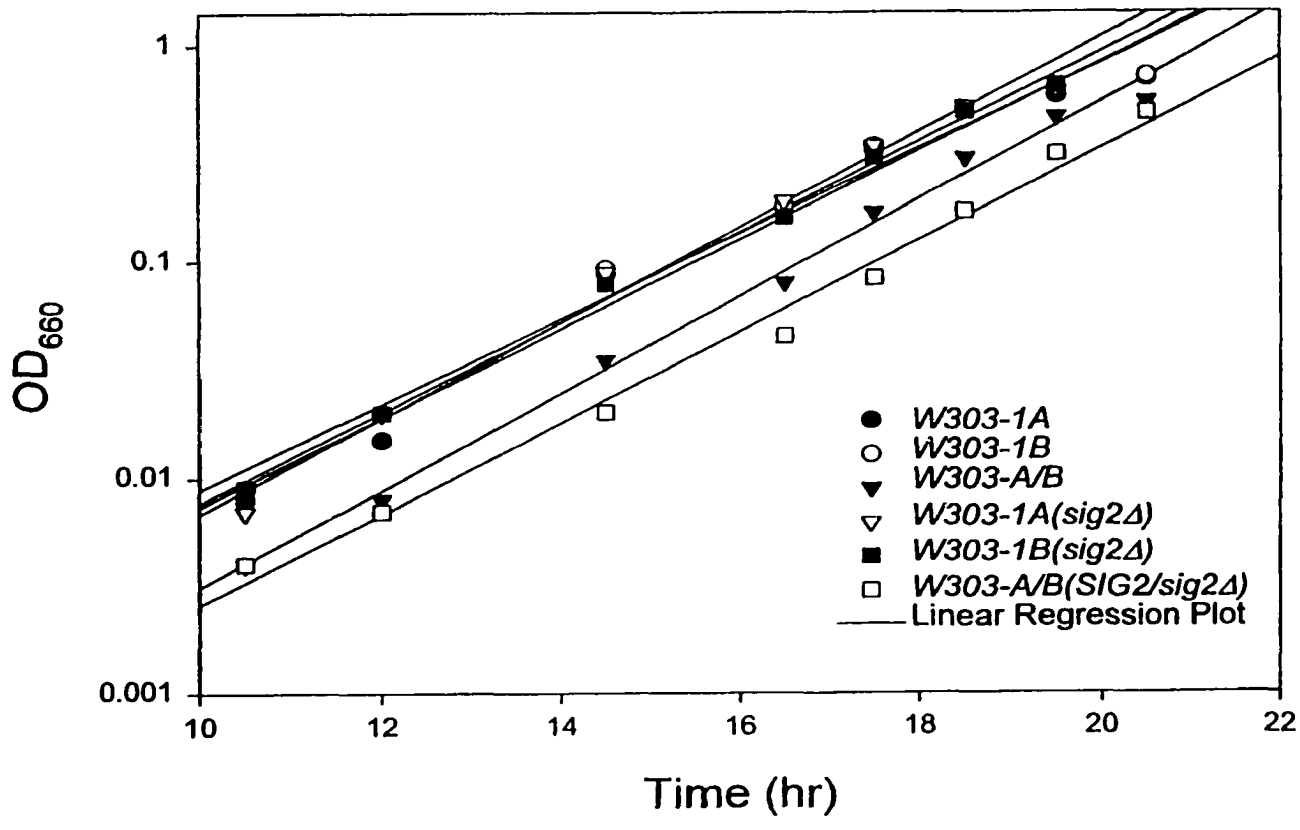

Figure 10: The cell morphology of **a** cells and the isogenic *Δycr089w*. Cells were grown at 30^{0}C in YNB supplemented with uracil and harvested at 0.1 O.D. Cells were viewed in a bright field microscope and photographed at 100X.

10A
Normal wild type **a** cells

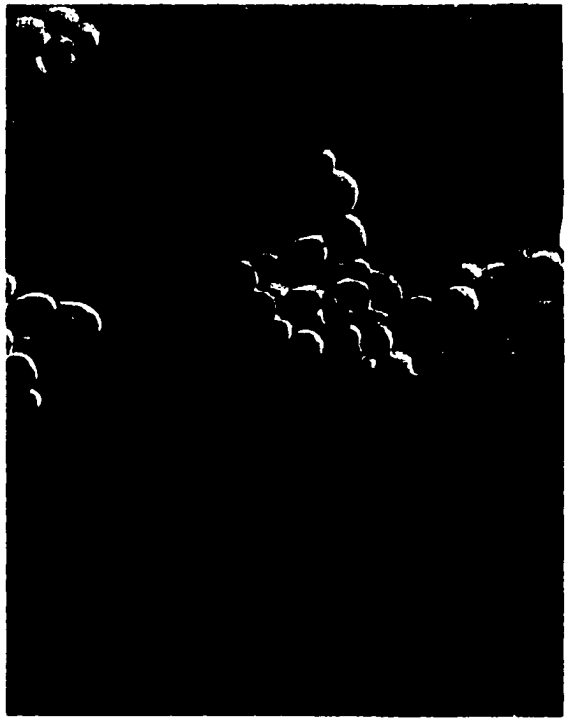

10B
Δycr089w **a** cells

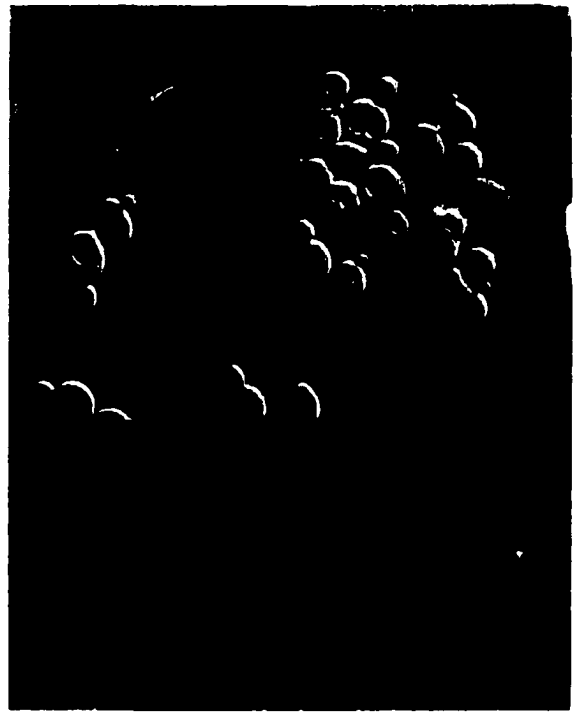

Figure 11: The cell morphology of **a** cells and the isogenic *Δycr089w*. Cells were grown t 30°C in YNB supplemented with uracil and harvested at 1.5 O.D.. Cells were viewed by a bright field microscopy.

11A
Normal wild type **a** cells 40X

11B
Δycr089w **a** cells 40X

11D
Δycr089w **a** cells 100X

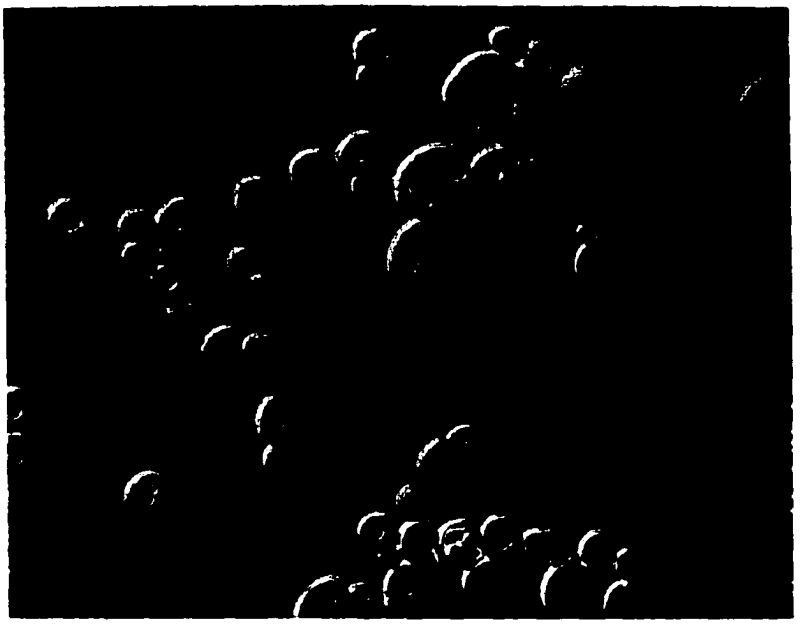

11C
Normal wild type **a** cells 100X

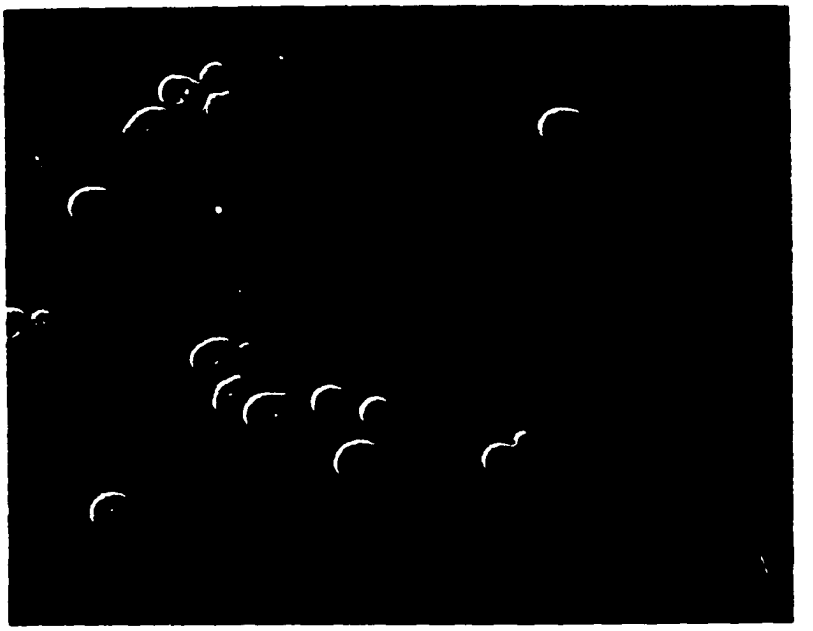

Figure 12: The cell morphology of α cells and the isogenic *Δycr089w*. Cells were grown at 30°C in YNB supplemented with uracil and harvested at 1.5 O.D.. Cells were viewed by bright field microscopy.

12A
normal wild type α cells 40X

12B
Δycr089w α cells 40X

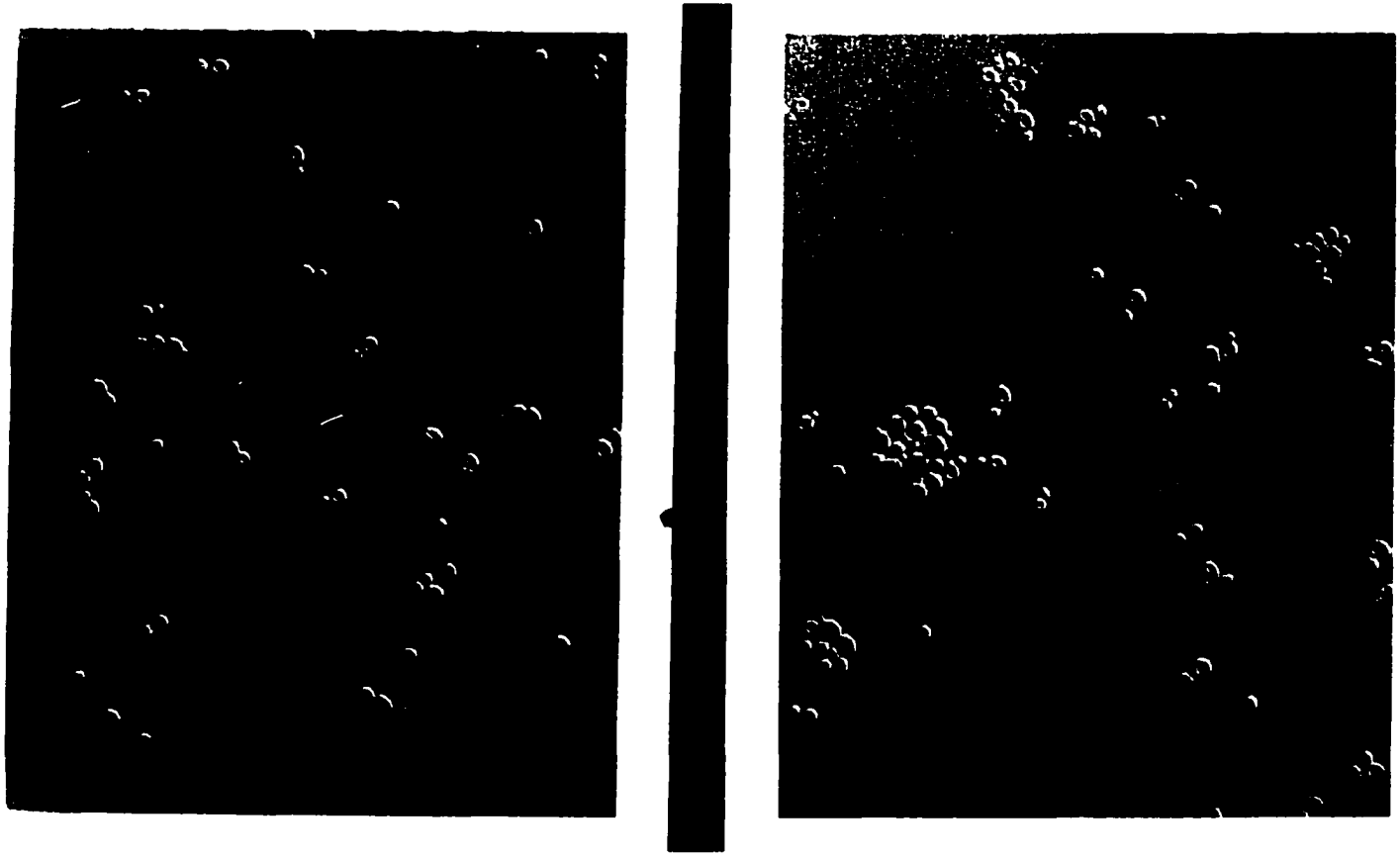

12D
Δycr089w α cells 100X

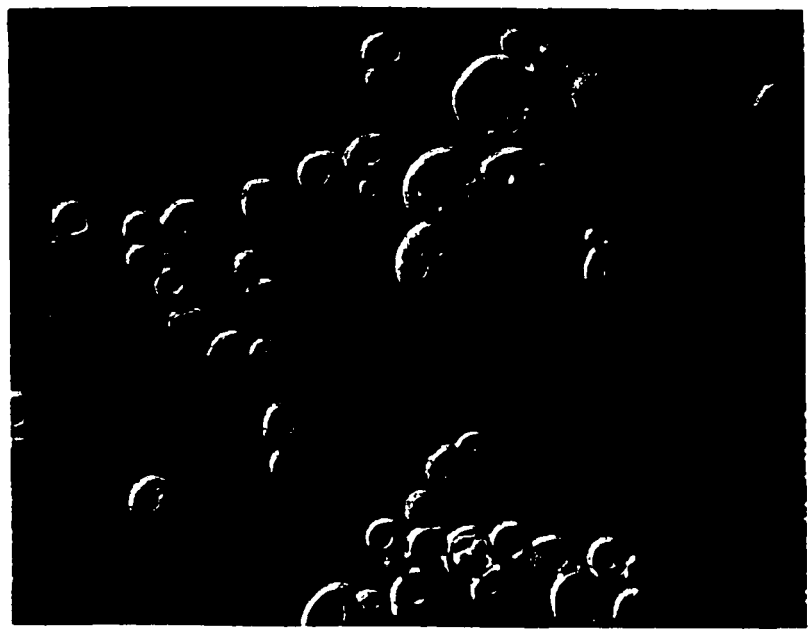

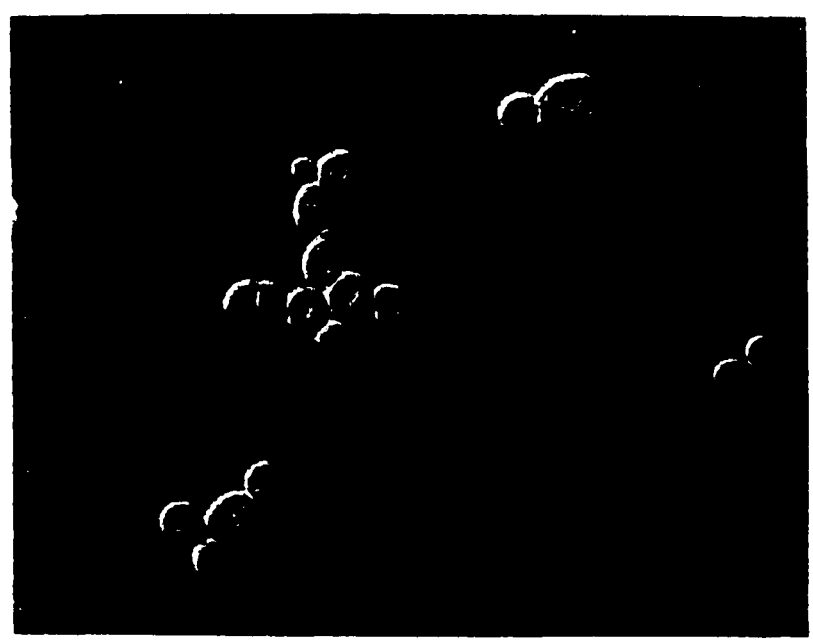

12C
normal wild type α cells 100X

Figure 13: The cell morphology of **a**/α cells and the isogenic *Δycr089w*. Cells were grown at 30^{0}C in YNB supplemented with uracil and harvested at 1.5 O.D.. Cells were viewed by bright field microscopy.

13A
normal wild type **a**/α cells 40X

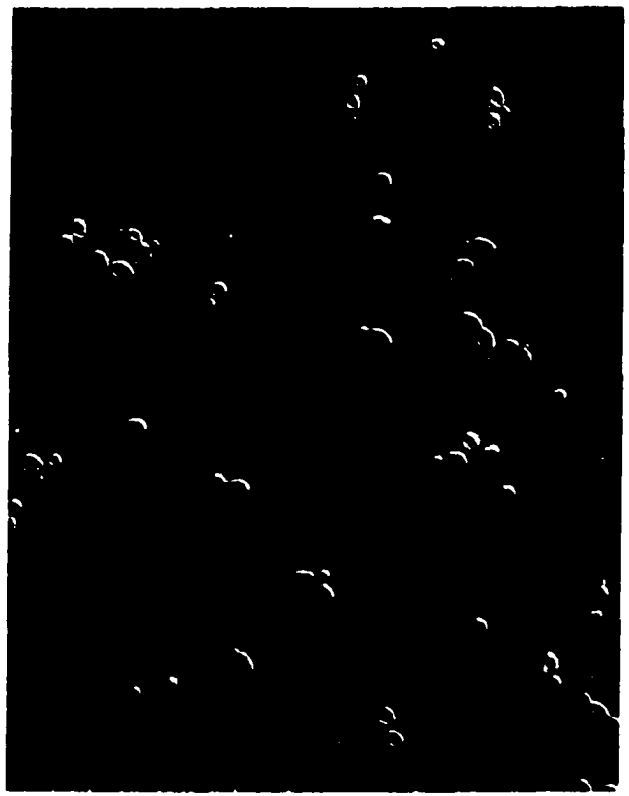

13B
Δycr089w/YCR089W **a**/α cells 40X

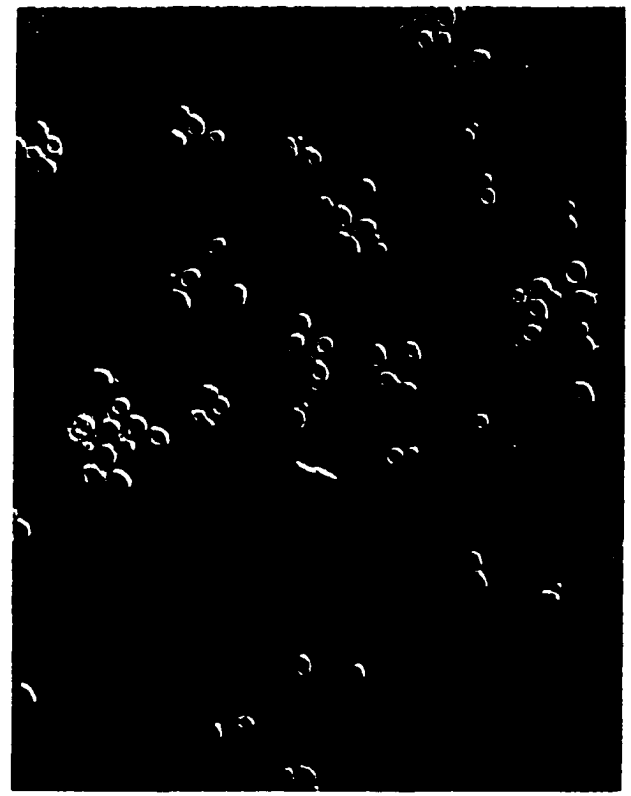

Figure 14: Spheroplast formation assay. *W303-1A* were grown at 30^{0}C in the media indicated to either mid log (0.2 OD_{660} or stationary (1.5 OD_{660}) phase. Zymolyase was then added to 30 ug/ml, and the cells incubated for the time indicated.
Optical density was then measured to indicate the degree of cell lysis.

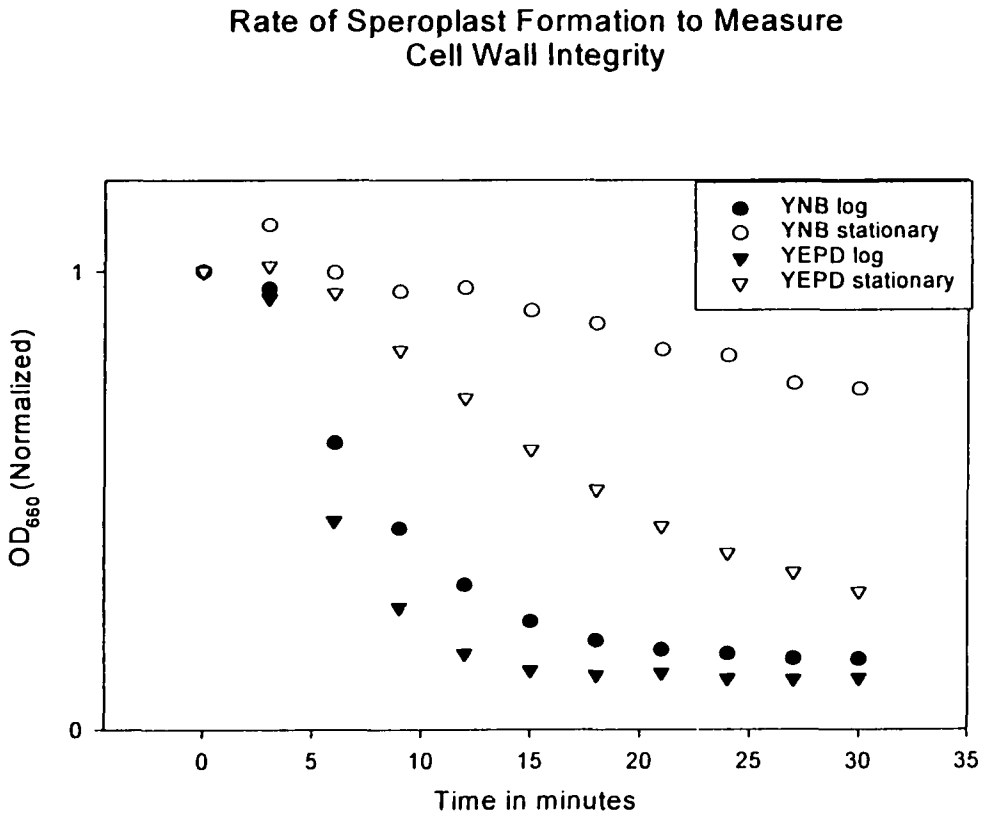

Figure 15: Wild type *W303-1A* and its isogenic *Δycr089w* were measured for their ability to resist Zymolyase digestion. Cells were treated as described in Figure 14.

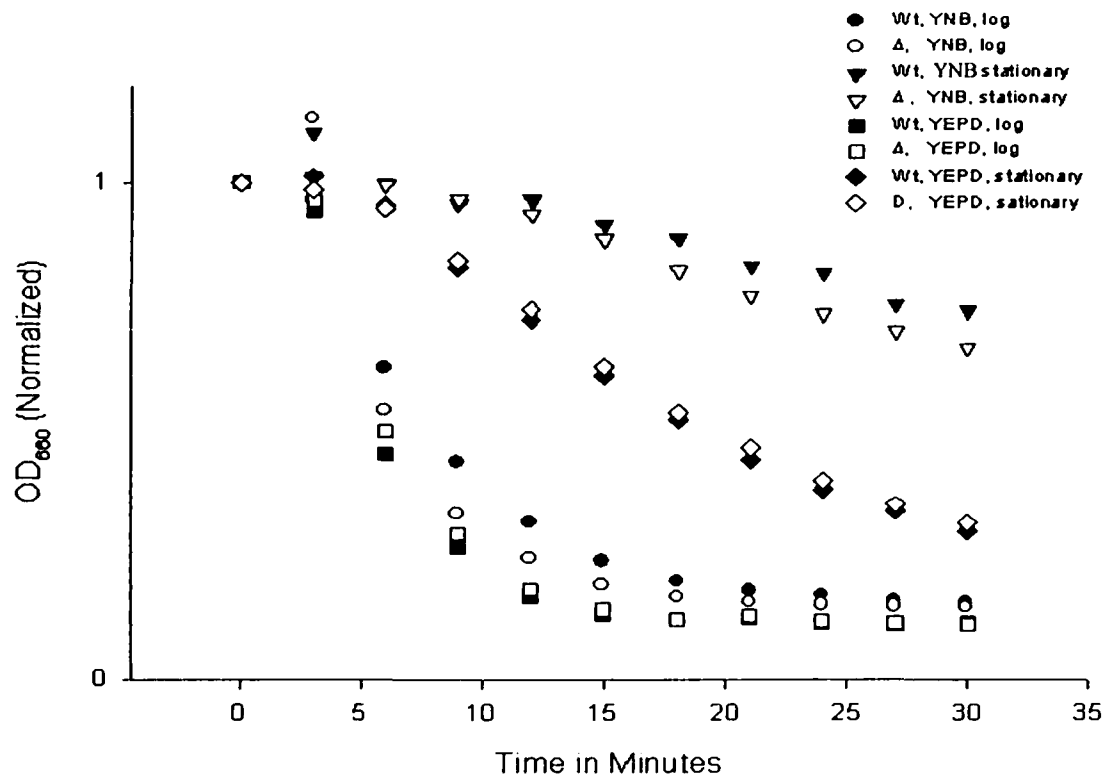

Figure 16: Wild type *W303-1A* and the isogenic *Δycr089w* were grown in YNB supplemented with uracil at th temperature indicated. Cells were subjected to the spheroplast formation assay as described in Figure 14.

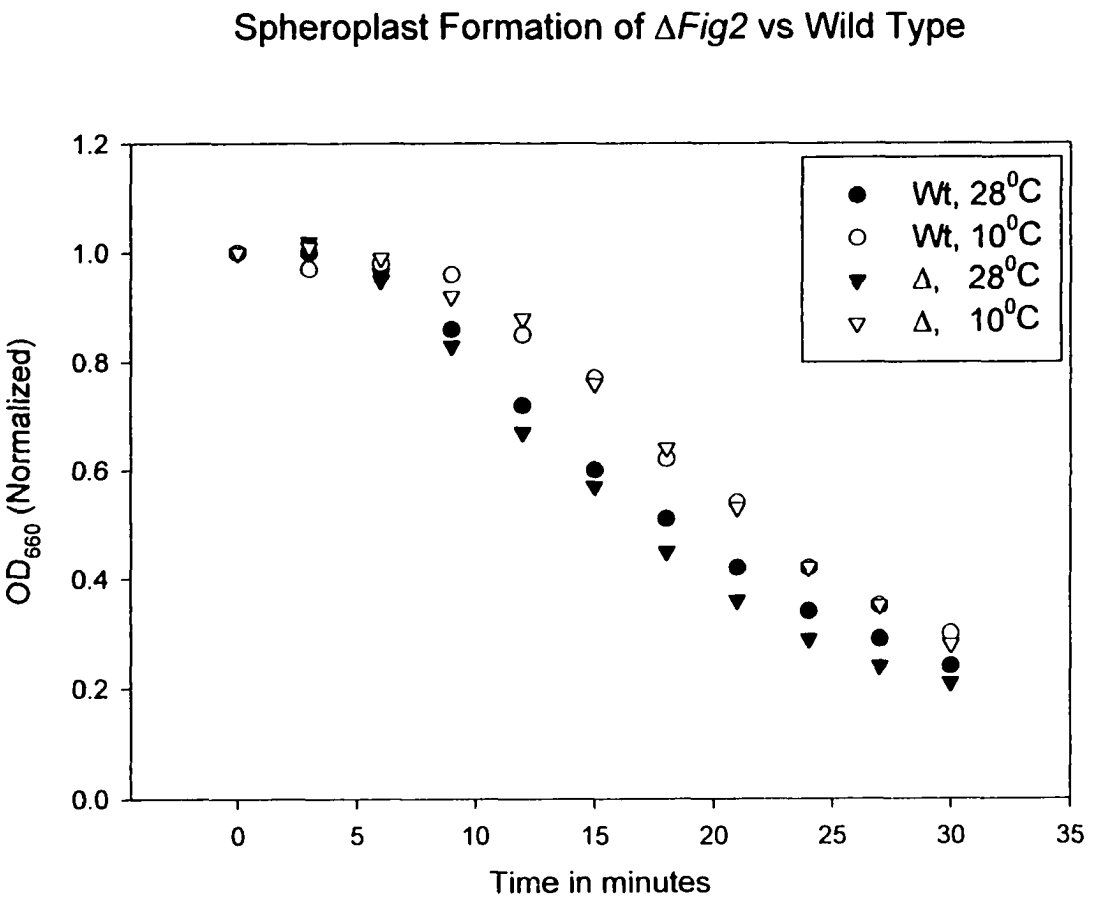

Figure 17. a Cells were grown at 30^{0}C in YNB supplemented with amino acids until cells reached O.D.=0.2 Cells were then treated with α factor at 400 ng/ml for 4 hours.

17A
2180-1A (40X)

17B
W303-1A (40X)

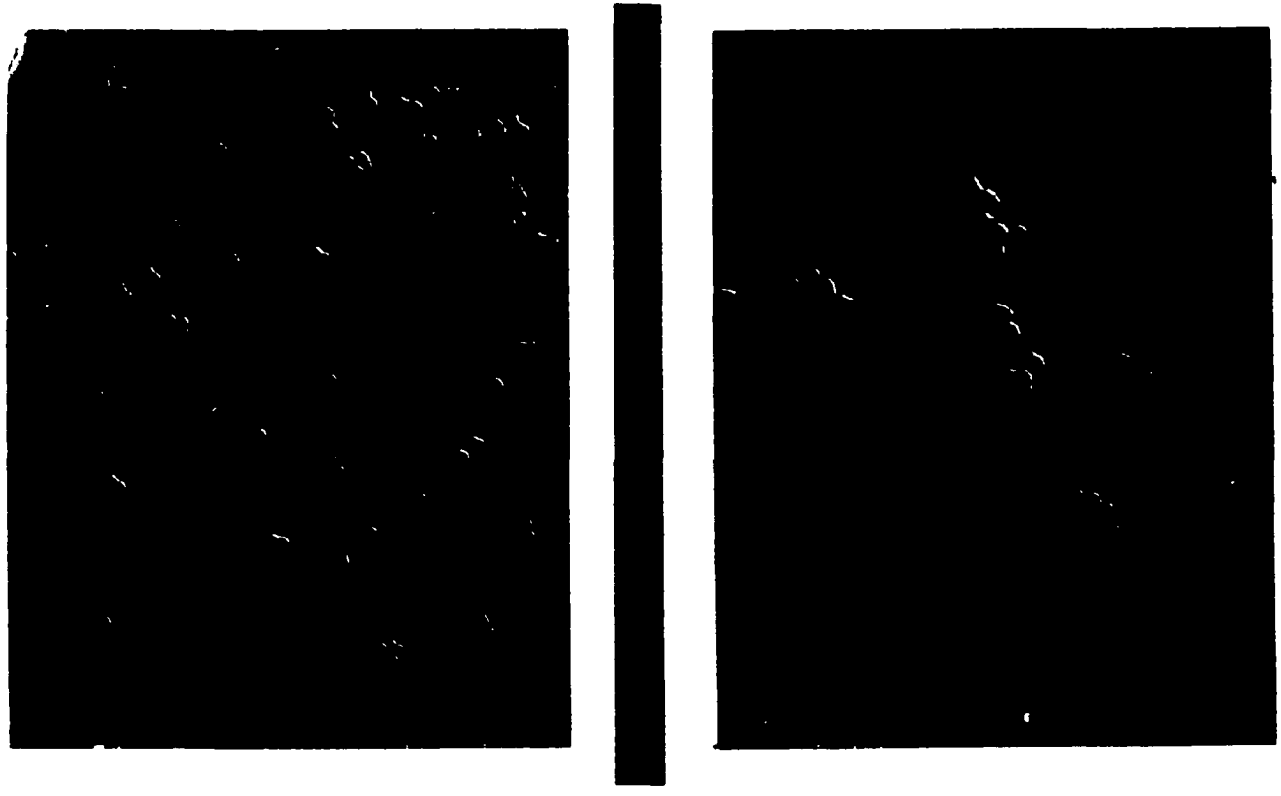

Figure 18. a *Δycr089w* and *W303-1A* were grown at 30^{0}C in YNB supplemented with amino acids until O.D.=0.2. Cells were then treated with α factor at 400 ng/ml for 4 hours.

18A

W303-1A(40X)

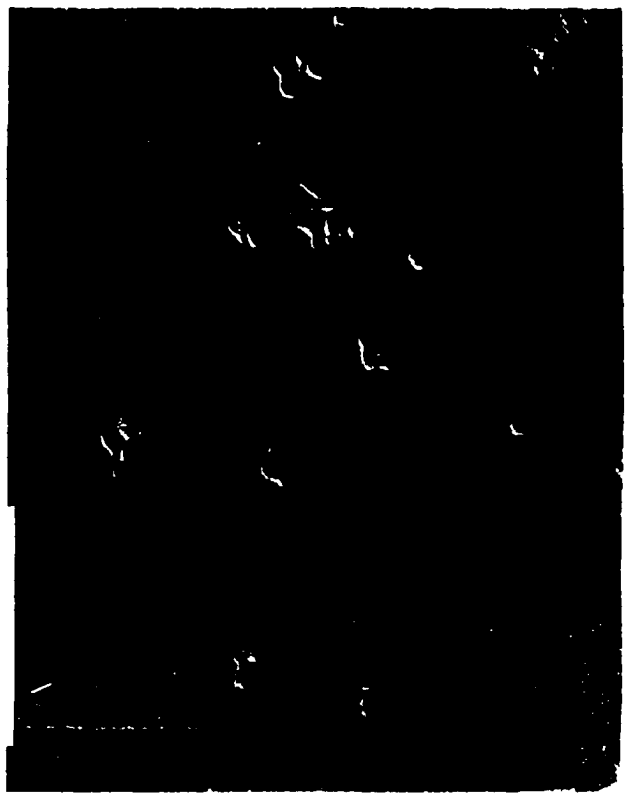

18B

Δycr089w (40X)

Figure 19. Northern analysis of constitutive expression of *YCR089W* in wild type *W303-1A*, *W303-1B*, and *W303-A/B*, and their corresponding disruptants. Total RNA was isolated from the cells indicated, run in formaldehyde gel, and transferred onto nylon membranes.
Lane 1: *W303-1A*. Lane 2: *W303-1B, Lane3: W303-A/B.* Lane4-6: Disruptants of Lane1-3 respectively.

19A

^{32}P actin probes (40 min exposure)

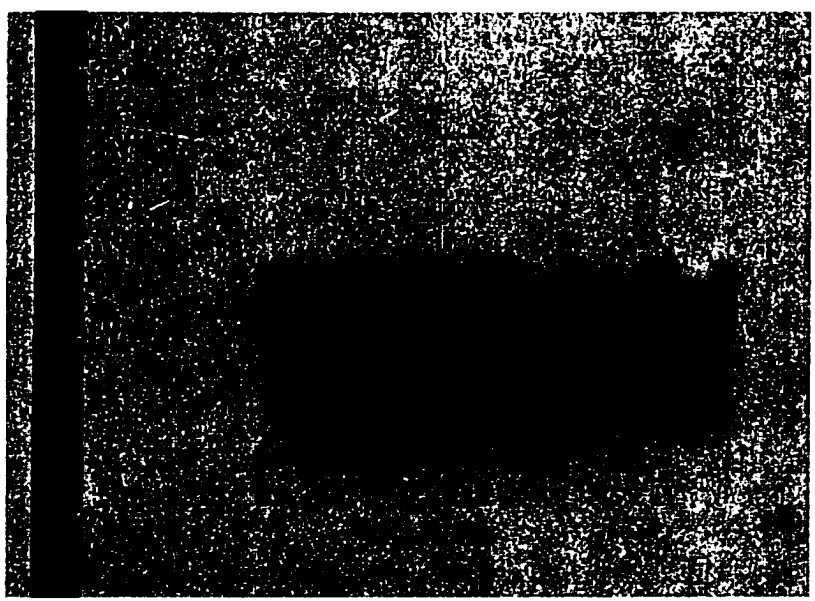

19B

^{32}P *YCR089W* probes (10 days exposure)

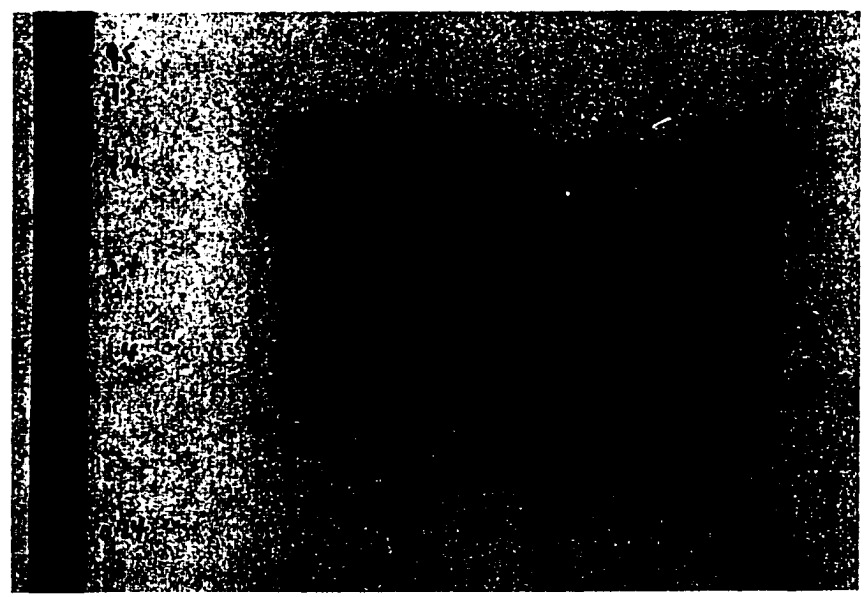

Figure 20. RNA protection assay of expression of *YCR089W* induced by pheromones. PolyA RNA's were isolated from **a** or α cells that were induced or uninduced with the appropriate pheromone. The PolyA RNA was hybridized to a ^{32}P RNA fragments . Lane 1: **a** cell. Lane 2: **a** cells exposed to pheromone. Lane 3: α cells. Lane 4: α cells exposed to pheromone.

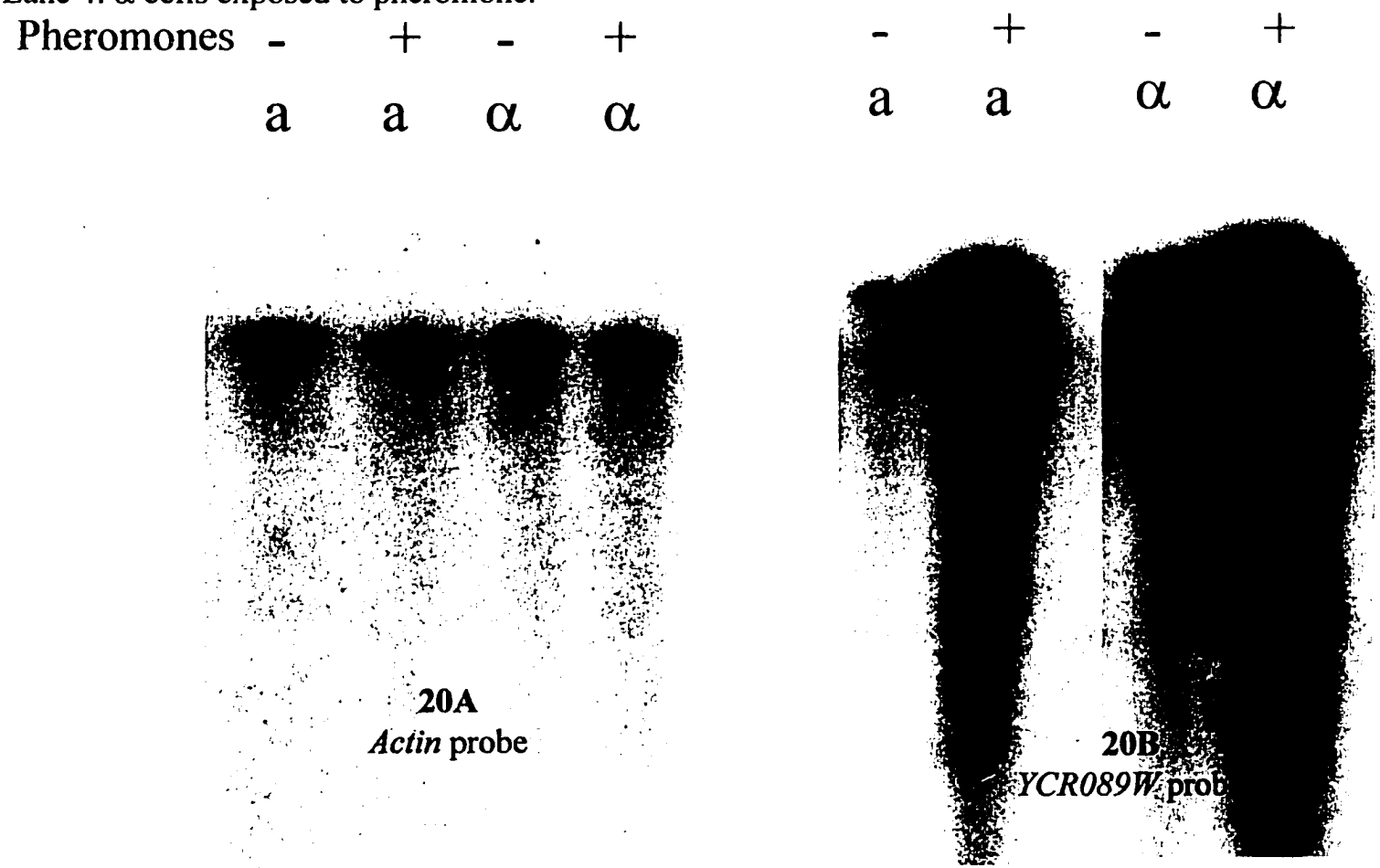

Figure 21. Observation of α cell containing a *YCR089W-GFP* construct. Cells were grown in YNB media until mid log phase. The cells were then induced with **a** factor. After 2 hours, cells were resuspended in TE buffer and stored at 4^0C for 18 hours.

21A
Bright field

21B
Under UV excitation

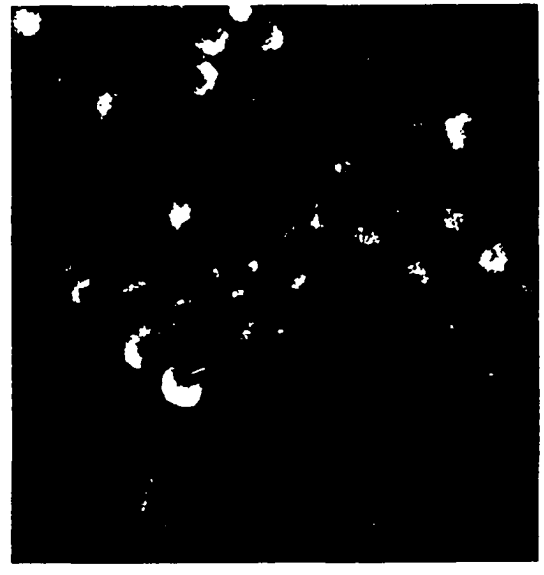

Figure 22. Observation of a cells containing a *YCR089W-GFP* construct. Cells were grown in YNB media until mid log phase. The cells were then induced with α factor. After 2 hours, cells were resuspended in TE buffer and stored at 4^0C for 18 hours.

22A
Bright field

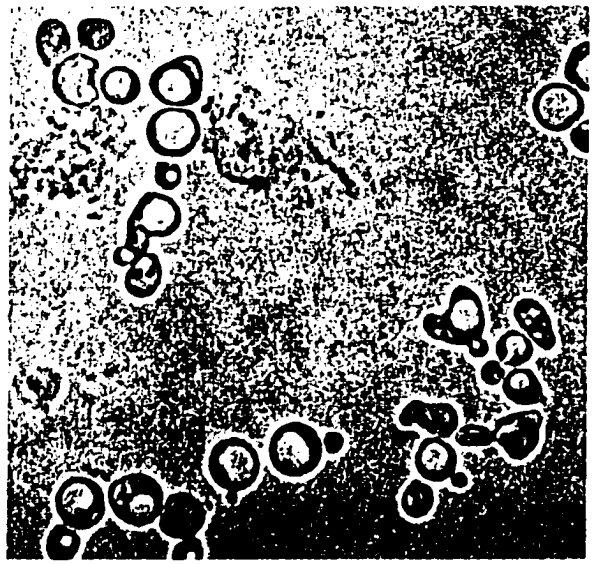

22B
Under UV excitation

Figure 23. Haploid cells of wild type and their corresponding *Δycr089w* mutants were assayed for their ability to agglutinate in various combination as indicated. The measurement of Agglutination Index was as described in Materials and Methods.

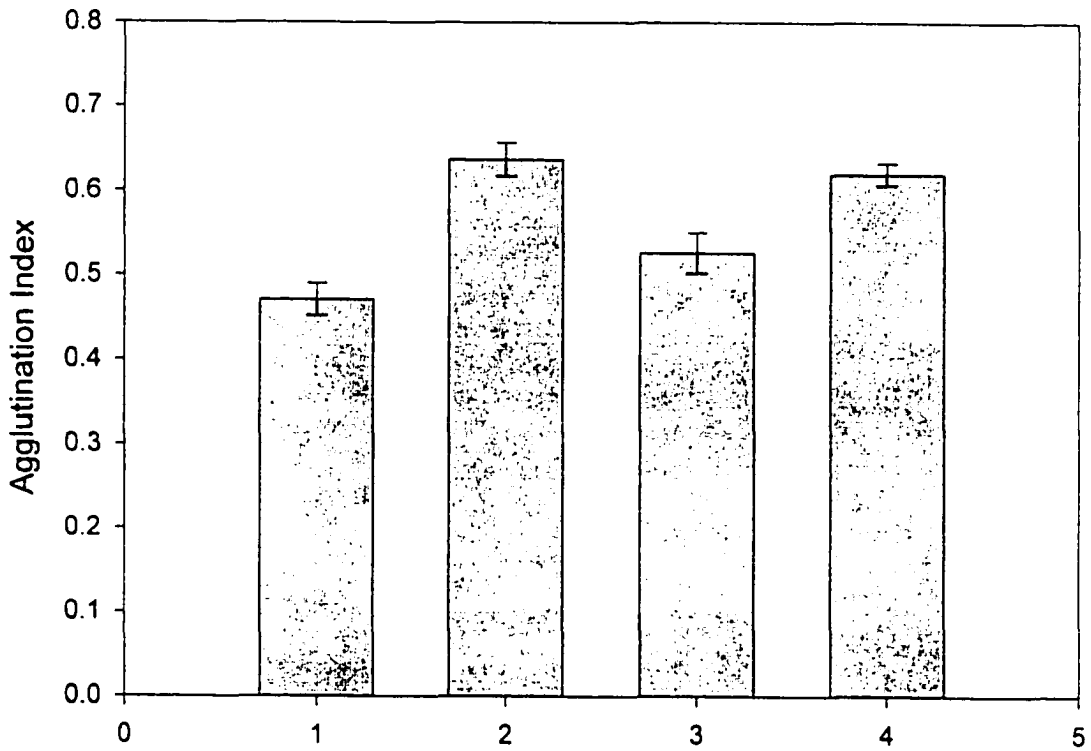

1 a X α
2 a X α(*Δycr089w*)
3 a(*Δycr089w*) X α
4 a(*Δycr089w*) X α(*Δycr089w*)

Figure 24. **a** or α cells containing *ycr089w* deletion were transfromed with multicopy plasmids expressing *YCR089W* or with vector alone. Agglutination assays were then performed on cells pairs as indicated. All **a** cells were induced by a factor understandard conditions.

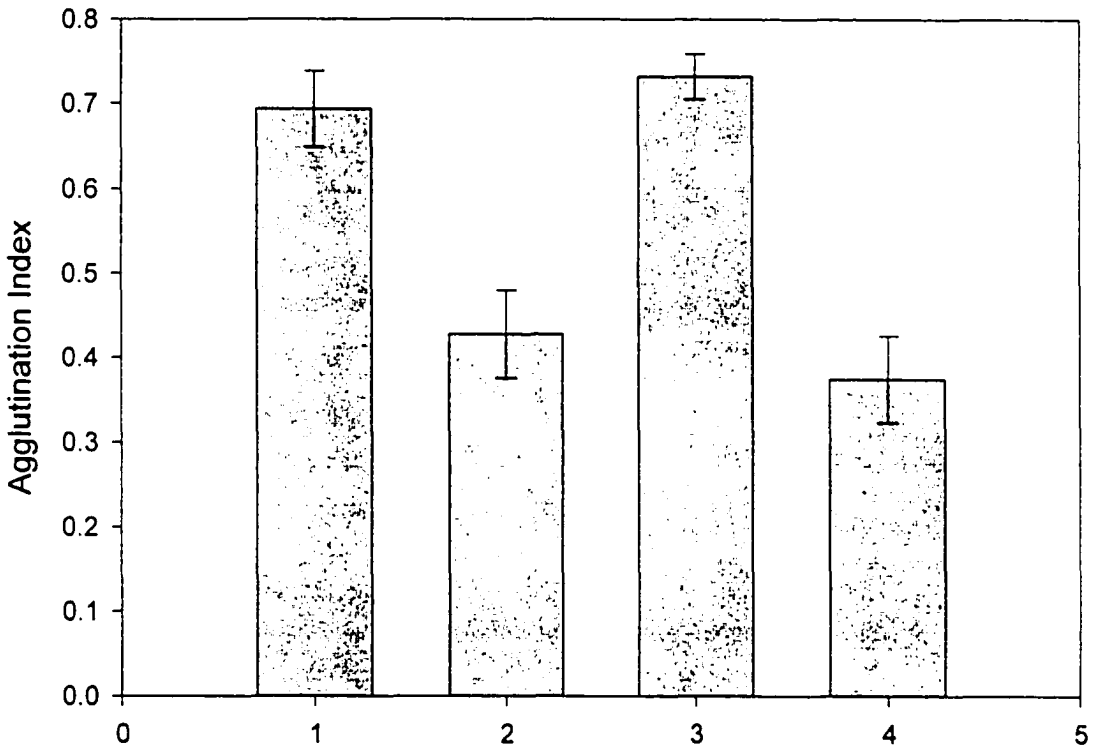

1 Δ**a** (vector alone) X Δα (vector alone)
2 Δ**a** (vector alone) X Δα (multicopy *YCR089W*)
3 Δ**a** (multicopy *YCR089W*) X Δα (vector alone)
4 Δ**a** (multicopy *YCR089W*) X Δα (multicopy *YCR089W*)

Fig 25. α and α(Δ*ycr089w*) were induced with **a** factor at the concentrations indicated. Agglutination assays were then performed with wild type a cells.

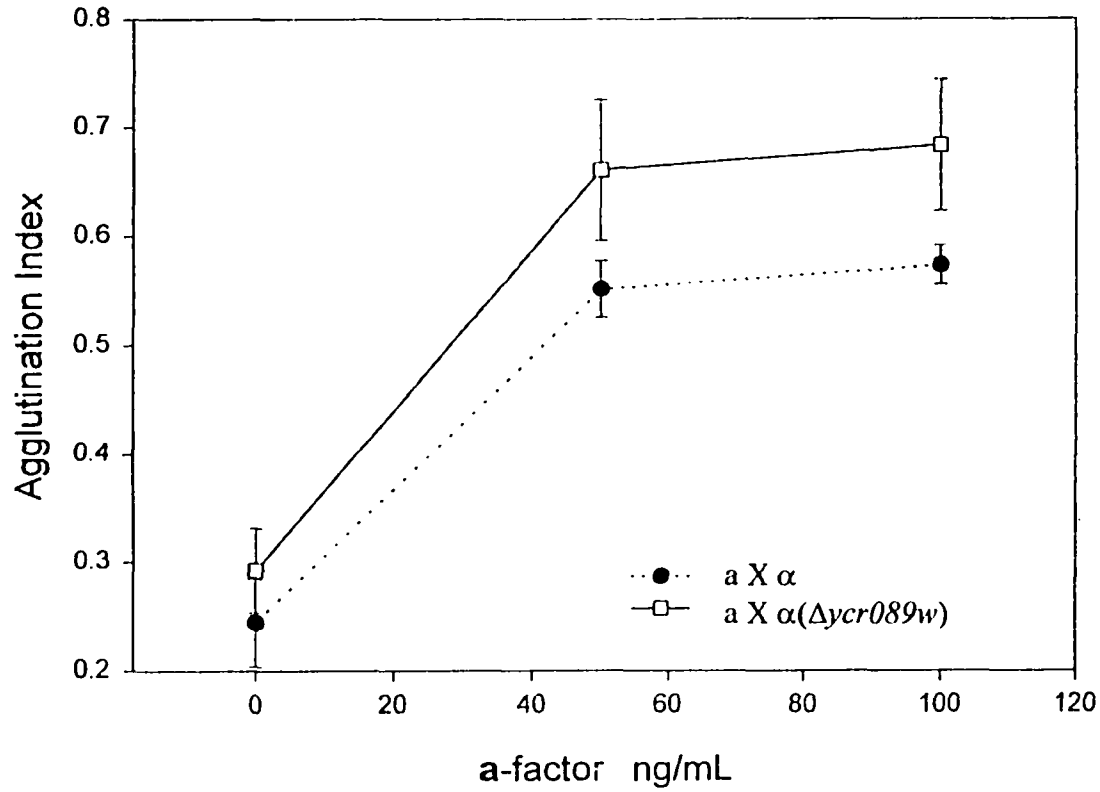

Figure 26. **a** and **a**(Δ*ycr089w*) cells were induced with α-factor at the concentrations indicated for 60 minutes. Cells were then agglutinated with wild type α cells, and the Agglutination Index was recorded.

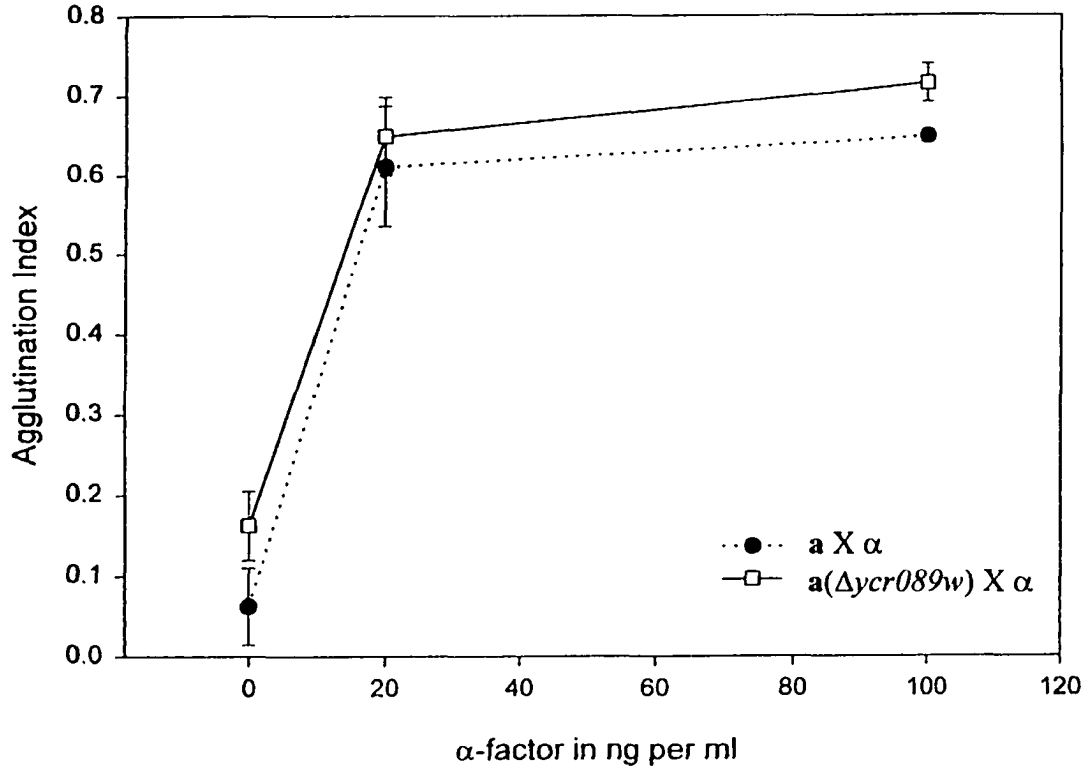

Figure 27. Agglutination of wild type cells and Δ*ycr089w* was measured as in Figure 23. **a** cells were induced with α-factor for different times as indicated.

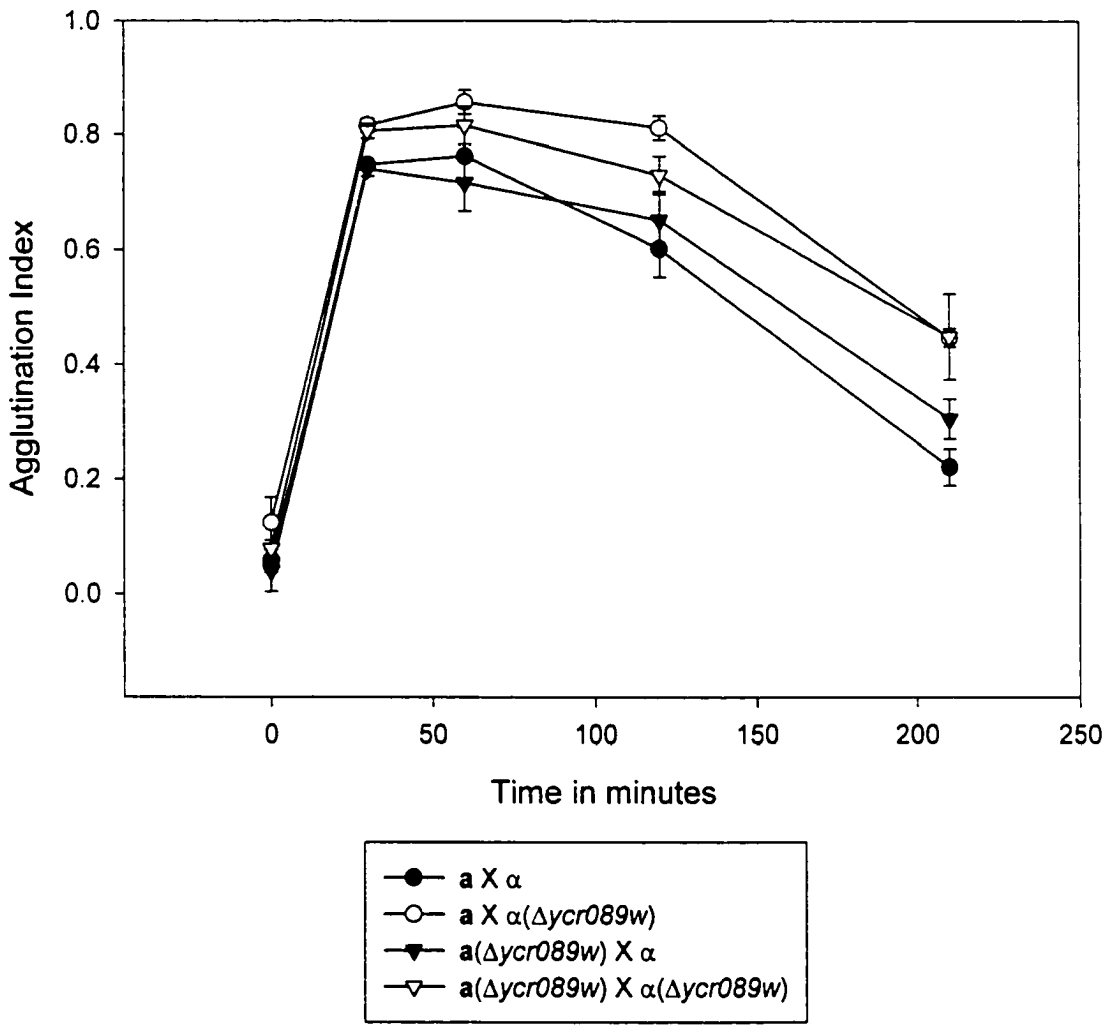

Figure 28. RNA protection assays (RPA) were performed to quantitate α-agglutinin transcription under the influence of the overexpression of *YCR089W*. Phero indicates cells that were induced with the appropriate pheromone. 089W OE indicates cells that contained a multicopy *YCR089W* plasmid. Lane 9 is a control in which no yeast polyA RNA was added. Lane 10 was a control where no RNase was added. The two blots below were identical except one blot was probed for actin, while the other was probed with the α-agglutinin gene.

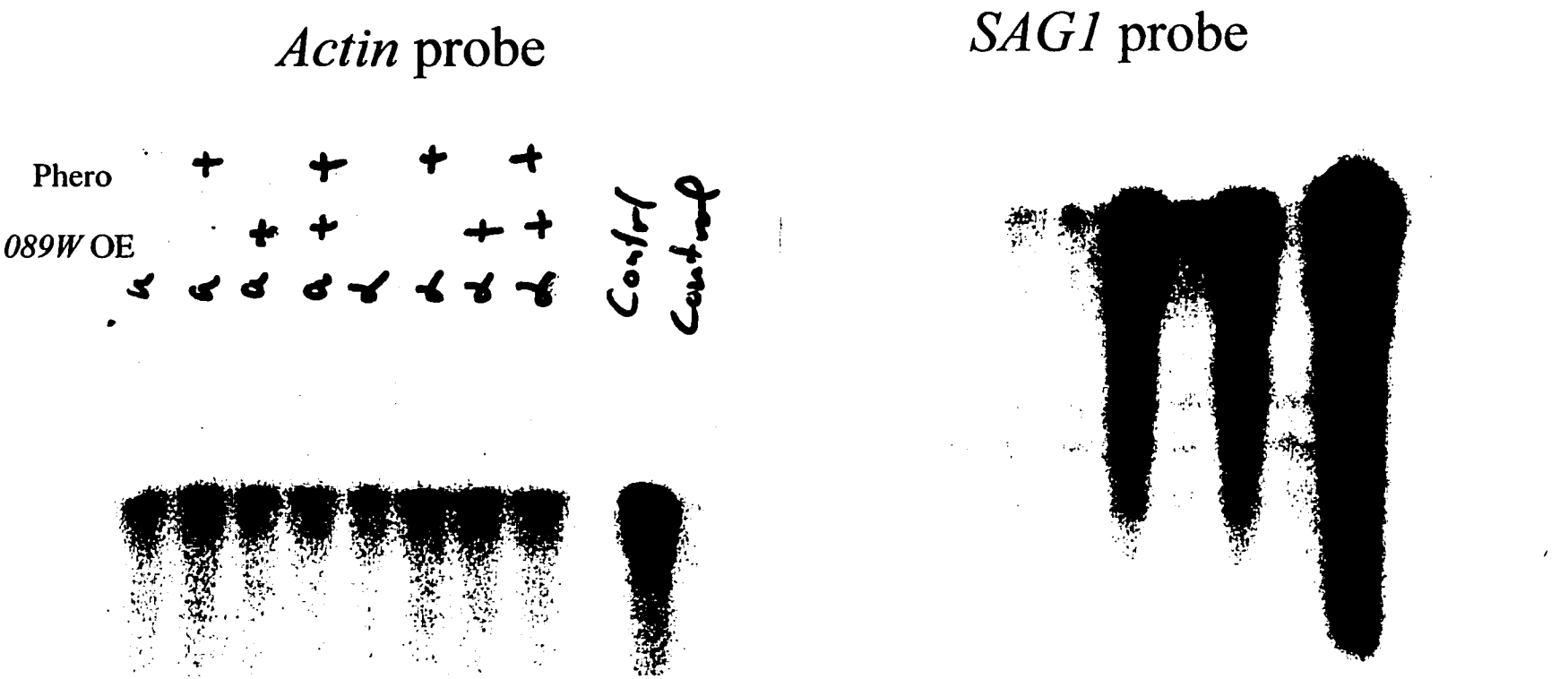

Figure 29. Qualitative Mating. Approximately 1 cm^2 of Tester strains *N435-1A* or *N435-2A* were scraped from plates and suspended in equal amount of YEPD. Cells were spread on pre-warmed YNB minimal plates. 10 µl of cells to be tested were layered on the top of the tester strains. Diploids grew in YNB minimal plates whereas neither haploids would grow due to their auxotropic markers. 29A: Tester strain were **a** cells. Cells tested were *W303*. Columns from left to right a, α, a/α. Rows from top to bottom were wild types, *ycr089wΔ*, *ycr089wΔ* and *aga1Δ*, and *aga1Δ*. 29B: Tester strain were α cells. Cells tested were *W303*. Columns from left to right a, α, a/α. Rows from top to bottom were wild types, *ycr089wΔ*, *ycr089wΔ* and *aga1Δ*(strain not available at the time and was not tested), and *aga1Δ*.

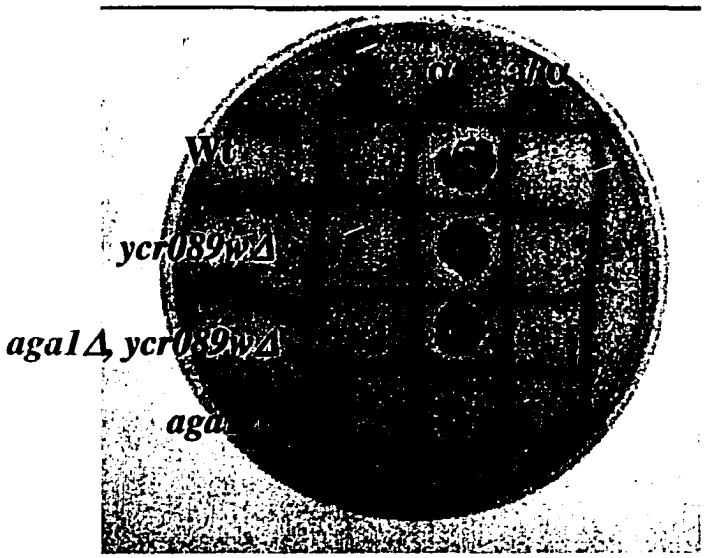

29A

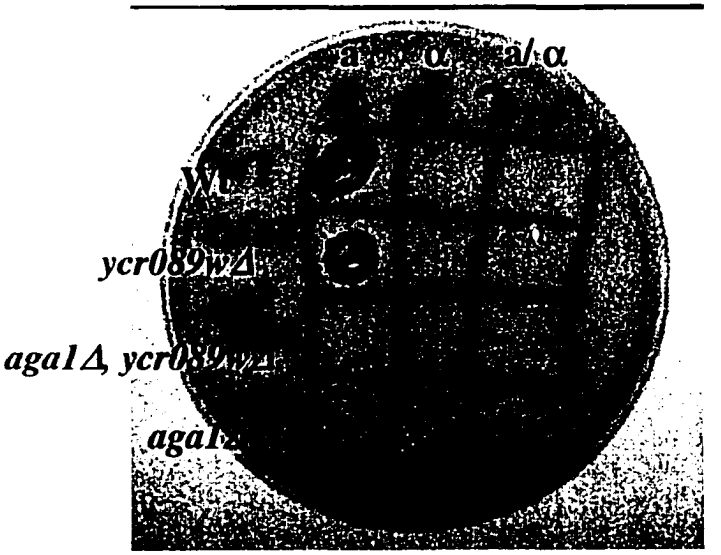

29B

References

Agrawal, b., Krantz, M. J., Reddish, M. A., Longenecker, B. M. 1998. Cancer-associated Muc1 mucin inhibits human T-cell proliferation, which is reversible by IL-2. *Nature Medicine* 4:43

Akada, R., Kallal, L., Johnson, D. I., Kurjan, J. 1996. Genetic relationships between the G protein beta gamma complex, Ste5p, Ste20p and Cdc42p: investigation of effector roles in the yeast pheromone response pathway. *Genetics* 143:103-17

Amberg, D. C., Zahner, J. E., Mulholland, J. W., Pringle, J. R., Botstein, D. 1997. Aip3p/Bud6p, a yeast actin-interacting protein that is involved in morphogenesis and the selection of bipolar bud sites. *Mol Biol Cell* 8:729-53

Anaissie, E. J., Kontoyiannis, D. P., Vartivarian, S., Kantarjian, H. M., O'Brien, S., et al. 1993. Effectiveness of an oral triazole for opportunistic mold infections in patients with cancer: experience with SCH 39304. *Clin Infect Dis* 17:1022-31

Angiolella, L., Facchin, M., Stringaro, A., Maras, B., Simonetti, N., Cassone, A. 1996. Identification of a glucan-associated enolase as a main cell wall protein of Candida albicans and an indirect target of lipopeptide antimycotics. *J Infect Dis* 173:684-90

Ballou, C. E. 1982. *Yeast cell wall and cell surface* New York: Cold Spring Harbor Laboratory. 335-360 pp.

Barug, D., de Groot, C. 1983. Microscopic studies of Candida albicans and Torulopsis glabrata after in vitro treatment with bifonazole. Freeze fracture electron microscopy. *Arzneimittelforschung* 33:538-45

Benghezal, M., Lipke, P. N., Conzelmann, A. 1995. Identification of six complementation classes involved in the biosynthesis of glycosylphosphatidylinositol anchors in Saccharomyces cerevisiae. *J Cell Biol* 130:1333-44

Betz, R., Crabb, J. W., Meyer, H. E., Wittig, R., Duntze, W. 1987. Amino acid sequences of a-factor mating peptides from Saccharomyces cerevisiae. *J Biol Chem* 262:546-8

Betz, R., Duntze, W. 1979. Purification and partial characterization of a factor, a mating hormone produced by mating-type-a cells from Saccharomyces cerevisiae. *Eur J Biochem* 95:469-75

Boguslawski, G. 1986. Polymyxin B nonapeptide inhibits mating in Saccharomyces cerevisiae. *Antimicrob Agents Chemother* 29:330-2

Bozzola, J. J., Mehta, R. J., Nisbet, L. J., Valenta, J. R. 1984. The effect of aculeacin A and papulacandin B on morphology and cell wall ultrastructure in Candida albicans. *Can J Microbiol* 30:857-63

Brake, A., Brenner, C., Najarian, R., Laybourn, P., Merryweather, J., eds. 1985. *Structure of genes encoding precursors of the yeast peptide mating pheromone a-factor*. New York: Cold Spring Harbor Laboratory. 103-8 pp.

Bruschi, C. V., Comer, A. R., Howe, G. A. 1987. Specificity of DNA uptake during whole cell transformation of S. cerevisiae. *Yeast* 3:131-7

Brzobohaty, B., Kovac, L. 1986. Factors enhancing genetic transformation of intact yeast cells modify cell wall porosity. *J Gen Microbiol* 132:3089-93

Burkholder, A. C., Hartwell, L. H. 1985. The yeast alpha-factor receptor: structural properties deduced from the sequence of the STE2 gene. *Nucleic Acids Res* 13:8463-75

Bussey, H. 1991. K1 killer toxin, a pore-forming protein from yeast. *Mol Microbiol* 5:2339-43

Cappellaro, C., Baldermann, C., Rachel, R., Tanner, W. 1994. Mating type-specific cell-cell recognition of Saccharomyces cerevisiae: cell wall attachment and active sites of a- and alpha-agglutinin. *Embo J* 13:4737-44

Cappellaro, C., Hauser, K., Mrsa, V., Watzele, M., Watzele, G., et al. 1991. Saccharomyces cerevisiae a- and alpha-agglutinin: characterization of their molecular interaction. *Embo J* 10:4081-8

Cappellaro, C., Mrsa, V., Tanner, W. 1998. New potential cell wall glucanases of Saccharomyces cerevisiae and their involvement in mating. *J Bacteriol* 180:5030-7

Caro, L. H., Tettelin, H., Vossen, J. H., Ram, A. F., van den Ende, H., Klis, F. M. 1997. In silicio identification of glycosyl-phosphatidylinositol-anchored plasma-membrane and cell wall proteins of Saccharomyces cerevisiae. *Yeast* 13:1477-89

Chan, A. K., Lockhart, D. C., von Bernstorff, W., Spanjaard, R. A., Joo, H. G., et al. 1999. Soluble MUC1 secreted by human epithelial cancer cells mediates immune suppression by blocking T-cell activation. *Int J Cancer* 82:721-6

Chant, J., Pringle, J. R. 1991. Budding and cell polarity in Saccharomyces cerevisiae. *Curr Opin Genet Dev* 1:342-50

Chenevert, J., Corrado, K., Bender, A., Pringle, J., Herskowitz, I. 1992. A yeast gene (BEM1) necessary for cell polarization whose product contains two SH3 domains. *Nature* 356:77-9

Choi, K. Y., Satterberg, B., Lyons, D. M., Elion, E. A. 1994. Ste5 tethers multiple protein kinases in the MAP kinase cascade required for mating in S. cerevisiae. *Cell* 78:499-512

Chuang, J. S., Schekman, R. W. 1996. Differential trafficking and timed localization of two chitin synthase proteins, Chs2p and Chs3p [published erratum appears in J Cell Biol 1996 Dec;135(6 Pt 2):1925]. *J Cell Biol* 135:597-610

Crandall, M., Egel, R., Mackay, V. L. 1977. Physiology of mating in three yeasts. *Adv Microb Physiol* 15:307-98

Crotchfelt, K. A., Pare, B., Gaydos, C., Quinn, T. C. 1998. Detection of Chlamydia trachomatis by the Gen-Probe AMPLIFIED Chlamydia Trachomatis Assay (AMP CT) in urine specimens from men and women and endocervical specimens from women. *J Clin Microbiol* 36:391-4

de Nobel, H., Pike, J., Lipke, P. N., Kurjan, J. 1995. Genetics of a-agglutunin function in Saccharomyces cerevisiae. *Mol Gen Genet* 247:409-15

De Nobel, J. G., Klis, F. M., Munnik, T., Priem, J., van den Ende, H. 1990. An assay of relative cell wall porosity in Saccharomyces cerevisiae, Kluyveromyces lactis and Schizosaccharomyces pombe. *Yeast* 6:483-90

De Sampaio, G., Bourdineaud, J. P., Lauquin, G. J. 1999. A constitutive role for GPI anchors in Saccharomyces cerevisiae: cell wall targeting. *Mol Microbiol* 34:247-56

Dean, N. 1995. Yeast glycosylation mutants are sensitive to aminoglycosides. *Proc Natl Acad Sci U S A* 92:1287-91

Debono, M., Gordee, R. S. 1994. Antibiotics that inhibit fungal cell wall development. *Annu Rev Microbiol* 48:471-97

Debono, M., Turner, W. W., LaGrandeur, L., Burkhardt, F. J., Nissen, J. S., et al. 1995. Semisynthetic chemical modification of the antifungal lipopeptide echinocandin B (ECB): structure-activity studies of the lipophilic and geometric parameters of polyarylated acyl analogs of ECB. *J Med Chem* 38:3271-81

Dielbandhoesing, S. K., Zhang, H., Caro, L. H. P., van der Vaart, J. M., Klis, F. M., et al. 1998. Specific cell wall proteins confer resistance to nisin upon yeast cells. *Appl Environ Microbiol* 64:4047-52

Dietzel, C., Kurjan, J. 1987. The yeast SCG1 gene: a G alpha-like protein implicated in the a- and alpha-factor response pathway. *Cell* 50:1001-10

Diment, A. V., Blinova, M. I. 1976. [The effect of cycloheximide on DNA replication. II. Antibiotic resistance following L cell treatment with hydroxyurea]. *Tsitologiia* 18:225-7

Dmochowska, A., Dignard, D., Henning, D., Thomas, D. Y., Bussey, H. 1987. Yeast KEX1 gene encodes a putative protease with a carboxypeptidase B- like function involved in killer toxin and alpha-factor precursor processing. *Cell* 50:573-84

Dolan, J. W., Kirkman, C., Fields, S. 1989. The yeast STE12 protein binds to the DNA sequence mediating pheromone induction. *Proc Natl Acad Sci U S A* 86:5703-7

Douglas, C. M., Foor, F., Marrinan, J. A., Morin, N., Nielsen, J. B., et al. 1994. The Saccharomyces cerevisiae FKS1 (ETG1) gene encodes an integral membrane protein which is a subunit of 1,3-beta-D-glucan synthase. *Proc Natl Acad Sci U S A* 91:12907-11

Dranginis, A. M. 1986. Regulation of cell type in yeast by the mating-type locus. *Trends in Biochemical Sciences* 11:328-331

Dranginis, A. M. 1990. Binding of yeast a1 and alpha 2 as a heterodimer to the operator DNA of a haploid-specific gene. *Nature* 347:682-5

Duffus, J. H., Levi, C., Manners, D. J. 1982. Yeast cell-wall glucans. *Adv Microb Physiol* 23:151-81

Dutcher, J. D. 1968. The discovery and development of amphotericin B. *Dis Chest* 54:296-8

Edwards, S. R., Braley, R., Chaffin, W. L. 1999. Enolase is present in the cell wall of Saccharomyces cerevisiae. *FEMS Microbiol Lett* 177:211-6

Erdman, S., Lin, L., Malczynski, M., Snyder, M. 1998. Pheromone-regulated genes required for yeast mating differentiation. *J Cell Biol* 140:461-83

Eroles, P., Sentandreu, M., Elorza, M. V., Sentandreu, R. 1997. The highly immunogenic enolase and Hsp70p are adventitious Candida albicans cell wall proteins. *Microbiology* 143:313-20

Evangelista, M., Blundell, K., Longtine, M. S., Chow, C. J., Adames, N., et al. 1997. Bni1p, a yeast formin linking cdc42p and the actin cytoskeleton during polarized morphogenesis. *Science* 276:118-22

Fields, S., Herskowitz, I. 1987. Regulation by the yeast mating-type locus of STE12, a gene required for cell-type-specific expression. *Mol Cell Biol* 7:3818-21

Fleet, G. H. 1985. Composition and structure of yeast cell walls. *Curr Top Med Mycol* 1:24-56

Foor, F., Parent, S. A., Morin, N., Dahl, A. M., Ramadan, N., et al. 1992. Calcineurin mediates inhibition by FK506 and cyclosporin of recovery from alpha-factor arrest in yeast. *Nature* 360:682-4

Franzin, L., Pennazio, M., Cabodi, D., Paolo Rossini, F., Gioannini, P. 2000. Clarithromycin and amoxicillin susceptibility of Helicobacter pylori strains isolated from adult patients with gastric or duodenal ulcer in Italy. *Curr Microbiol* 40:96-100

Friis, J., Roman, H. 1968. The effect of the mating-type alleles on intragenic recombination in yeast. *Genetics* 59:33-6

Fuller, R., Brake, A., Sterne, R., Kunisawa, R., Barnes, D., eds. 1986. *Post-translational processing events in the maturation of yeast peromone precursors*. New York: Liss. 461-76 pp.

Gehrung, S., Snyder, M. 1990. The SPA2 gene of Saccharomyces cerevisiae is important for pheromone- induced morphogenesis and efficient mating. *J Cell Biol* 111:1451-64

Gimeno, C. J., Ljungdahl, P. O., Styles, C. A., Fink, G. R. 1992. Unipolar cell divisions in the yeast Saccharomyces cerevisiae lead to gilamentous growth: regulation by starvation and RAS. *Cell* 68:1077-1090

Goffeau, A., Barrell, B. G., Bussey, H., Davis, R. W., Dujon, B., et al. 1996. Life with 6000 genes [see comments]. *Science* 274:546, 563-7

Gruler, H. 1981. Quantitative picture analysis of freeze-fracture electron-micrographs. *Acta Histochem Suppl* 23:55-74

Haber, J. E. 1992. Mating-type gene switching in Saccharomyces cerevisiae. *Trends Genet* 8:446-52

Haber, J. E. 1998. Mating-type gene switching in Saccharomyces cerevisiae. *Annu Rev Genet* 32:561-99

Hagen, D. C., Bruhn, L., Westby, C. A., Sprague, G. F., Jr. 1993. Transcription of alpha-specific genes in Saccharomyces cerevisiae: DNA sequence requirements for activity of the coregulator alpha 1. *Mol Cell Biol* 13:6866-75

Hagen, D. C., McCaffrey, G., Sprague, G. F., Jr. 1986. Evidence the yeast STE3 gene encodes a receptor for the peptide pheromone a factor: gene sequence and implications for the structure of the presumed receptor. *Proc Natl Acad Sci U S A* 83:1418-22

Hamada, K., Fukuchi, S., Arisawa, M., Baba, M., Kitada, K. 1998a. Screening for glycosylphosphatidylinositol (GPI)-dependent cell wall proteins in Saccharomyces cerevisiae. *Mol Gen Genet* 258:53-9

Hamada, K., Terashima, H., Arisawa, M., Kitada, K. 1998b. Amino acid sequence requirement for efficient incorporation of glycosylphosphatidylinositol-associated proteins into the cell wall of Saccharomyces cerevisiae. *J Biol Chem* 273:26946-53

Harsay, E., Bretscher, A. 1995. parallet secretory pathways tothe cell surface in yeast. *J Cell Biol* 131:297-310

Hartland, R. P., Vermeulen, C. A., Klis, F. M., Sietsma, J. H., Wessels, J. G. 1994. The linkage of (1-3)-beta-glucan to chitin during cell wall assembly in Saccharomyces cerevisiae. *Yeast* 10:1591-9

Hartwell, L. H. 1980. Mutants of Saccharomyces cerevisiae unresponsive to cell division control by polypeptide mating hormone. *J Cell Biol* 85:811-22

Hasson, M. S., Blinder, D., Thorner, J., Jenness, D. D. 1994. Mutational activation of the STE5 gene product bypasses the requirement for G protein beta and gamma subunits in the yeast pheromone response pathway. *Mol Cell Biol* 14:1054-65

Hauser, K., Tanner, W. 1989. Purification of the inducible alpha-agglutinin of S. cerevisiae and molecular cloning of the gene. *FEBS Lett* 255:290-4

Heoprich, P. D. 1995. Antifungal chemotherapy. *Progress in Drug Research* 44:87-127

Herscovics, A., Orlean, P. 1993. Glycoprotein biosynthesis in yeast. *Faseb J* 7:540-50

Heude, M., Fabre, F. 1993. a/alpha-control of DNA repair in the yeast Saccharomyces cerevisiae: genetic and physiological aspects. *Genetics* 133:489-98

Ho, J. J., Kim, Y. S. 1994. Serological pancreatic tumor markers and the MUC1 apomucin. *Pancreas* 9:674-91

Inokoshi, J., Tomoda, H., Hashimoto, H., Watanabe, A., Takeshima, H., Omura, S. 1994. Cerulenin-resistant mutants of Saccharomyces cerevisiae with an altered fatty acid synthase gene. *Mol Gen Genet* 244:90-6

Ito, H., Fukuda, Y., Murata, K., Kimura, A. 1983. Transformation of intact yeast cells treated with alkali cations. *J Bacteriol* 153:163-8

Jackson, C. L., Konopka, J. B., Hartwell, L. H. 1991. S. cerevisiae alpha pheromone receptors activate a novel signal transduction pathway for mating partner discrimination. *Cell* 67:389-402

Jarvis, E. E., Hagen, D. C., Sprague, G. F., Jr. 1988. Identification of a DNA segment that is necessary and sufficient for alpha-specific gene control in Saccharomyces cerevisiae: implications for regulation of alpha-specific and a-specific genes. *Mol Cell Biol* 8:309-20

Jiang, B., Sheraton, J., Ram, A. F., Dijkgraaf, G. J., Klis, F. M., Bussey, H. 1996. CWH41 encodes a novel endoplasmic reticulum membrane N-glycoprotein involved in beta 1,6-glucan assembly. *J Bacteriol* 178:1162-71

Julius, D., Blair, L., Brake, A., Sprague, G., Thorner, J. 1983. Yeast alpha factor is processed from a larger precursor polypeptide: the essential role of a membrane-bound dipeptidyl aminopeptidase. *Cell* 32:839-52

Julius, D., Brake, A., Blair, L., Kunisawa, R., Thorner, J. 1984. Isolation of the putative structural gene for the lysine-arginine- cleaving endopeptidase required for processing of yeast prepro-alpha- factor. *Cell* 37:1075-89

Kam, J. L., Regimbald, L. H., Hilgers, J. H., Hoffman, P., Krantz, M. J., et al. 1998. MUC1 synthetic peptide inhibition of intercellular adhesion molecule-1 and MUC1 binding requires six tandem repeats. *Cancer Res* 58:5577-81

Kanbe, T., Morishita, M., Ito, K., Tomita, K., Utsunomiya, K., Ishiguro, A. 1996. Evidence for the presence of immunoglobulin E antibodies specific to the cell wall phosphomannoproteins of Candida albicans in patients with allergies. *Clin Diagn Lab Immunol* 3:645-50

Kappeli, O., Walther, P., Mueller, M., Fiechter, A. 1984. Structure of the cell surface of the yeast Candida tropicalis and its relation to hydrocarbon transport. *Arch Microbiol* 138:279-82

Kapteyn, J. C., Van Egmond, P., Sievi, E., Van Den Ende, H., Makarow, M., Klis, F. M. 1999. The contribution of the O-glycosylated protein Pir2p/Hsp150 to the construction of the yeast cell wall in wild-type cells and beta 1,6- glucan-deficient mutants. *Mol Microbiol* 31:1835-44

Klar, A. J., Fogel, S., Radin, D. N. 1979. Switching of a mating-type a mutant allele in budding yeast Saccharomyces cerevisiae. *Genetics* 92:759-76

Klar, A. J., Hicks, J. B., Strathern, J. N. 1982. Directionality of yeast mating-type interconversion. *Cell* 28:551-61

Klebe, R. J., Harriss, J. V., Sharp, Z. D., Douglas, M. G. 1983. A general method for polyethylene-glycol-induced genetic transformation of bacteria and yeast. *Gene* 25:333-41

Kobayashi, O., Hayashi, N., Kuroki, R., Sone, H. 1998. Region of FLO1 proteins responsible for sugar recognition. *J Bacteriol* 180:6503-10

Kollar, R., Petrakova, E., Ashwell, G., Robbins, P. W., Cabib, E. 1995. Architecture of the yeast cell wall. The linkage between chitin and beta(1-->3)-glucan. *J Biol Chem* 270:1170-8

Kondo, K., Inouye, M. 1991. TIP1, a cold shock-inducible gene of Saccharomyces cerevisiae. *J Biol Chem* 266:17537-17544

Konopka, J. B., Jenness, D. D., Hartwell, L. H. 1988. The C-terminus of the S. cerevisiae alpha-pheromone receptor mediates an adaptive response to pheromone. *Cell* 54:609-20

Kowalski, L. R., Kondo, K., Inouye, M. 1995. Cold-shock induction of a family of TIP1-related proteins associated with the membrane in Saccharomyces cerevisiae. *Mol Microbiol* 15:341-53

Kurjan, J. 1985. Alpha-factor structural gene mutations in Saccharomyces cerevisiae: effects on alpha-factor production and mating. *Mol Cell Biol* 5:787-96

Kurjan, J. 1992. Pheromone response in yeast. *Annu Rev Biochem* 61:1097-129

Kurjan, J., Herskowitz, I. 1982. Structure of a yeast pheromone gene (MFalpha): a putative alpha-factor precursor contains four tandem copies of mature alpha-factor. *Cell* 30:933-43

Kurjan, J., Lipke, P. N. 1986. Agglutination and mating activity of the MF alpha 2-encoded alpha- factor analog in Saccharomyces cerevisiae. *J Bacteriol* 168:1472-5

Lafuente, M. J., Gancedo, C. 1999. Disruption and basic functional analysis of six novel ORFs of chromosome XV from Saccharomyces cerevisiae. *Yeast* 15:935-43

Lagow, E., DeSouza, M. M., Carson, D. D. 1999. Mammalian reproductive tract mucins. *Hum Reprod Update* 5:280-92

Lagunas, R., DeJuan, C., Benito, B. 1986. Inhibition of biosynthesis of Saccharomyces cerevisiae sugar transport system by tunicamycin. *J Bacteriol* 168:1484-6

Lan, M. S., Batra, S. K., Qi, W. N., Metzgar, R. S., Hollingsworth, M. A. 1990. Cloning and sequencing of a human pancreatic tumor mucin cDNA. *J. Biol. Chem.* 256:15294-15299

Leberer, E., Dignard, D., Harcus, D., Thomas, D. Y., Whiteway, M. 1992. The protein kinase homologue Ste20p is required to link the yeast pheromone response G-protein beta gamma subunits to downstream signalling components. *Embo J* 11:4815-24

Lee, B. N., Elion, E. A. 1999. The MAPKKK Ste11 regulates vegetative growth through a kinase cascade of shared signaling components. *Proc Natl Acad Sci U S A* 96:12679-84

Lee, J. W., Kelly, P., Lecciones, J., Coleman, D., Gordee, R., et al. 1990. Cilofungin (LY121019) shows nonlinear plasma pharmacokinetics and tissue penetration in rabbits. *Antimicrob Agents Chemother* 34:2240-5

Lim, S. T., Jue, C. K., Moore, C. W., Lipke, P. N. 1995. Oxidative cell wall damage mediated by bleomycin-Fe(II) in Saccharomyces cerevisiae. *J Bacteriol* 177:3534-9

Linnemans, W. A., Boer, P., Elbers, P. F. 1977. Localization of acid phosphatase in Saccharomyces cerevisiae: a clue to cell wall formation. *J Bacteriol* 131:638-44

Lipke, P. N., Chen, M. H., de Nobel, H., Kurjan, J., Kahn, P. C. 1995. Homology modeling of an immunoglobulin-like domain in the Saccharomyces cerevisiae adhesion protein alpha-agglutinin. *Protein Sci* 4:2168-78

Lipke, P. N., Kurjan, J. 1992. Sexual agglutination in budding yeasts: structure, function, and regulation of adhesion glycoproteins. *Microbiol Rev* 56:180-94

Lipke, P. N., Taylor, A., Ballou, C. E. 1976. Morphogenic effects of alpha-factor on Saccharomyces cerevisiae a cells. *J Bacteriol* 127:610-8

Lipke, P. N., Wojciechowicz, D., Kurjan, J. 1989. AG alpha 1 is the structural gene for the Saccharomyces cerevisiae alpha-agglutinin, a cell surface glycoprotein involved in cell-cell interactions during mating. *Mol Cell Biol* 9:3155-65

Lo, W. S., Dranginis, A. M. 1996. FLO11, a yeast gene related to the STA genes, encodes a novel cell surface flocculin. *J Bacteriol* 178:7144-51

Lo, W. S., Dranginis, A. M. 1998. The cell surface flocculin Flo11 is required for pseudohyphae formation and invasion by Saccharomyces cerevisiae. *Mol Biol Cell* 9:161-71

Lu, C. F., Montijn, R. C., Brown, J. L., Klis, F., Kurjan, J., et al. 1995. Glycosyl phosphatidylinositol-dependent cross-linking of alpha-agglutinin and beta 1,6-glucan in the Saccharomyces cerevisiae cell wall. *J Cell Biol* 128:333-40

Madden, K., Snyder, M. 1992. Specification of sites for polarized growth in Saccharomyces cerevisiae and the influence of external factors on site selection. *Mol Biol Cell* 3:1025-35

Mago, N., Khuller, G. K. 1989. Influence of lipid composition on the sensitivity of Candida albicans to antifungal agents. *Indian J Biochem Biophys* 26:30-3

Manners, D. J., Masson, A. J., Patterson, J. C. 1973a. The structure of a beta-(1 leads to 3)-D-glucan from yeast cell walls. *Biochem J* 135:19-30

Manners, D. J., Masson, A. J., Patterson, J. C., Bjorndal, H., Lindberg, B. 1973b. The structure of a beta-(1--6)-D-glucan from yeast cell walls. *Biochem J* 135:31-6

Manning, B. D., Padmanabha, R., Snyder, M. 1997. The Rho-GEF Rom2p localizes to sites of polarized cell growth and participates in cytoskeletal functions in Saccharomyces cerevisiae. *Mol Biol Cell* 8:1829-44

Marichal, P., Koymans, L., Willemsons, S., Bellens, D., Verhasselt, P., et al. 1999. Contribution of mutations in the cytochrome P450 14alpha-demethylase (Rrg11p, Cyp51p) to azole resistance in Candida albicans. *Microbiology* 145:2701-13

Marsh, L., Herskowitz, I. 1988. STE2 protein of Saccharomyces kluyveri is a member of the rhodopsin/beta-adrenergic receptor family and is responsible for recognition of the peptide ligand alpha factor. *Proc Natl Acad Sci U S A* 85:3855-9

Marsh, L., Rose, M. D., eds. 1997. *Pathway of cell fusion during mating.* New York: Cold Spring Harbor Laboratory Press. 827-888 pp.

Mazur, P., Morin, N., Baginsky, W., el-Sherbeini, M., Clemas, J. A., et al. 1995. Differential expression and function of two homologous subunits of yeast 1,3-beta-D-glucan synthase. *Mol Cell Biol* 15:5671-81

McMurrough, I., Rose, A. H. 1967. Effect of growth rate and substrate limitation on the composition and structure of the cell wall of Saccharomyces cerevisiae. *Biochem J* 105:189-203

Miyajima, I., Nakafuku, M., Nakayama, N., Brenner, C., Miyajima, A., et al. 1987. GPA1, a haploid-specific essential gene, encodes a yeast homolog of mammalian G protein which may be involved in mating factor signal transduction. *Cell* 50:1011-9

Mizoguchi, J., Saito, T., Mizuno, K., Hayano, K. 1977. On the mode of action of a new antifungal antibiotic, aculeacin A: inhibition of cell wall synthesis in Saccharomyces cerevisiae. *J Antibiot (Tokyo)* 30:308-13

Mizuno, K., Yagi, A., Satoi, S., Takada, M., Hayashi, M. 1977. Studies on aculeacin. I. Isolation and characterization of aculeacin A. *J Antibiot (Tokyo)* 30:297-302

Moore, S. A. 1983. Comparison of dose-response curves for alpha factor-induced cell division arrest, agglutination, and projection formation of yeast cells. Implication for the mechanism of alpha factor action. *J Biol Chem* 258:13849-56

Mormeneo, S., Marcilla, A., Iranzo, M., Sentandreu, R. 1994. Structural mannoproteins released by beta-elimination from Candida albicans cell walls. *FEMS Microbiol Lett* 123:131-6

Mormeneo, S., Zueco, J., Iranzo, M., Sentandreu, R. 1989. O-linked mannose composition of secreted invertase of Saccharomyces cerevisiae. *FEMS Microbiol Lett* 48:271-4

Moukadiri, I., Armero, J., Abad, A., Sentandreu, R., Zueco, J. 1997. Identification of a mannoprotein present in the inner layer of the cell wall of Saccharomyces cerevisiae. *J Bacteriol* 179:2154-62

Mrsa, V., Ecker, M., Strahl-Bolsinger, S., Nimtz, M., Lehle, L., Tanner, W. 1999. Deletion of new covalently linked cell wall glycoproteins alters the electrophoretic mobility of phosphorylated wall components of Saccharomyces cerevisiae. *J Bacteriol* 181:3076-86

Mrsa, V., Seidl, T., Gentzsch, M., Tanner, W. 1997. Specific labelling of cell wall proteins by biotinylation. Identification of four covalently linked O-mannosylated proteins of Saccharomyces cerevisiae. *Yeast* 13:1145-54

Mrsa, V., Tanner, W. 1999. Role of NaOH-extractable cell wall proteins Ccw5p, Ccw6p, Ccw7p and Ccw8p (members of the Pir protein family) in stability of the Saccharomyces cerevisiae cell wall. *Yeast* 15:813-20

Nasmyth, K. 1983. Molecular analysis of a cell lineage. *Nature* 302:670-6

Nguyen, T. H., Fleet, G. H., Rogers, P. L. 1998. Composition of the cell walls of several yeast species. *Appl Microbiol Biotechnol* 50:206-12

Ohsumi, Y., Anraku, Y. 1985. Specific induction of Ca2+ transport activity in MATa cells of Saccharomyces cerevisiae by a mating pheromone, alpha factor. *J Biol Chem* 260:10482-6

Oliver, S. G., van der Aart, Q. J., Agostoni-Carbone, M. L., Aigle, M., Alberghina, L., et al. 1992. The complete DNA sequence of yeast chromosome III [see comments]. *Nature* 357:38-46

Olson, M. V., ed. 1991. . New York: Cold Spring Harbor Laboratory. 1-39 pp.

Orlean, P., ed. 1997. *Biogenesis of Yeast Wall and Surface Component.* New York: Cold Spring Harbor laboratory Press

Orlean, P., Ammer, M., Watzele, M., W., T. 1986. Synthesis of an O-glycosylated cell surface protein induced in yeast by alpha-factor. *Proc. Natl. Acad. Sci.* 83:6263

Oshima, Y., Takano, I. 1971. Mating types in Saccharomyces: their convertibility and homothallism. *Genetics* 67:327-35

Oskouian, B., Saba, J. D. 1999. YAP1 confers resistance to the fatty acid synthase inhibitor cerulenin through the transporter Flr1p in Saccharomyces cerevisiae. *Mol Gen Genet* 261:346-53

Osumi, M., Shimoda, C., Yanagishima, N. 1974. Mating reaction in Saccharomyces cerevisiae. V. Changes in the fine structure during the mating reaction. *Arch Mikrobiol* 97:27-38

Palkova, Z., Janderova, B., Gabriel, J., Zikanova, B., Pospisek, M., Forstova, J. 1997. Ammonia mediates communication between yeast colonies. *Nature* 390:532-6

Pancholi, V., Fischetti, V. A. 1992. A major surface protein on group A streptococci is a glyceraldehyde-3-3phosphate-dehydrogenase with multiple binding activity. *J Exp Med* 176:415-26

Pancholi, V., Fischetti, V. A. 1998. alpha-enolase, a novel strong plasmin(ogen) binding protein on surface of pathogenic streptococci. *J Biol Chem* 273:14503-15

Pastor, F. I., Herrero, E., Sentandreu, R. 1982. Metabolism of Saccharomyces cerevisiae envelope mannoproteins. *Arch Microbiol* 132:144-8

Patterton, H. G., Simpson, R. T. 1994. Nucleosomal location of the STE6 TATA box and Mat alpha 2p-mediated repression. *Mol Cell Biol* 14:4002-10

Philips, J., Herskowitz, I. 1997. Osmotic balance regulates cell fusion during mating in Saccharomyces cerevisiae. *J Cell Biol* 138:961-74

Powers, S., Michaelis, S., Broek, D., Santa Anna, S., Field, J., et al. 1986. RAM, a gene of yeast required for a functional modification of RAS proteins and for production of mating pheromone a-factor. *Cell* 47:413-22

Prasad, K. R., Rosoff, P. M. 1992. Characterization of the energy-dependent, mating factor-activated Ca2+ influx in Saccharomyces cerevisiae. *Cell Calcium* 13:615-26

Ram, A. F., Kapteyn, J. C., Montijn, R. C., Caro, L. H., Douwes, J. E., et al. 1998a. Loss of the plasma membrane-bound protein Gas1p in Saccharomyces cerevisiae results in the release of beta1,3-glucan into the medium and induces a compensation mechanism to ensure cell wall integrity. *J Bacteriol* 180:1418-24

Ram, A. F., Van den Ende, H., Klis, F. M. 1998b. Green fluorescent protein-cell wall fusion proteins are covalently incorporated into the cell wall of Saccharomyces cerevisiae. *FEMS Microbiol Lett* 162:249-55

Ramon, A. M., Montero, M., Sentandreu, R., Valentin, E. 1999. Yarrowia lipolytica cell wall architeture:interaction of Ywp1, a mycelial protein, wtih other wall components and the effect of its depletion. *Res Microbiol* 150:95-103

Read, E. B., Okamura, H. H., Drubin, D. G. 1992. Actin- and tubulin-dependent functions during Saccharomyces cerevisiae mating projection formation. *Mol Biol Cell* 3:429-44

Regimbald, L. H., Pilarski, L. M., Longenecker, B. M., Reddish, M. A., Zimmermann, G., Hugh, J. C. 1996. The breast mucin MUCI as a novel adhesion ligand for endothelial intercellular adhesion molecule 1 in breast cancer. *Cancer Res* 56:4244-9

Rex, J. H., Rinaldi, M. G., Phaller, M. A. 1995. Resistance of Candida species to fluconazole. *Antimicrob Agents Chemother* 39:1-8

Roemer, T., Madden, K., Chang, J., Snyder, M. 1996. Selection of axial growth sites in yeast requires Axl2p, a novel plasma membrane glycoprotein. *Genes Dev* 10:777-93

Rose, M. C. 1992. Mucins: structure, function, and role in pulmonary diseases [see comments]. *Am J Physiol* 263:L413-29

Rothstein, S. J., Lahners, K. N., Lazarus, C. M., Baulcombe, D. C., Gatenby, A. A. 1987. Synthesis and secretion of wheat alpha-amylase in Saccharomyces cerevisiae. *Gene* 55:353-6

Roy, A., Lu, C. F., Marykwas, D. L., Lipke, P. N., Kurjan, J. 1991. The AGA1 product is involved in cell surface attachment of the Saccharomyces cerevisiae cell adhesion glycoprotein a-agglutinin. *Mol Cell Biol* 11:4196-206

Samani, N. J., Morgan, K., Brammar, W. J., Swales, J. D. 1987. Detection of renin messenger RNA in rat tissues: increased sensitivity using an RNAse protection technique. *J Hypertens Suppl* 5:S19-21

Sambrook, S., Fritsch, E. F., Maniatis, T. 1989. *Molecular Cloning a laboratory manual* New York: Cold Spring Harbor Laboratory Press

Samuel, J., Longenecker, B. M. 1995. Development of active specific immunotherapeutic agents based on cancer- associated mucins. *Pharm Biotechnol* 6:875-90

Sanders, S. L., Herskowitz, I. 1996. The bud4 protein of yeast, required for axial budding, is localized to the mother-bud neck in a cell cycle-dependent manner. *J Cell Biol* 134:413-27

Schmitt, M. I., Radler, F. 1990. Blockage of cell wall receptors for yeast killer toxin KT28 with antimannoprotein antibodies. *Antimicrob Agents Chemother* 34:1615-8

Segall, J. E. 1993. Polarization of yeast cells in spatial gradients of alpha mating factor. *Proc Natl Acad Sci U S A* 90:8332-6

Sengupta, P., Cochran, B. H. 1990. The PRE and PQ box are functionally distinct yeast pheromone response elements. *Mol Cell Biol* 10:6809-12

Sentandreu, M., Elorza, M. V., Valentin, E., Sentandreu, R., Gozalbo, D. 1995. Cloning of cDNAs coding for Candida albicans cell surface proteins. *J Med Vet Mycol* 33:105-11

Seregni, E., Botti, C., Massaron, S., Lombardo, C., Capobianco, A., et al. 1997. Structure, function and gene expression of epithelial mucins. *Tumori* 83:625-32

Shaw, J. A., Mol, P. C., Bowers, B., Silverman, S. J., Valdivieso, M. H., et al. 1991. The function of chitin synthases 2 and 3 in the Saccharomyces cerevisiae cell cycle. *J Cell Biol* 114:111-23

Sherman, F. 1998. Introduction to the Genetics and Molecular Biology of the Yeast Saccharomyces cerevisiae. . Vol. 2000

Sheu, Y. J., Santos, B., Fortin, N., Costigan, C., Snyder, M. 1998. Spa2p interacts with cell polarity proteins and signaling components involved in yeast cell morphogenesis. *Mol Cell Biol* 18:4053-69

Shimoda, C., Yanagishima, N. 1975. Mating reaction in Saccharomyces cerevisiae. VIII. Mating-type-specific substances responsible for sexual cell agglutination. *Antonie Van Leeuwenhoek* 41:521-32

Shimoi, H., Kitagaki, H., Ohmori, H., Iimura, Y., Ito, K. 1998. Sed1p is a major cell wall protein of Saccharomyces cerevisiae in the stationary phase and is involved in lytic enzyme resistance. *J Bacteriol* 180:3381-7

Simon, M. N., De Virgilio, C., Souza, B., Pringle, J. R., Abo, A., Reed, S. I. 1995. Role for the Rho-family GTPase Cdc42 in yeast mating-pheromone signal pathway. *Nature* 376:702-5

Singh, A., Chen, E. Y., Lugovoy, J. M., Chang, C. N., Hitzeman, R. A. 1983. Saccharomyces cerevisiae contains two discrete genes-coding for the alpha-factor pheromone. *nucleic Acids Res* 11:4049-63

Sipiczki, M., Ferenczy, L. 1977. Protoplast fusion of Schizosaccharomyces pombe Auxotrophic mutants of identical mating-type. *Mol Gen Genet* 151:77-81

Smits, G. J., Kapteyn, J. C., van den Ende, H., Klis, F. M. 1999. Cell wall dynamics in yeast. *Curr Opin Microbiol* 2:348-52

Sohnle, P. G., Hahn, B. L., Fassel, T. A., Kushnaryov, V. M. 1998. Analysis of fluconazole effect on Candida albicans viability during extended incubations. *Med Mycol* 36:29-36

Soni, L. M., Burattini, M. N., Pignatari, A. C., Gompertz, O. F., Colombo, A. L. 1999. Comparative study of agar diffusion test and the NCCLS macrobroth method for in vitro susceptibility testing of Candida spp [In Process Citation]. *Mycopathologia* 145:131-5

Sprague, G. F., Jr., Blair, L. C., Thorner, J. 1983a. Cell interactions and regulation of cell type in the yeast Saccharomyces cerevisiae. *Annu Rev Microbiol* 37:623-60

Sprague, G. F., Jr., Jensen, R., Herskowitz, I. 1983b. Control of yeast cell type by the mating type locus: positive regulation of the alpha-specific STE3 gene by the MAT alpha 1 product. *Cell* 32:409-15

Staab, J. F., Sundstrom, P. 1998. Genetic organization and sequence analysis of the hypha-specific cell wall protein gene HWP1 of Candida albicans. *Yeast* 14:681-6

Stotzler, D., Duntze, W. 1976. Isolation and characterization of four related peptides exhibiting alpha factor activity from Saccharomyces cerevisiae. *Eur J Biochem* 65:257-62

Strader, C. D., Sigal, I. S., Register, R. B., Candelore, M. R., Rands, E., Dixon, R. A. F. 1987. Identification of residues required for ligand binding to the beta-adrenergic receptor. *Proc Natl Acad Sci USA* 84:4384-88

Strathern, J., Hicks, J., Herskowitz, I. 1981. Control of cell type in yeast by the mating type locus. The alpha 1- alpha 2 hypothesis. *J Mol Biol* 147:357-72

Taylor-Papadimitriou, J., Burchell, J., Miles, D. W., Dalziel, M. 1999. MUC1 and cancer. *Biochim Biophys Acta* 1455:301-13

Terrance, K., Lipke, P. N. 1981. Sexual agglutination in Saccharomyces cerevisiae. *J Bacteriol* 148:889-96

Tkacz, J. S., MacKay, V. L. 1979. Sexual conjugation in yeast. Cell surface changes in response to the action of mating hormones. *J Cell Biol* 80:326-33

Tokunaga, M., Niimi, M., Kusamichi, M., Koike, H. 1990. Initial attachment of Candida albicans cells to buccal epithelial cells. Demonstration of ultrastructure with the rapid-freezing technique. *Mycopathologia* 111:61-8

Trueheart, J., Boeke, J. D., Fink, G. R. 1987. Two genes required for cell fusion during yeast conjugation: evidence for a pheromone-induced surface protein. *Mol Cell Biol* 7:2316-28

Udden, M. M., Finkelstein, D. B. 1978. Reaction order of Saccharomyces cerevisiae alpha-factor-mediated cell cycle arrest and mating inhibition. *J Bacteriol* 133:1501-7

Udenfriend, S., Kodukula, K. 1995. How glycosylphosphatidylinositol-anchored membrane proteins are made. *Annu. Rev. Biochem.* 64:563-591

Valentin, E., Herrero, E., Pastor, F. I. J., Sentandreu, R. 1984. Solubilization and analysis of mannoprotein molecules from the cell wall of Saccharomyces cerevisiae. *J. Gen. Microbiol.* 130:1419

Valentin, E., Herrero, E., Rico, H., Miragall, F., Sentandreu, R. 1987. Cell wall mannoproteins during the population growth phases in Saccharomyces cerevisiae. *Arch Microbiol* 148:88-94

Valtz, N., Herskowitz, I. 1996. Pea2 protein of yeast is localized to sites of polarized growth and is required for efficient mating and bipolar budding. *J Cell Biol* 135:725-39

Van Arsdell, S. W., Stetler, G. L., Thorner, J. 1987. The yeast repeated element sigma contains a hormone-inducible promoter. *Mol Cell Biol* 7:749-59

van der Vaart, J. M., Caro, L. H., Chapman, J. W., Klis, F. M., Verrips, C. T. 1995. Identification of three mannoproteins in the cell wall of Saccharomyces cerevisiae. *J Bacteriol* 177:3104-10

Vanden Bossche, H., Marichal, P., Gorrens, J., Coene, M. C. 1990. Biochemical basis for the activity and selectivity of oral antifungal drugs. *Br J Clin Pract Suppl* 71:41-6

Vartivarian, S. E., Reyes, G. H., Jacobson, E. S., James, P. G., Cherniak, R., et al. 1989. Localization of mannoprotein in Cryptococcus neoformans. *J Bacteriol* 171:6850-2

von Mensdorff-Pouilly, S., Verstraeten, A. A., Kenemans, P., Snijdewint, F. G. 2000. Survival in early breast cancer patients is favorably influenced by a natural humoral immune response to polymorphic epithelial mucin. *J. Clin. Oncol.* 18:574-83

Wakamatsu, K., Okada, A., Miyazawa, T., Masui, Y., Sakakibara, S., Higashijima, T. 1987. Conformations of yeast alpha-mating factor and analog peptides as bound to phospholipid bilayer. Correlation of membrane-bound conformation with physiological activity. *Eur J Biochem* 163:331-8

Wakamatsu, K., Okada, A., Suzuki, M., Higashijima, T., Masui, Y., et al. 1986. Nuclear-magnetic-resonance studies on the conformation of membrane- bound alpha-mating factor. Transferred nuclear Overhauser effect analysis. *Eur J Biochem* 154:607-15

Walsh, M. D., Luckie, S. M., Cummings, M. C., Antalis, T. M., McGuckin, M. A. 1999. Heterogeneity of MUC1 expression by human breast carcinoma cell lines in vivo and in vitro [In Process Citation]. *Breast Cancer Res Treat* 58:255-66

Watkins, P. A., Lu, J. F., Steinberg, S. J., Gould, S. J., Smith, K. D., Braiterman, L. T. 1998. Disruption of the Saccharomyces cerevisiae FAT1 gene decreases very long-chain fatty acyl-CoA synthetase activity and elevates intracellular very long-chain fatty acid concentrations. *J Biol Chem* 273:18210-9

Watzele, G., Tanner, W. 1989. Cloning of the glutamine:fructose-6-phosphate amidotransferase gene from yeast. Pheromonal regulation of its transcription. *J Biol Chem* 264:8753-8

Weiler, K. S., Broach, J. R. 1992. Donor locus selection during Saccharomyces cerevisiae mating type interconversion responds to distant regulatory signals. *Genetics* 132:929-42

Wesseling, J., van der Valk, S. W., Hilkens, J. 1996. A mechanism for inhibition of E-cadherin-mediated cell-cell adhesion by the membrane-associated mucin episialin/MUC1. *Mol Biol Cell* 7:565-77

Wesseling, J., van der Valk, S. W., Vos, H. L., Sonnenberg, A., Hilkens, J. 1995. Episialin (MUC1) overexpression inhibits integrin-mediated cell adhesion to extracellular matrix components. *J Cell Biol* 129:255-65

Wilkinson, L. E., Pringle, J. R. 1974. Transient G1 arrest of S. cerevisiae cells of mating type alpha by a factor produced by cells of mating type a. *Exp Cell Res* 89:175-87

Wilson, K. L., Herskowitz, I. 1984. Negative regulation of STE6 gene expression by the alpha 2 product of Saccharomyces cerevisiae. *Mol Cell Biol* 4:2420-7

Wilson, K. L., Herskowitz, I. 1987. STE16, a new gene required for pheromone production by a cells of Saccharomyces cerevisiae. *Genetics* 115:441-9

Winterford, C. M., Walsh, M. D., Leggett, B. A., Jass, J. R. 1999. Ultrastructural localization of epithelial mucin core proteins in colorectal tissues. *J Histochem Cytochem* 47:1063-74

Winzeler, E. A., Shoemaker, D. D., Astromoff, A., Liang, H., Anderson, K., et al. 1999. Functional characterization of the S. cerevisiae genome by gene deletion and parallel analysis. *Science* 285:901-6

Wojciechowicz, D., Lipke, P. N. 1989. Alpha-agglutinin expression in Saccharomyces cerevisiae. *Biochem Biophys Res Commun* 161:46-51

Woodcock, D. M., Williamson, M. R., Doherty, J. P. 1996. A sensitive RNase protection assay to detect transcripts from potentially functional human endogenous L1 retrotransposons. *Biochem Biophys Res Commun* 222:460-5

Xing, P. X., Lees, C., Lodding, J., Prenzoska, J., Poulos, G., et al. 1998. Mouse mucin 1 (MUC1) defined by monoclonal antibodies. *Int J Cancer* 76:875-83

Yamaguchi, H., Hiratani, T., Baba, M., Osumi, M. 1985. Effect of aculeacin A, a wall-active antibiotic, on synthesis of the yeast cell wall. *Microbiol Immunol* 29:609-23

Yanagishima, N. 1986. Sexual differentiation and interactions in yeasts. *Microbiol Sci* 3:45-9

Yun, D. J., Ibeas, J. I., Lee, H., Coca, M. A., Narasimhan, M. L., et al. 1998. Osmotin, a plant antifungal protein, subverts signal transduction to enhance fungal cell susceptibility. *Mol Cell* 1:807-17

Yun, D. J., Zhao, Y., Pardo, J. M., Narasimhan, M. L., Damsz, B., et al. 1997. Stress proteins on the yeast cell surface determine resistance to osmotin, a plant antifungal protein. *Proc Natl Acad Sci U S A* 94:7082-7

Zhao, C., Jung, U. S., Garrett-Engele, P., Roe, T., Cyert, M. S., Levin, D. E. 1998. Temperature-induced expression of yeast FKS2 is under the dual control of protein kinase C and calcineurin. *Mol Cell Biol* 18:1013-22

Zhao, Z. S., Leung, T., Manser, E., Lim, L. 1995. Pheromone signalling in Saccharomyces cerevisiae requires the small GTP- binding protein Cdc42p and its activator CDC24. *Mol Cell Biol* 15:5246-57

Zhou, Z., Gartner, A., Cade, R., Ammerer, G., Errede, B. 1993. Pheromone-induced signal transduction in Saccharomyces cerevisiae requires the sequential function of three protein kinases. *Mol Cell Biol* 13:2069-80

Zlotnik, H., Fernandez, M. P., Bowers, B., Cabib, E. 1984. Saccharomyces cerevisiae mannoproteins form an external cell wall layer that determines wall porosity. *J Bacteriol* 159:1018-26

Zueco, J., Mormeneo, S., Sentandreu, R. 1986. Temporal aspects of the O-glycosylation of Saccharomyces cerevisiae mannoproteins. *Biochim. Biophys. Acta* 884:93